



**UNIL** | Université de Lausanne

Unicentre

CH-1015 Lausanne

<http://serval.unil.ch>

---

*Year : 2012*

## ROLES OF ACID-SENSING ION CHANNELS (ASICs) IN PERIPHERAL NEUROPEPTIDE SECRETION AND PAIN

BOILLAT Aurélien

BOILLAT Aurélien, 2012, ROLES OF ACID-SENSING ION CHANNELS (ASICs) IN  
PERIPHERAL NEUROPEPTIDE SECRETION AND PAIN

Originally published at : Thesis, University of Lausanne

Posted at the University of Lausanne Open Archive.  
<http://serval.unil.ch>

### **Droits d'auteur**

L'Université de Lausanne attire expressément l'attention des utilisateurs sur le fait que tous les documents publiés dans l'Archive SERVAL sont protégés par le droit d'auteur, conformément à la loi fédérale sur le droit d'auteur et les droits voisins (LDA). A ce titre, il est indispensable d'obtenir le consentement préalable de l'auteur et/ou de l'éditeur avant toute utilisation d'une oeuvre ou d'une partie d'une oeuvre ne relevant pas d'une utilisation à des fins personnelles au sens de la LDA (art. 19, al. 1 lettre a). A défaut, tout contrevenant s'expose aux sanctions prévues par cette loi. Nous déclinons toute responsabilité en la matière.

### **Copyright**

The University of Lausanne expressly draws the attention of users to the fact that all documents published in the SERVAL Archive are protected by copyright in accordance with federal law on copyright and similar rights (LDA). Accordingly it is indispensable to obtain prior consent from the author and/or publisher before any use of a work or part of a work for purposes other than personal use within the meaning of LDA (art. 19, para. 1 letter a). Failure to do so will expose offenders to the sanctions laid down by this law. We accept no liability in this respect.



UNIL | Université de Lausanne

Faculté de biologie  
et de médecine

**Département de Pharmacologie et de Toxicologie**

**ROLES OF ACID-SENSING ION CHANNELS (ASICs) IN PERIPHERAL  
NEUROPEPTIDE SECRETION AND PAIN**

**Thèse de doctorat en Neurosciences**

présentée à la

Faculté de Biologie et de Médecine  
de l'Université de Lausanne

par

**Aurélien BOILLAT**

Titulaire d'un Master en Biologie Médicale de l'Université de Lausanne, Suisse

**Jury**

Prof. Jean-Pierre Hornung, Président

Dr. Stephan Kellenberger, Directeur

Dr. Alexandre Bouron, Expert

Dr. Marc Suter, Expert

Lausanne 2012

***Programme doctoral interuniversitaire en Neurosciences  
des Universités de Lausanne et Genève***



UNIL | Université de Lausanne



**UNIVERSITÉ  
DE GENÈVE**

**Programme doctoral interuniversitaire en Neurosciences  
des Universités de Lausanne et Genève**

# Imprimatur

Vu le rapport présenté par le jury d'examen, composé de

<b>Président</b>	Monsieur Prof. Jean-Pierre <b>Hornung</b>
<b>Directeur de thèse</b>	Monsieur Dr Stephan <b>Kellenberger</b>
<b>Co-directeur de thèse</b>	
<b>Experts</b>	Monsieur Dr Alexandre <b>Bouron</b>
	Monsieur Dr Marc <b>Suter</b>

le Conseil de Faculté autorise l'impression de la thèse de

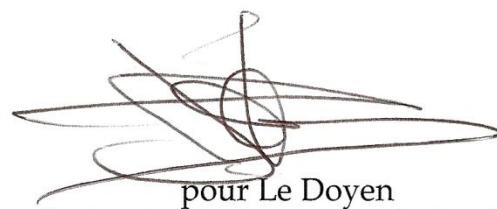
**Monsieur Aurélien Boillat**

Master ès sciences en biologie médicale de l'Université de Lausanne

intitulée

**ROLE OF ACID-SENSING ION CHANNELS (ASICs) IN PERIPHERAL  
NEUROPEPTIDE SECRETION AND PAIN.**

Lausanne, le 17 août 2012



pour Le Doyen  
de la Faculté de Biologie et de Médecine

Prof. Jean-Pierre Hornung

## Acknowledgments

I would like to thank Stephan Kellenberger for the continuous support, patience, and his constructive comments on my work.

I also thank former and present members of the laboratory: Omar Alijevic, Maxime Blanchard, Gaetano Bonifacio, Benoîte Bargeton, Gaetano Bonifacio, Cédric Laedermann, François Pascaud, Olivier Poirot, Sophie Roy. I would specially thank Maxime Blanchard for the scientific and general discussion we had, and for the patch-clamp experiments he performed for me.

I wish to thank Laurent Schild and all the members of his laboratory for sharing their results almost every Monday morning for five years.

I also wish to thank Jean-Pierre Hornung, Alexandre Bouron and Marc Suter for accepting to be president and members of the jury of my thesis.

Finally, I would like to thank my parents and my sister for their support all these years.

## Abstract

Acid-sensing ion channels (ASICs) are non-voltage-gated sodium channels activated by an extracellular acidification. They are widely expressed in neurons of the central and peripheral nervous system. ASICs have a role in learning, the expression of fear, in neuronal death after cerebral ischemia, and in pain sensation. Tissue damage leads to the release of inflammatory mediators. There is a subpopulation of sensory neurons which are able to release the neuropeptides calcitonin gene-related peptide (CGRP) and substance P (SP). Neurogenic inflammation refers to the process whereby peripheral release of the neuropeptides CGRP and SP induces vasodilation and extravasation of plasma proteins, respectively. Our laboratory has previously shown that calcium-permeable homomeric ASIC1a channels are present in a majority of CGRP- or SP-expressing small diameter sensory neurons.

In the first part of my thesis, we tested the hypothesis that a local acidification can produce an ASIC-mediated calcium-dependant neuropeptide secretion. We have first verified the co-expression of ASICs and CGRP/SP using immunocytochemistry and in-situ hybridization on dissociated rat dorsal root ganglion (DRG) neurons. We found that most CGRP/SP-positive neurons also expressed ASIC1a and ASIC3 subunits. Calcium imaging experiments with Fura-2 dye showed that an extracellular acidification can induce an increase of intracellular  $Ca^{2+}$  concentration, which is essential for secretion. This increase of intracellular  $Ca^{2+}$  concentration is, at least in some cells, ASIC-dependent, as it can be prevented by amiloride, an ASIC antagonist, and by Psalmotoxin (PcTx1), a specific ASIC1a antagonist. We identified a sub-population of neurons whose acid-induced  $Ca^{2+}$  entry was completely abolished by amiloride, an amiloride-resistant population which does not express ASICs, but rather another acid-sensing channel, possibly transient receptor potential vanilloïde 1 (TRPV1), and a population expressing both  $H^{+}$ -gated channel types. Voltage-gated calcium channels ( $Ca_v$ s) may also mediate  $Ca^{2+}$  entry. Co-application of the  $Ca_v$ s inhibitors ( $\omega$ -conotoxin MVIIC, Mibefradil and Nifedipine) reduced the  $Ca^{2+}$  increase in neurons expressing ASICs during an acidification to pH 6. This indicates that ASICs can depolarise the neuron and activate  $Ca_v$ s. Homomeric ASIC1a are  $Ca^{2+}$ -permeable and allow a direct entry of  $Ca^{2+}$  into the cell; other ASICs mediate an indirect entry of  $Ca^{2+}$  by inducing a membrane depolarisation that activates  $Ca_v$ s. We showed with a secretion assay that CGRP secretion can be induced by extracellular acidification in cultured rat DRG neurons. Amiloride and PcTx1 were not able to inhibit the secretion at acidic pH, but BCTC, a TRPV1 inhibitor was able to decrease the secretion induced by an extracellular acidification in our *in vitro* secretion assay.

In conclusion, these results show that in DRG neurons a mild extracellular acidification can induce a calcium-dependent neuropeptide secretion. Even if our data show that ASICs can mediate an increase of intracellular  $Ca^{2+}$  concentration, this appears not to be sufficient to trigger neuropeptide secretion. TRPV1, a calcium channel whose activation induces a sustained current – in contrary of ASICs – played in our experimental conditions a predominant role in neurosecretion.

In the second part of my thesis, we focused on the role of ASICs in neuropathic pain. We used the spared nerve injury (SNI) model which consists in a nerve injury that induces symptoms of neuropathic pain such as mechanical allodynia. We have previously shown that the SNI model modifies ASIC currents in dissociated rat DRG neurons. We hypothesized that ASICs could play a role in the development of mechanical allodynia. The SNI model was performed on ASIC1a, -2, and -3 knockout mice and wild type littermates. We measured mechanical allodynia on these mice with calibrated von Frey filaments. There were no differences between the wild-type and the ASIC1, or ASIC2 knockout mice. ASIC3 null mice were less sensitive than wild type mice at 21 day after SNI, indicating a role for ASIC3. Finally, to investigate other possible roles of ASICs in the perception of the environment, we measured the baseline heat responses. We used two different models; the tail flick model and the hot plate model. ASIC1a null mice showed increased thermal allodynia behaviour in the hot plate test at three different temperatures (49, 52, 55°C) compared to their wild type littermates. On the contrary, ASIC2 null mice showed reduced thermal allodynia behaviour in the hot plate test compared to their wild type littermates at the three same temperatures.

We conclude that ASIC1a and ASIC2 in mice can play a role in temperature sensing. It is currently not understood how ASICs are involved in temperature sensing and what the reason for the opposed effects in the two knockout models is.

## Résumé

Les canaux sensibles aux protons (ASICs) sont des canaux sodiques non voltages dépendants activés par une acidification extracellulaire. Ils sont largement exprimés dans les neurones du système nerveux central et périphérique. Les ASICs ont un rôle dans l'apprentissage, l'expression de la peur, dans la mort neuronale après une ischémie cérébrale, ainsi que dans la sensation de douleur. Un dommage tissulaire conduit au relâchement de médiateurs inflammatoires. Il y a une sous-population de neurones sensoriels qui sont capables de relâcher les neuropeptides calcitonin gene-related peptide (CGRP) et substance P (SP). L'inflammation neurogénique réfère au processus lorsque le relâchement périphérique de neuropeptides CGRP et SP induit respectivement la vasodilatation et l'extravasation de plasma. Notre laboratoire a montré précédemment que les canaux homomériques ASIC1a sont présents dans la majorité des neurones de petits diamètres exprimant le CGRP et la SP.

Dans la première partie de ma thèse, nous avons testé l'hypothèse selon laquelle une acidification locale peut produire une sécrétion de peptide médiée par les ASICs. Nous avons tout d'abord vérifié la co-expression des ASICs et de CGRP/SP en utilisant l'immunocytochimie et l'hybridation in-situ sur des neurones dissociés de ganglions de racine dorsale (DRG). Nous avons trouvé que la plupart des neurones positifs pour CGRP/SP exprimaient aussi les sous-unités ASIC1a et ASIC3. Des expériences d'imagerie calcique avec le colorant Fura-2 ont montré qu'une acidification extracellulaire peut induire une augmentation de  $Ca^{2+}$  intracellulaire, qui est essentielle pour la sécrétion. Cette augmentation de concentration de  $Ca^{2+}$  intracellulaire est, au moins dans certaines cellules, dépendant d'ASIC, car elle peut être empêchée par l'amiloride, un antagoniste d'ASIC et par la Psalmotoxine (PcTx1), un antagoniste spécifique d'ASIC1a. Nous avons identifié une sous-population de neurones dans laquelle l'entrée de  $Ca^{2+}$  a été complètement abolie par l'amiloride, une population résistante à l'amiloride qui n'exprime pas d'ASICs, mais plutôt un autre canal sensible aux protons, possiblement TRPV1, et une population exprimant les deux types de canaux sensibles aux protons. Les canaux calciques voltage dépendants ( $Ca_v$ s) peuvent aussi médier l'entrée de calcium. La co-application des inhibiteurs de  $Ca_v$ s ( $\omega$ -conotoxin MVIIC, Mibefradil et Nifedipine) a réduit l'augmentation de  $Ca^{2+}$  dans des neurones exprimant des ASICs lors d'une acidification à pH 6. Cela indique que les ASICs peuvent dépolariser les neurones et activer les  $Ca_v$ s. Les ASIC1a homomériques sont perméables au calcium et permettent une entrée directe de calcium dans la cellule; les autres ASICs médient une entrée indirecte de  $Ca^{2+}$  en induisant une dépolarisation de la membrane qui active les  $Ca_v$ s. Nous avons montré avec un essai de sécrétion que la sécrétion de CGRP peut être induite par une acidification extracellulaire des neurones de DRG de rats. L'Amiloride et la PcTx1 n'ont pas pu inhiber la sécrétion à pH acide, mais le BCTC, un inhibiteur de TRPV1a été capable de diminuer, dans notre essai de sécrétion in vitro, la sécrétion lors d'une acidification extracellulaire.

Pour conclure, ces résultats montrent que dans les neurones de DRG, une légère acidification peut induire une sécrétion de neuropeptides dépendante  $Ca^{2+}$ . Même si nos données montrent que les canaux ASICs peuvent médier une augmentation de la concentration de  $Ca^{2+}$  intracellulaire, cela n'apparaît pas comme suffisant pour activer la sécrétion de neuropeptides. TRPV1, un canal calcique dont l'activation induit un courant soutenu – au contraire des ASICs – a joué, avec nos conditions expérimentales, un rôle prédominant dans la sécrétion.

Dans une deuxième partie de ma thèse, nous nous sommes concentrés sur le rôle des ASICs dans la douleur neuropathique. Nous avons utilisé le modèle SNI qui consiste en une blessure du nerf qui induit des symptômes de douleurs neuropathiques comme une allodynie mécanique. Nous avons précédemment montré que le modèle SNI modifie les courants ASICs dans des neurones de DRG de rat dissociés. Nous avons émis l'hypothèse que les ASICs pourraient jouer un rôle dans le développement de l'allodynie mécanique. Le modèle SNI a été effectué sur des souris knockout pour ASIC1a, -2, et -3 et des souris de type sauvage. Nous avons mesuré l'allodynie mécanique sur ces souris avec des filaments von Frey calibrés. Il n'y avait pas de différence entre les souris sauvages et les souris ASIC1a et ASIC2 knockout. Les souris ASIC3 knockout étaient moins sensibles que les souris sauvages 21 jours après le SNI, indiquant un rôle des ASIC3. Finalement, pour investiguer d'autres rôles possibles des ASICs dans la perception de l'environnement, nous avons mesuré les réponses de base à la chaleur. Nous avons utilisé deux différents modèles; le modèle de « tail flick » et de la « plaque chaude ». Les souris ASIC1a knockout ont montré une augmentation de l'allodynie thermique dans le modèle de la « plaque chaude » à trois différentes températures (49, 52, 55°C) comparé aux souris de type sauvage. Au contraire, Les souris ASIC2 knockout ont montré une diminution de l'allodynie thermique dans le modèle de la « plaque chaude » comparé aux souris de type sauvage aux trois mêmes températures.

Nous concluons que les ASIC1a et les ASIC2 dans les souris peuvent jouer un rôle dans la sensation de la température. On ne comprend actuellement pas comment les ASICs sont impliqués dans la sensation de température et quelles sont les raisons des effets opposés dans les deux modèles knockout.

## Résumé à un large public

### Rôle des canaux sensibles à l'acidification (ASICs) dans la sécrétion périphérique de neuropeptides et dans la douleur

Les neurones sont les principales cellules du système nerveux. Leur fonction principale est la transmission de signaux. Cette signalisation se fait grâce au passage d'ions (particules chargées) à travers des canaux présents dans la membrane plasmique, qui délimite la cellule. Ces canaux sont généralement fermés et peuvent s'ouvrir après avoir été stimulés. Je me suis principalement intéressé à un canal nommé ASIC. Ce canal est normalement fermé et s'ouvre quand l'environnement devient acide. L'ouverture du canal ASIC permet d'activer les neurones. Les ASICs ont un rôle dans l'apprentissage, l'expression de la peur, dans la mort neuronale après une attaque cérébrale, et dans la sensation de douleur. Lors d'une blessure, une inflammation se produit. Elle est accompagnée d'une acidification qui va activer les ASICs et permettre la transmission d'un message de douleur au cerveau.

Lors de ma thèse, j'ai étudié le rôle des ASICs dans les neurones sensoriels lors d'une acidification périphérique. Nous avons formulé l'hypothèse que ces neurones peuvent sécréter des médiateurs qui peuvent induire ou maintenir l'inflammation. Afin de vérifier cette hypothèse, j'ai vérifié, chez le rat, si les canaux ASICs étaient présents dans les mêmes neurones sensoriels que ces médiateurs. J'ai aussi vérifié si l'activation des ASICs par une acidification permet l'entrée de calcium dans la cellule. Nous savons que cette entrée de  $Ca^{2+}$  est nécessaire pour la sécrétion. Finalement, j'ai vérifié si l'activation des ASICs permet la sécrétion des médiateurs importants pour l'inflammation. Des expériences de marquage des ASICs et des médiateurs m'ont permis de montrer qu'ils étaient présents dans les mêmes neurones. Des expériences d'imagerie m'ont permis de montrer que l'activation des ASICs permet une entrée de calcium dans les neurones. Des expériences de sécrétion de médiateurs m'ont permis de montrer que les canaux ASICs ne sont pas impliqués dans la sécrétion de ces médiateurs. J'ai pu mettre en évidence qu'un autre canal appelé TRPV1, lui aussi activé par une acidification, était responsable de cette sécrétion.

Je me suis aussi intéressé au rôle possible des ASICs dans la douleur neuropathique. La douleur neuropathique est une douleur chronique qui apparaît lors d'une lésion d'un nerf lors d'une maladie ou suite à un accident. Il avait été précédemment observé dans notre groupe de recherche que lors d'une lésion du nerf sciatique provoquant une douleur neuropathique chez le rat, des changements de ses canaux ASICs avaient lieu. C'est pourquoi j'ai étudié le rôle des ASICs dans la perception de la douleur neuropathique après une lésion du nerf sciatique chez la souris. Pour ce faire j'ai utilisé trois différents types de souris chez qui, à chaque fois, une différente forme d'ASIC avait été supprimé. J'ai comparé à chaque fois la douleur ressentie après la lésion du nerf par une souris ne possédant pas une certaine forme d'ASIC avec la douleur ressentie par une souris normale. J'ai pu montrer que deux formes d'ASICs n'avaient pas de rôle dans la douleur perçue par les souris, Les souris ne possédant pas une variante spécifique d'ASICs ressentaient un peu moins de douleur que les souris normales, ce qui nous indique, bien que les effets soient petits, que cette variante du canal est impliquée dans cette forme de douleur.

Ces résultats confirment un rôle des ASICs dans l'activité des neurones sensoriels et dans la douleur, notamment un rôle, quoi que limité, dans la douleur neuropathique.



## List of Abbreviations

AP: action potential	RAMP1: receptor activity-modifying protein 1
APETx2: sea anemone peptide toxin 2	rTRPV1: rat TRPV1
ASIC: acid-sensing ion channel	SNAP25: Synaptosomal-associated protein 25
ATP: adenosine triphosphate	SNARE: SNAP (Soluble NSF Attachment Protein)
BCTC : N-(4-Tertiarybutylphenyl)-4-(3-cholorpyridin-2-yl)tetrahydropryazine-1(2H)-carbox-amide	REceptor
CAP1: adenylate cyclase-associated protein 1	SNI: spared nerve injury
cASIC1a: chicken ASIC1a	SP: substance P
Cav: voltage-gated calcium channel	SSI: steady-state inactivation
CFA: complete freud's adjuvant	TNF- $\alpha$ : tumor necrosis factor $\alpha$
CGRP: calcitonin gene related peptide	TPEN: N,N'-Ethylenebis[bis(2-pyridyl)amine]
CLR: calcitonin receptor-like receptor	TrkA: tyrosine kinase receptor A
CNS: central nervous system	TRPA1: transient receptor potential ankyrin 1
COX: cyclooxygenase	TRPM8: transient receptor potential melastatin 8
CTPC: (2R)-4-(3-chloro-2pyridinyl)-2-methyl-N-[4-(tri-fluoromethyl)phenyl]-1 piperazonecarboxamide	TRPV1: transient teceptor potential vanilloid 1
DRG: dorsal root ganglion	TRPV2: transient teceptor potential vanilloid 2
DTNB: 5,5'-dithio-bis-(2-nitrobenzoic acid)	TTX: tetrodotoxin
DTT: dithiothreitol	WT: wild type
EC50: half maximal effective concentration	
EIA: enzyme immunoassay	
ENaC: epithelial sodium channel	
FaNaC: FMRF-amide-gated ion channel	
FMRFamide: Phe-Met-Arg-Phe amide	
GDNF: glial-derived neurotrophic factor	
GMQ: 2-guanidine-4-methylquinazoline	
hASIC1a: human ASIC1a	
IB4: isolectin B4	
IC50: half maximal inhibitory concentration	
IEM: Inherited erythromelalgia	
IL-1 $\beta$ : interleukin-1 $\beta$	
IL-6: interleukin-6	
KO: knockout	
MAPK: mitogen-activated protein kinase	
MitTx: Micrurus tener tener toxin	
Nav: voltage-gated sodium channel	
NGF: nerve growth factor	
NK1: neurokinin 1	
NMDA: N-Methyl-D-aspartic acid	
NPAF: neuropeptide AF	
NPFF: neuropeptide FF	
NPSF: neuropeptide SF	
NSAID: non-steroidal anti-inflammatory drug	
PAG: periaqueductal grey	
PCR: polymerase chain reaction	
PcTx1: psalmotoxin 1	
pH50: half maximal effective concentration of protons	
PI3K: phosphoinositide 3-kinase	
PKA: protein kinase A	
PLC: phospholipase C	
PNS: peripheral nervous system	



## Table of content

<i>Acknowledgments</i> .....	<i>II</i>
<i>Abstract</i> .....	<i>II</i>
<i>Résumé</i> .....	<i>III</i>
<i>Résumé à un large public</i> .....	<i>IV</i>
<i>List of Abbreviations</i> .....	<i>V</i>
<i>Table of content</i> .....	<i>VI</i>
<i>List of Figures</i> .....	<i>IX</i>
<i>List of Tables</i> .....	<i>X</i>
<b>1. Introduction</b> .....	<b>1</b>
<b>1.1 The peripheral nervous system</b> .....	<b>1</b>
1.1.1 General organization .....	1
1.1.2 Distinct types of pain.....	3
1.1.3 The nociceptors .....	3
1.1.4 Projections of afferent fibers in the spinal cord.....	4
1.1.5 Effects of a peripheral injury on nociception .....	5
<b>1.2 The Acid-Sensing Ion Channels (ASICs)</b> .....	<b>7</b>
1.2.1 The ENaC/degenerin family.....	7
1.2.2 Genes and splice variants .....	8
1.2.3 Structure .....	8
1.2.4 Biophysical properties .....	9
1.2.5 ASIC modulators and activators.....	10
1.2.6 Pharmacology.....	13
<b>1.3 ASICs in the central nervous system</b> .....	<b>14</b>
1.3.1 Expression pattern .....	14
1.3.2 Role of ASIC1a in memory and fear.....	15
1.3.3 Role of ASIC1a in cerebral ischemia .....	15
<b>1.4 ASICs in the peripheral nervous system</b> .....	<b>16</b>
1.4.1 Mechanosensation .....	17
1.4.2 Nociception .....	18
1.4.3 Taste and hearing .....	20
1.4.4 Molecular basis of signal detection and propagation .....	21
1.4.5 Neuropeptides and their peripheral targets.....	25

<b>1.5</b>	<b>Aims of the Thesis.....</b>	<b>28</b>
1.5.1	Role of ASICs in neuropeptide secretion .....	28
1.5.2	Role of ASICs in neuropathic pain.....	28
<b>2.</b>	<b>Materials and methods.....</b>	<b>29</b>
<b>2.1</b>	<b>DRG neuron isolation and culture.....</b>	<b>29</b>
<b>2.2</b>	<b>Immunocytochemistry .....</b>	<b>29</b>
2.2.1	Test of ASIC2 antibody.....	30
<b>2.3</b>	<b>In-situ hybridization.....</b>	<b>31</b>
2.3.1	Preparation of cells.....	31
2.3.2	Labelling of oligonucleotides .....	31
2.3.3	Hybridization and detection of the oligonucleotides .....	32
2.3.4	Solutions.....	33
2.3.5	Oligonucleotides sequences .....	33
2.3.6	Test of in-situ hybridization probes against ASIC subunits .....	34
<b>2.4</b>	<b>Microscopy and cell counting.....</b>	<b>36</b>
<b>2.5</b>	<b>Calcium imaging.....</b>	<b>36</b>
<b>2.6</b>	<b>In vitro CGRP secretion assay with DRG neurons .....</b>	<b>37</b>
<b>2.7</b>	<b>CGRP enzyme immunoassay.....</b>	<b>37</b>
<b>2.8</b>	<b>Animal surgery .....</b>	<b>38</b>
<b>2.9</b>	<b>Behaviour .....</b>	<b>39</b>
2.9.1	Von Frey monofilaments.....	39
2.9.2	Hot plate.....	39
2.9.3	Tail flick.....	40
<b>3.</b>	<b>Results.....</b>	<b>41</b>
<b>3.1</b>	<b>Distribution of ASICs, TRPV1 and neuropeptides in rat DRG neurons .....</b>	<b>41</b>
3.1.1	ASIC1, -2 and TRPV1 are preferentially localised in peptidergic neurons.....	41
3.1.2	In situ hybridization experiment confirm that ASIC subunits are preferentially expressed in the peptidergic population of small neurons .....	42
<b>3.2</b>	<b>Functional experiments with calcium imaging on cells in culture .....</b>	<b>46</b>
3.2.1	Heterologous expressed ASIC1a and TRPV1 are activated by extracellular acidification .....	46
3.2.2	Amiloride prevents the ASIC-induced Ca <sup>2+</sup> entry in a population of DRG neurons.....	48
3.2.3	Psalmotoxin inhibits the activation of ASICs in a population of DRG neurons .....	50
3.2.4	Ca <sub>v</sub> inhibitors reduce the amplitude of ASIC-mediated Ca <sup>2+</sup> increase in DRG neurons .....	52
3.2.5	Ca <sub>v</sub> inhibitors do not affect PcTx1-sensitive Ca <sup>2+</sup> entry.....	54

<b>3.3</b>	<b>CGRP secretion assay on dissociated DRG neurons.....</b>	<b>55</b>
3.3.1	BCTC reduces CGRP secretion induced by an extracellular acidification in DRG neurons .....	55
<b>3.4</b>	<b>Behavioural experiments on ASIC1, ASIC2 and ASIC3 null mice. ....</b>	<b>58</b>
3.4.1	Mechanical allodynia-like behaviour induced by spared nerve injury (SNI) is not different from wild type in ASIC1a, -2 and 3 null mice .....	58
3.4.2	ASIC2 null mice exhibit a reduced thermal allodynia-like behavior in the hot plate test .....	60
<b>4.</b>	<b>Discussion.....</b>	<b>63</b>
<b>4.1</b>	<b>Expression of the different ASIC subunits and of neuropeptides.....</b>	<b>63</b>
4.1.1	Advantages and limitations of immunocytochemistry and in-situ hybridization .....	63
4.1.2	Comparison between the labelling of ASICs and the different types of ASIC currents .....	64
4.1.3	Comparison of the results of expression of ASICs, TRPV1, CGRP and SP with the literature .....	64
<b>4.2</b>	<b>Increase of intracellular calcium concentration via ASICs and TRPV1.....</b>	<b>66</b>
4.2.1	Effect of amiloride on the intracellular Ca <sup>2+</sup> concentration of CHO cells expressing ASIC1a .....	66
4.2.2	Effect of amiloride on the intracellular Ca <sup>2+</sup> concentration of DRG neurons .....	66
4.2.3	Effect of PcTx1 on the intracellular Ca <sup>2+</sup> concentration of DRG neurons .....	66
4.2.4	Effect of Ca <sub>v</sub> s on the intracellular Ca <sup>2+</sup> concentration of DRG neurons .....	67
4.2.5	Comparison of our results on ASICs and TRPV1 function in DRG neurons with the literature ....	68
<b>4.3</b>	<b>Secretion of CGRP from DRG neurons .....</b>	<b>69</b>
4.3.1	Extracellular acidification induces CGRP secretion .....	69
4.3.2	Role of ASICs in acid-induced CGRP secretion .....	70
4.3.3	Role of Ca <sub>v</sub> s in acid-induced CGRP secretion .....	70
4.3.4	Role of TRPV1 in acid-induced CGRP secretion .....	71
4.3.5	Role of Na <sub>v</sub> s in acid-induced CGRP secretion .....	71
4.3.6	Comparison of our results on CGRP secretion from DRG neurons with the literature .....	72
<b>4.4</b>	<b>Behavioural experiments with mice.....</b>	<b>73</b>
4.4.1	Mechanical allodynia-like behaviour induced by SNI .....	73
4.4.2	Thermal allodynia-like behaviour in the tail flick and the hot plate test .....	74
<b>4.5</b>	<b>Conclusion.....</b>	<b>75</b>
<b>4.6</b>	<b>Perspectives.....</b>	<b>76</b>
<b>5.</b>	<b>Annexes .....</b>	<b>77</b>
<b>5.1</b>	<b>Supplementary images of in-situ hybridization on DRG neurons.....</b>	<b>77</b>
<b>6.</b>	<b>References .....</b>	<b>80</b>

## List of Figures

Figure 1 : Description of small-diameter (A $\delta$ ), medium- to large-diameter (A $\alpha$ , $\beta$ ) myelinated afferent fibres and small-diameter unmyelinated afferent fibres (C).....	2
Figure 2 : Connections between primary afferent fibers and the dorsal horn .....	4
Figure 3 : The molecular complexity of the primary afferent nociceptor is illustrated by its response to inflammatory mediators released at the site of tissue injury. ....	6
Figure 4 : Macroscopic inward current of ASIC1a recorded at -70 mV after rapid pH change from 7.4 to 6 in <i>Xenopus</i> oocytes.....	8
Figure 5 : Structure of chicken ASIC1 .....	9
Figure 6 : Proportion of small IB4-negative (left) and IB4-positive neurones (right) without ASIC current (white), and type 1 (hatched), type 2 (black) and type 3 (cross-hatched) .....	16
Figure 7 : Calcitonin gene-related peptide (CGRP) receptor and transduction pathways.....	26
Figure 8: Use of Fab fragments for labelling and blocking.....	30
Figure 9: Test of ASIC2 antibody on ASIC2 knock-out DRG.....	31
Figure 10 : Test of in-situ hybridization probes (antisense and sense) for ASIC1a, -1b, -2a, -2b and -3 in CHO cells. ....	35
Figure 11 : Co-expression of ASIC1, -2, and TRPV1 with neuropeptides in DRG neurons .....	42
Figure 12 : Example of staining of ASIC1a with in-situ hybridization on DRG neurons.....	43
Figure 13 : ASIC subunits are preferentially expressed in the peptidergic population of small DRG neurons .....	44
Figure 14 : A large population of neurons express both ASIC1a/1b and ASIC 3.....	45
Figure 15 : Effect of amiloride and BCTC on ASIC1a and TRPV1 stably expressed in CHO cells ....	47
Figure 16 : Amiloride inhibits the acid-induced Ca <sup>2+</sup> entry in a sub-population of DRG neurons .....	48
Figure 17 : Acid-induced fluorescence of the amiloride-insensitive neurons desensitizes less than the fluorescence of the full amiloride-sensitive neurons.....	50
Figure 18 : PcTx1 inhibits ASIC1a in a population of DRG neurons.....	51
Figure 19 : Ca <sub>v</sub> inhibitors reduced the pH6-induced increase of Ca <sup>2+</sup> concentration in an amiloride-sensitive population of neurons.....	53
Figure 20 : Ca <sub>v</sub> inhibitors had no effect on the pH6-induced increase of Ca <sup>2+</sup> concentration in an PcTx1-sensitive population of neurons .....	54
Figure 21 : Effect of extracellular acidification on CGRP secretion.....	56
Figure 22 : Co-application of TTX and lidocaine reduce acid-mediated CGRP secretion .....	58
Figure 23 : Mechanical withdrawal threshold decreases significantly in ipsilateral paws after SNI for both ASIC3 knockout mice and wild type mice.....	59
Figure 24 : Relative frequencies of paw withdrawal are not significantly different in both wild type and null mice following SNI .....	60
Figure 25 : ASIC1a and ASIC2 null mice showed a significant difference in thermal with the hot plate test .....	62
Figure 26: Schematic drawing of a neuron expressing ion channels .....	68
Figure S1: Example of staining of ASIC1b with in-situ hybridization on DRG neurons .....	77
Figure S2: Example of staining of ASIC2a with in-situ hybridization on DRG neurons .....	78
Figure S3: Example of staining of ASIC2b with in-situ hybridization on DRG neurons .....	78
Figure S4: Example of staining of ASIC3 with in-situ hybridization on DRG neurons .....	79

## List of Tables

Table 1 : List of ASIC subunits sense oligonucleotides.....	34
Table 2 : List of ASIC subunits anti-sense oligonucleotides .....	34

# 1. Introduction

## 1.1 The peripheral nervous system

### 1.1.1 General organization

The somatic sensory system mediates a range of sensations: touch, pressure, vibration, limb position, heat, cold, and pain. These sensations are transduced by receptors at the membrane of the terminal endings of the axons, localized in the skin, organs, and muscles. The cell bodies of sensory neurons are localized in a series of ganglia that lie alongside the spinal cord and the brainstem and are considered part of the peripheral nervous system (PNS). Neurons in the dorsal root ganglia (DRG) and in the cranial nerve ganglia transmit information on peripheral events to the central nervous system (CNS) and ultimately the brain. Action potentials generated in afferent fibers by the activation of different receptors at the peripheral endings propagate along the axons to the central endings, passing the cell bodies located in ganglia. The central endings make synapses with central neurons in the spinal cord.

The fundamental mechanism of sensory transduction, defined as the process of converting a stimulus into an electrical signal, can be described as a stimulus that alters the permeability of channels in the afferent nerve endings, generating a transmembrane potential difference called receptor potential. If the magnitude of the depolarization is sufficient and reaches a threshold, action potentials are generated along the axon toward the other ending of the axon. The rate of action potential firing is more or less proportional to the amplitude of the depolarization. Endings of afferent fibers can be encapsulated by specialized receptor cells (mechanoreceptors) that act as sensors of the somatic stimulations. Afferent fibers that do not have these specialized cells have free nerve endings. The free nerve endings have a role in the detection of painful stimuli.

Distinct classes of afferents can be defined, each of which making unique contributions to somatic sensations. Sensory afferents can be classified according to their axon diameter. Sensory afferents with the largest diameter (called Ia) are those that are linked to the sensory receptors in the muscles. Sensory afferents with smaller diameter fibers ( $A\beta$ ) mediate the touch sensation. Medium diameter myelinated ( $A\delta$ ) afferents that mediate acute, well-localized “first” or fast pain differ considerably from the larger diameter and rapidly conducting  $A\beta$  fibers that respond to innocuous mechanical stimulation. Information about pain and temperature is mediated by even smaller diameter fibers ( $A\delta$  and C).  $A\delta$  and C fibers have a higher threshold than  $A\beta$  fibers. Small diameter unmyelinated “C” fibers convey poorly localized, “second” or slow pain (Figure 1). The diameter of the fibers determines the speed of conduction. The larger is the diameter of the fibre, the faster is the speed of conduction (Basbaum *et al.*, 2009).

There are two major classes of nociceptors (Basbaum *et al.*, 2009). The A $\delta$  nociceptors can be subdivided into two main classes. Type I respond to both mechanical and chemical stimuli but have relatively high heat thresholds (>50°C). The type I fiber mediates the first pain provoked by intense mechanical stimuli. They will be sensitized in the case of tissue injury. Sensitization is defined as a lowering of the heat or mechanical threshold of response. Type II fibers have a much lower heat threshold, but a very high mechanical threshold. Activity of these afferents mediates the first acute pain to noxious heat. The unmyelinated C fibers are also heterogenous. Most C fibers are polymodal; they include a population that is both heat- and mechanically sensitive (Perl, 2007).

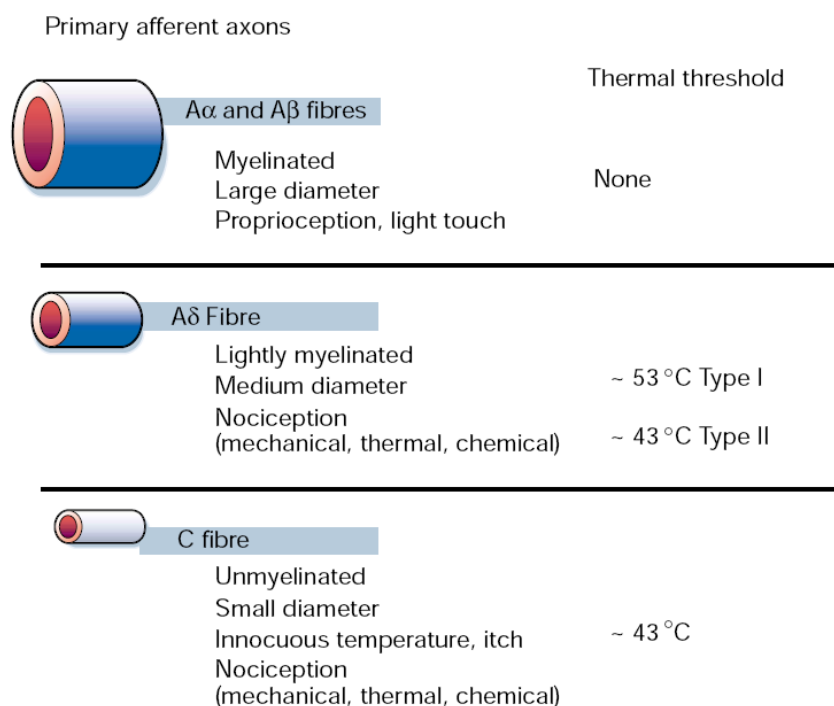


**Figure 1 : Description of small-diameter (A $\delta$ ), medium- to large-diameter (A $\alpha$ , $\beta$ ) myelinated afferent fibres and small-diameter unmyelinated afferent fibres (C)**  
(Julius and Basbaum 2001)

Another feature of sensory afferents is the size of the receptive field. The receptive field of a sensory neuron is defined as the area of the skin surface over which stimulation results in a significant change in the rate of action potentials of that neuron. The size of the receptive field is dependant of the innervation of the skin. The receptive fields in regions with dense innervation (lips, fingers) are relatively small compared to those in the forearm or back that are innervated by a smaller number of afferent fibers. Sensory afferents are also differentiated by the temporal dynamics of their response to sensory stimuli. Some afferents, which are called rapidly adapting, fire rapidly when a stimulus is first presented, and afterwards stop firing in the presence of continued stimulation. Other afferents generate a sustained discharge in the presence of continuous stimulus. Rapidly adapting afferents are particularly effective to provide information about stimulations that are changing, such as those



produced by stimulus caused by movements. In contrast, slowly adapting afferents provide information about the spatial attributes of the stimulus, such as size and shape (Purves, 2008).

### **1.1.2 Distinct types of pain**

According to The International Association for the Study of Pain, pain is defined as "an unpleasant sensory and emotional experience associated with actual or potential tissue damage, or described in terms of such damage". Indeed, pain is a multidimensional sensory experience that is intrinsically unpleasant and associated with hurting and soreness. It may vary in intensity (mild, moderate, or severe), quality (sharp, burning, or dull), duration (transient, intermittent, or persistent), and referral (superficial or deep, localized or diffuse). Pain has also strong cognitive and emotional components which can be described as suffering. Several distinct types exist: nociceptive, inflammatory which are adaptive; neuropathic and functional which are maladaptive. Adaptive pain is very useful for an organism to be protected against injury or to promote healing when the injury has occurred. Maladaptive pain, in contrast, occurs under pathological state of the nervous system. This type pain is considered as a disease. The sensory experience of acute pain caused by a noxious stimulus is mediated by the nociceptive system. Functional pain is due to an abnormal responsiveness or function of the nervous system. Several diseases cause this type of pain such as for example, fibromyalgia or irritable bowel syndrome. To prevent damage to tissue, we have learned to associate noxious stimuli with danger that must be avoided. We have linked noxious stimuli with pain, an unpleasant sensation. If tissue damage occurs despite the nociceptive defensive system, the body needs to protect itself against noxious, potentially damaging stimuli to promote healing of the injured tissue. The goal of the inflammatory pain is to allow the body to recover from the injury by increasing the sensitivity of the injured part until repair is complete, minimizing further damage. Maladaptive pain is uncoupled from a noxious stimulus or healing tissue. Such pain may occur in response to damage to the nervous system (neuropathic pain) or result from abnormal operation of the nervous system (functional pain). Neuropathic pain may result from lesions to the peripheral nervous system, as for example in patients with diabetic polyneuropathy, or to the central nervous system, such as for example in patients with multiple sclerosis or spinal cord injury (Woolf, 2004).

### **1.1.3 The nociceptors**

Intense thermal, mechanical, or chemical stimuli are detected by a subpopulation of peripheral nerve fibers, called nociceptors. The process of detection of these stimuli by the nociceptors is called nociception. The cell bodies of nociceptors innervating the body are located in the DRG. The cell bodies innervating the face are located in the trigeminal ganglion. These neurons are pseudo-unipolar and they have both peripheral and central axonal branches that innervate respectively their target organ and the spinal cord. Nociceptors are excited only when stimulus intensities reach the noxious range.

Neuroanatomical and molecular characterization of nociceptors has demonstrated their heterogeneity, especially for the C fibers (Snider & McMahon, 1998). For example, the peptidergic population of C nociceptors releases the neuropeptides substance P (SP) and calcitonin-gene related peptide (CGRP); this population also expresses the TrkA neurotrophin receptor, which responds to nerve growth factor (NGF). The nonpeptidergic population of C nociceptors expresses the cRet neurotrophin receptor which is activated by glial-derived neurotrophic factor (GDNF). Almost all the nociceptors of the nonpeptidergic population bind Griffonia simplicifolia isolectin B4 (IB4) and express specific purinergic receptor subtypes, one of the most important being P2X<sub>3</sub> (Basbaum *et al.*, 2009). Nociceptors can also be distinguished according to their differential expression of channels that confer sensitivity for example to heat (TRPV1), cold (TRPM8), extracellular acidification (ASICs, TRPV1), or chemical irritants (TRPA1) (Julius & Basbaum, 2001). The majority of proteins synthesized by the DRG or trigeminal ganglion cells are distributed to both central and peripheral terminals, due to the particular pseudo-unipolar morphology of these neurons. The biochemical equivalency of central and peripheral terminals means that the nociceptors can send and receive messages from either ends (Basbaum *et al.*, 2009).

#### 1.1.4 Projections of afferent fibers in the spinal cord

Primary afferent nerve fibers project to the dorsal horn of the spinal cord. The dorsal horn has a precise laminar organisation characterized by distinct anatomical localization (Figure 2). A $\delta$  nociceptors project to lamina I as well as to the deeper dorsal horn (lamina V). The A $\beta$  fibers, which respond to light touch, project to the deep laminae (III, IV, and V).

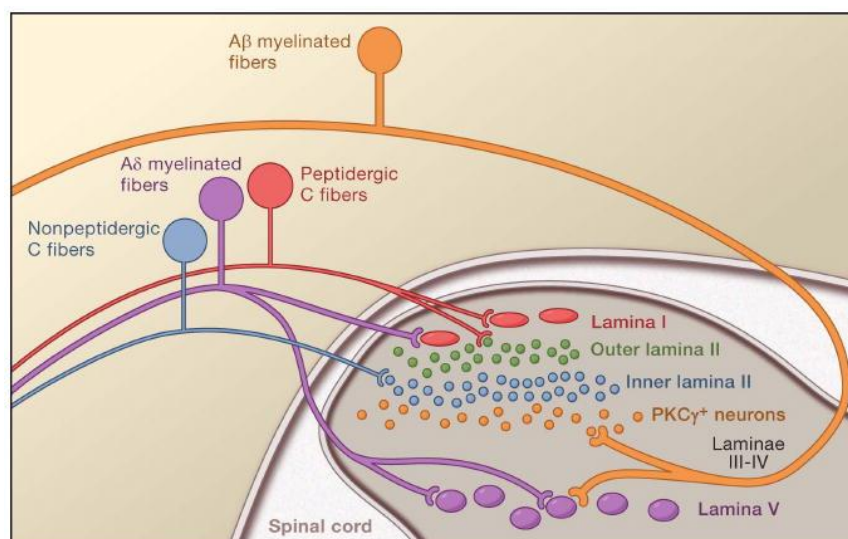


**Figure 2 : Connections between primary afferent fibers and the dorsal horn**  
(Basbaum *et al.*, 2009)

The nonpeptidergic C fibers terminate in the mid-region of lamina II. The most ventral part of lamina II, which is characterized by the presence of excitatory interneurons, is targeted predominantly by myelinated nonnociceptive afferents. Spinal cord neurons within lamina I are generally responsive to noxious stimulation (via A $\delta$  and C fibers), neurons in laminae III and IV are primarily responsive to innocuous stimulation (via A $\beta$ ), and neurons in lamina V receive a convergent nonnoxious and noxious input via direct, monosynaptic, A $\delta$  and A $\beta$  inputs and indirect (polysynaptic) C fiber inputs. Projection neurons within laminae I and V constitute the major output from the dorsal horn to the brain. These neurons are at the origin of multiple ascending pathways. One of them is the spinothalamic tract, which carries pain messages to the thalamus and is particularly relevant to the sensory-discriminative aspects of the pain experience, that is, where is the stimulus and how intense is it. Another is the spinoreticulothalamic tract, which carries pain to the brainstem and may be more relevant to poorly localized pain. From these brainstem and thalamic loci, information reaches cortical structures. There is no single brain area essential for pain. Rather, pain results from activation of a distributed group of structures, some of which are more associated with the sensory-discriminative properties (such as the somatosensory cortex) and others with the emotional aspects (such as the anterior cingulate gyrus and insular cortex). Pain results from activation of a distributed group of structures, some of which are more associated with the sensory-discriminative properties and others with the emotional aspects. Imaging studies on healthy subjects with experimental pain models or on patients with clinical pain conditions have demonstrated activation of prefrontal cortical areas, as well as regions not generally associated with pain processing (such as the basal ganglia and cerebellum). (Basbaum *et al.*, 2009)

### **1.1.5 Effects of a peripheral injury on nociception**

#### **1.1.5.1 Sensitization**

Nociceptors do not only signal acute pain, but also contribute to persistent and pathological pain conditions that occur in the case of injury. Allodynia is defined as a pain induced by a stimulus which normally does not provoke pain. Allodynia can result from two different conditions: increased excitability of postsynaptic neurons in the dorsal horn following high levels of activity in the nociceptive afferents (central sensitization), or lowering of nociceptor activation thresholds (peripheral sensitization) (Purves, 2008). With central sensitization, pain can be produced by activity in non-nociceptive primary sensory fibres. Peripheral sensitization results from the exposure of nociceptor terminals to products of tissue damage and inflammation, referred to as the “inflammatory soup” (Basbaum *et al.*, 2009) (Figure 3).

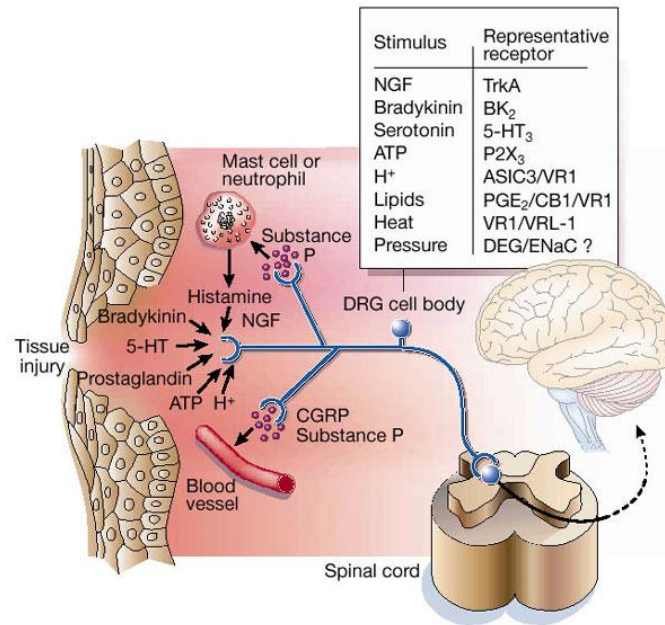


**Figure 3 : The molecular complexity of the primary afferent nociceptor is illustrated by its response to inflammatory mediators released at the site of tissue injury.**  
(Julius & Basbaum, 2001)

These compounds include extracellular protons, arachidonic acid and other lipid metabolites, serotonin, bradykinin, nucleotides and NGF, all of which can interact with receptors or ion channels on sensory nerve endings, increasing their response.

### 1.1.5.2 Neurogenic inflammation

Nociceptors conduct information not only in an afferent way toward the spinal cord, but also in an efferent way. Electrical activity of nociceptors due to the activation of terminals by local depolarization, axonal reflexes or dorsal horn reflexes, can release peptides and neurotransmitters (for example, SP, CGRP and ATP) from their peripheral terminals. An axonal reflex results from a stimulus applied to one branch of a nerve, which creates an impulse that moves centrally to the point of division of the nerve, where it is reflected down other branches to the free termini innervating, for example, the skin. These released factors are able to facilitate production of the inflammatory soup by promoting the release of factors from neighbouring non-neuronal cells (release of histamine from mast cells) and vascular tissue (vasodilatation, plasma extravasation), a phenomenon known as neurogenic inflammation (Julius & Basbaum, 2001).

### 1.1.5.3 Inflammatory mediators

NGF is produced in the setting of tissue injury and constitutes an important component of the inflammatory soup. NGF acts directly on peptidergic C fiber nociceptors, which express the NGF receptor tyrosine kinase, TrkA (Chao, 2003). NGF produces hypersensitivity to heat and mechanical stimuli through two different mechanisms. Rapidly after its release, NGF binds to its receptor, TrkA

activating downstream signaling pathways, including phospholipase C (PLC), mitogen-activated protein kinase (MAPK), and phosphoinositide 3-kinase (PI3K). It results in potentiation of target proteins at the peripheral nociceptor terminal, most notably TRPV1, leading to a rapid change in cellular and behavioral sensitivity (Chuang *et al.*, 2001). Later, NGF is retrogradely transported to the nucleus of the nociceptor, where it promotes increased expression of substance P, TRPV1 and Nav1.8 (Chao, 2003). These changes in gene expression enhance excitability of the nociceptor and amplify the neurogenic inflammatory response. Injury promotes the release of numerous cytokines as interleukin-1 $\beta$  (IL-1 $\beta$ ) and IL-6, and tumor necrosis factor  $\alpha$  (TNF- $\alpha$ ). Their main contribution to pain hypersensitivity is to potentiate the inflammatory response and increase the production of proalgesic agents (such as prostaglandins, NGF, bradykinin, and extracellular protons) (Basbaum *et al.*, 2009). In inflammatory conditions proinflammatory mediators NGF, serotonin, interleukin-1, and bradykinin increase ASIC transcript levels *in vivo*. If applied together, these mediators are able to increase the amplitude of the ASIC-like currents on sensory neurons as well as the number of ASIC-expressing neurons. These proinflammatory mediators increase sensory neuron excitability (Mamet *et al.*, 2002).  $\alpha$ -eudesmol inhibits the presynaptic  $\omega$ -agatoxin IVA-sensitive (P/Q-type) Ca<sup>2+</sup> channels. Treatment with  $\alpha$ -eudesmol dose-dependently attenuated neurogenic vasodilation in facial skin following electrical stimulation of rat trigeminal ganglion.  $\alpha$ -eudesmol concentration-dependently inhibits the depolarization-evoked CGRP and SP release from sensory nerve terminals in spinal cord slices (Asakura *et al.*, 2000). The activation of TRPV1 receptors on sensory fibers produces calcium and sodium influx and the release of neuropeptides (Richardson & Vasko, 2002).

## 1.2 The Acid-Sensing Ion Channels (ASICs)

### 1.2.1 The ENaC/degenerin family

At the beginning of the 1990's, a new class of ion channels was identified. This new class is now known as the epithelial sodium channel (ENaC)/degenerin family. The first members of this family were discovered in a genetic screen of the mechanosensory pathway of *Caenorhabditis elegans*. Mutations in the *deg-1* gene induced a selective degeneration of the sensory neurons responsible for the light touch sensitivity (Chalfie *et al.*, 1993). This phenotype has given the name “degenerin” to this family of channels. At about the same time, the  $\alpha$ -subunit of ENaC was cloned (Canessa *et al.*, 1993). ENaC plays a crucial role in Na<sup>+</sup> reabsorption in the kidney. The amino acid sequence identity between the different ENaC/DEG subfamilies is about 15 to 20%. Based on their homology, a subfamily of neuronal channels was identified. It later appeared that these channels were activated by extracellular acidifications. They were consequently named Acid-Sensing Ion Channels (ASICs) (Waldmann *et al.*, 1997; Waldmann & Lazdunski, 1998). Another subfamily within the ENaC/DEG

family of ion channels was also cloned at that time, the FMRF-amide-gated ion channel (FaNaC) (Lingueglia *et al.*, 1995), which is present in the mollusc *Helix aspersa* (Kellenberger & Schild, 2002).

### 1.2.2 Genes and splice variants

Four different ASIC genes were identified; two of them exist in different splice variants. The ASIC1 gene has two splice variants (-1a, -1b), as the ASIC2 gene (-2a, -2b) (Kellenberger & Schild, 2002). The expression of the members of this new subfamily was analysed by Northern blotting and in situ hybridisation (Waldmann & Lazdunski, 1998; Biagini *et al.*, 2001) and shows a high expression in the central and peripheral nervous system. These channels were found to be non-voltage-activated sodium channels that are transiently activated by a rapid extracellular acidification (Figure 4) (Waldmann *et al.*, 1997).

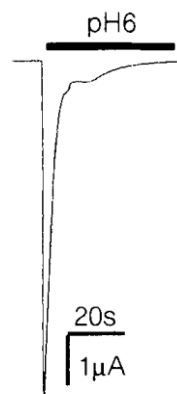


**Figure 4 :** Macroscopic inward current of ASIC1a recorded at -70 mV after rapid pH change from 7.4 to 6 in *Xenopus* oocytes. (Waldmann *et al.*, 1997)

ASIC1a, -1b, -2a and -3 can form functional homomultimeric as well as heteromultimeric channels (Hesseler *et al.*, 2004). ASIC2b needs to be coexpressed with ASIC1a, -1b, -2a or -3 to generate a proton-induced current (i.e. a current whose properties are different compared to the homomeric channel formed by the coexpressed subunit) (Lingueglia *et al.*, 1997). ASIC4 is not activated by protons and does not form functional channels with other ASIC subunits (Grunder *et al.*, 2000).

### 1.2.3 Structure

In 2007, the first crystal structure of ASIC was released by the group of Gouaux (Jasti *et al.*, 2007). They managed to crystallize a truncated version of chicken ASIC1 (cASIC1), lacking the two N- and C- endings of the protein. The previously predicted secondary structure was confirmed. Each ASIC subunit is composed of two intracellular endings, two transmembrane domains and a large extracellular loop (Figure 5). Although numerous biochemical experiments done on ENaC have shown that it has four subunits (Firsov *et al.*, 1998; Kosari *et al.*, 1998), the crystal structure of cASIC1 shows surprisingly a trimeric architecture. The transmembrane domain of  $\Delta$ ASIC1 is defined by two



long  $\alpha$ -helices from each of the three subunits. Surrounding the “wrist”-like junction between the transmembrane and extracellular domains are well ordered 'loops' that probably have a key role in coupling conformational changes in the extracellular domain to the ion channel pore. Shaped like a funnel, the trimeric extracellular domain is composed of a core of three large  $\beta$ -sheets, one per subunit, and decorating this central core are three smaller  $\beta$ -sheet and  $\alpha$ -helical domains (Jasti *et al.*, 2007). More recently, the same group managed to crystallize a functional ASIC by keeping the N-termini of the protein intact. This structure is identical to the first structure in the extracellular parts, and shows a more realistic configuration of the transmembrane parts (Gonzales *et al.*, 2009).



**Figure 5 : Structure of chicken ASIC1**

View of the homotrimeric  $\Delta$ ASIC1 structure. Each crystallographically independent subunit is in a different colour, a single chloride ion per subunit is shown as a green sphere and N-linked carbohydrate is shown in stick representation. The  $\Delta$ ASIC1 structure has a chalice-like shape with a large extracellular domain protruding as much as 80 Å from the membrane plane, a slender transmembrane domain, and a broadened 'base' defined by the cytoplasmic N and C termini. The transmembrane domain of  $\Delta$ ASIC1 is defined by two long  $\alpha$ -helices from each of the three subunits. On the cytoplasmic side of the membrane, the termini are frayed and we do not see well-ordered protein structure (Jasti *et al.*, 2007).

#### 1.2.4 Biophysical properties

ASIC channels are activated by a drop of the extracellular pH. The selectivity ratio for  $\text{Na}^+$  over  $\text{K}^+$  is around 10 (Kellenberger & Schild, 2002). Homomeric ASIC1a is also slightly permeant to  $\text{Ca}^{2+}$  ( $\text{PNa}^+/\text{PCa}^{2+} = 18:1$ ), contrary to other ASIC assemblies that are not  $\text{Ca}^{2+}$  permeant (Bassler *et al.*, 2001). To determine the pH dependence of activation, step pH changes from pH 7.4 to acidic solutions of different pH are performed. The measured current can be plotted as a function of the activating pH and fitted with a Hill equation. The Hill equation allows calculating the pH50 which is the pH that induces half of the maximal current. The pH50 measured at 25°C in CHO cells expressing homomeric ASICs is 6.6 for ASIC1a, 6.2 for ASIC1b, 4.0 for ASIC2a and 6.7 for ASIC3 (Blanchard & Kellenberger, 2011). All functional ASICs respond to extracellular acidification with a transient



current. ASIC3-containing homo- and heteromultimers produce currents with a sustained phase in addition to the transient phase. Due to inactivation, prolonged exposure to a slightly acidic pH can render ASICs non-responsive to a subsequent acidic stimulus. In voltage-gated Na<sup>+</sup> channels (Na<sub>v</sub>), this analogous property is called steady-state inactivation (SSI). The SSI represents the direct transition from the closed to the inactivated state during prolonged exposure to moderately acidic pH. For ASIC1a, the pH of half-maximal inactivation is about 7.2. Therefore, at pH more acidic than pH 7.4, an increasing fraction of ASIC1a channels is in the inactivated conformation from which they cannot be opened by acidification. SSI determines the fraction of channels that are available for opening. ASIC activation can be important for the neuronal signalling. For example, it has also been shown that ASICs can induce action potentials (AP) in hippocampal neurons. The probability of inducing APs correlates with current entry via ASICs. The type of electrical response of a neuron to acidification depends on the variation of the pH, on the expression level of ASICs in the neuron, and on the activity of the neuron at that moment (Vukicevic & Kellenberger, 2004).

### 1.2.5 ASIC modulators and activators

Until recently, no activators of ASICs other than protons were known. Recently, it has been shown that 2-guanidine-4-methylquinazoline (GMQ) causes persistent ASIC3 channel activation at a physiological pH (Yu *et al.*, 2010) with an EC<sub>50</sub> of about 1 mM. A snake toxin activating ASICs with an EC<sub>50</sub> ≥ 10 nM has also been recently identified (Bohlen *et al.*, 2011). All the other substances described in this section can only modulate the activation of ASICs by protons, but are unable to activate ASICs by themselves.

#### 1.2.5.1 Redox reagents

ASICs are modulated by redox reagents. It has been shown that the reducing agent dithiothreitol (DTT) at 1-2 mM reversibly potentiates proton-activated currents in the sensory ganglia and hippocampal neurons of rat, while the oxidizing reagent 5,5'-dithio-bis-(2-nitrobenzoic acid) (DTNB) at 5 mM causes their inhibition. The antioxidant tripeptide glutathione (its reduced form, g-l-glutamyl-l-cysteinyl-glycine, GSH) at 2 mM also potentiates proton-activated currents (Andrey *et al.*, 2005). Mouse cortical application of the reducing agents potentiated, whereas the oxidizing agents inhibited the ASIC currents, but no effect was seen on ASIC1 knock-out mice. Experiments done on CHO cells expressing homomeric ASICs have shown that ASIC1a, but not ASIC1b, -2a, -3 respond to redox agents (Chu *et al.*, 2006). The effect of DTT on hASIC1a was mimicked by the metal chelator TPEN, indicating that the effect of DTT could be due to relief of tonic inhibition by transition metal ions, in addition of the redox modulation (Cho & Askwith, 2007).

### 1.2.5.2 Divalent cations: $\text{Ca}^{2+}$ , $\text{Zn}^{2+}$ and $\text{Mg}^{2+}$

ASICs are modulated by  $\text{Ca}^{2+}$ ,  $\text{Zn}^{2+}$  and  $\text{Mg}^{2+}$ . Extracellular, divalent cations like  $\text{Ca}^{2+}$  and  $\text{Mg}^{2+}$  shift the steady-state inactivation of ASIC1a and ASIC1b to more acidic values, leading in some cases to a potentiation of the channel response which extends the dynamic range of ASIC  $\text{H}^+$  sensors. (Babini *et al.*, 2002). At higher concentrations,  $\text{Ca}^{2+}$  inhibits ASIC1a partially by a pore block with an  $\text{IC}_{50}$  of about 3.9 mM at pH 5.5, whereas ASIC1b is blocked with reduced affinity with an  $\text{IC}_{50} > 10$  mM at pH 4.7 (Paukert *et al.*, 2004). The ASIC2a homomeric current is partially inhibited by high  $\text{Ca}^{2+}$  concentration (de Weille & Bassilana, 2001). On ASIC3, decreasing  $[\text{Ca}^{2+}]$  opens the channel because it is thought that protons open ASIC3 releasing  $\text{Ca}^{2+}$  from a high-affinity binding site on the extracellular side of the pore. The bound  $\text{Ca}^{2+}$  could block permeation and the channel could only conduct current when multiple protons relieve this block. (Immke & McCleskey, 2003).  $\text{Zn}^{2+}$  at 100–300  $\mu\text{M}$  concentration potentiates the acid activation of homomeric and heteromeric ASIC2a-containing channels (*i.e.* ASIC2a, ASIC1a+2a, ASIC2a+3), but not of homomeric ASIC1a and ASIC3 (Baron *et al.*, 2001). On hippocampal neurons in primary culture, either low extracellular  $[\text{Ca}^{2+}]$  or high extracellular  $[\text{Zn}^{2+}]$  increased the amplitude of the ASIC-like currents (Gao *et al.*, 2004).  $\text{Zn}^{2+}$  inhibits ASIC currents in cultured mouse cortical neurons at nanomolar concentrations. At nanomolar concentrations,  $\text{Zn}^{2+}$  inhibits currents mediated by homomeric ASIC1a and heteromeric ASIC1a-ASIC2a channels expressed in CHO cells, without effect on homomeric ASIC2a and ASIC3 (Chu *et al.*, 2004).

### 1.2.5.3 FMRFamide and FMRFamide-related peptides

FMRFamide (Phe-Met-Arg-Phe amide) and related peptides are abundant in invertebrate nervous systems and can act as neurotransmitters and neuromodulators (Cottrell, 1989). FMRFamide is not expressed in mammals, but related peptides are expressed in the mammalian nervous system. It has been shown in various snail species that FMRFamide directly gates sodium channels called FaNaC (FMRFamide-activated  $\text{Na}^+$  channel) (Green *et al.*, 1994). The structural similarity between ASICs and FaNaC led to test the effect of FMRFamide peptides on ASICs. Inflammation induces expression of FMRFamide-related neuropeptides, which modulate pain. Neuropeptide FF at 50  $\mu\text{M}$  (NPFF, Phe-Leu-Phe-Gln-Pro-Gln-Arg-Phe amide) and FMRFamide at 50–100  $\mu\text{M}$  generated no current on their own but potentiated  $\text{H}^+$ -gated currents from cultured sensory neurons and heterologously expressed ASIC1 and ASIC3, but not ASIC2a (Askwith *et al.*, 2000). The heteromeric channel ASIC3 + 2a is even more sensitive to NPFF than to FMRFamide (Catarsi *et al.*, 2001). Knockout mice have demonstrated that ASIC3 plays a major role in mediating the sensory response to FMRFamide and FRRFamide. Deletion of ASIC3 attenuated the response to FMRFamide-related peptides, whereas the loss of ASIC1 increased the response. The loss of ASIC2 had no effect on FMRFamide-dependent enhancement of  $\text{H}^+$ -gated currents. (Xie *et al.*, 2002; Xie *et al.*, 2003). ASIC2a is able to increase the

response to peptides in heteromeric channels containing ASIC1a or ASIC3 subunits (Catarsi *et al.*, 2001; Askwith *et al.*, 2004; Lingueglia *et al.*, 2006). Exogenous and endogenous FMRFamide-related peptides at 50  $\mu\text{M}$  decreased the pH sensitivity of ASIC1a steady-state desensitization. During conditions that normally induced steady-state desensitization, these peptides enhanced ASIC1a activity (Sherwood & Askwith, 2008). Endogenous mammalian RFamide peptides such as NPPF, NPAF and NPSF are mainly expressed in the CNS, with high level in the spinal cord, where they can be released. NPPF is present in small and medium DRG neurons. NPPF has been implicated in a variety of physiological functions such as pain modulation and is increased in the spinal cord during chronic inflammation. FMRFamide-related peptides could have neuromodulatory effects, like the modulation of nociceptive responses on central and peripheral neurons, through their interaction with ASICs. This could have an important role in conditions such as chronic inflammation where the expression levels of both NPPF and ASICs are increased (Lingueglia *et al.*, 2006).

Dynorphin A at 50  $\mu\text{M}$  and big dynorphin at 50  $\mu\text{M}$  inhibit steady-state desensitization of ASIC1a and acid-activated currents in cortical neurons. Dynorphin potentiation of ASIC1a current is abolished in the presence of PcTx1, a specific inhibitor of homomeric ASIC1a. This suggests that dynorphins interact with ASIC1a to enhance channel activity. The neuroprotection induced by steady-state desensitization of ASIC1a is abolished in the presence of dynorphins. In other words, dynorphins enhance neuronal damage following ischemia by preventing steady-state desensitization of ASIC1a (Sherwood & Askwith, 2009).

#### *1.2.5.4 Serine proteases*

Ischemia or inflammation can induce an acidification of the extracellular milieu. This acidification is often accompanied with an increase in the activity of proteases. Serine proteases modulate the function of ASIC1a and ASIC1b but not of ASIC2a and ASIC3. Protease exposure shifts the pH dependence of ASIC1a activation and steady-state inactivation to more acidic pH. Exposing ASIC1a to serine proteases at physiological pH decreased the response to an acidic pH, compared to naive ASIC1a. Interestingly, the same experiment with a conditioning pH of 7.0 instead of 7.4 showed that the exposed ASIC1a is more activated than the unexposed (Poirot *et al.*, 2004). This regulation of ASIC function by serine proteases is linked to channel cleavage. Trypsin, a serine protease, cleaves ASIC1a with a similar time course as it changes ASIC1a function, whereas ASIC1b, whose function is not modified by trypsin, is not cleaved. Trypsin cleaves ASIC1a at Arg-145, in the N-terminal part of the extracellular loop (Vukicevic *et al.*, 2006). The closely related channel ENaC is responsible for  $\text{Na}^+$  transport in many epithelia, including kidney and lung. Many factors have a role in regulating ENaC activity. The first evidence of a role of proteases in the regulation of ENaC was shown in a *Xenopus* kidney epithelial cell line (A6). Exposure of the apical membrane to the protease inhibitor aprotinin reduced transepithelial sodium transport. CAP1, a serine protease expressed in kidney, gut, lung, skin

and ovary, increased the activity of the sodium channel by two- to threefold (Vallet *et al.*, 1997). Proteolysis of ENaC subunits has a key role in this process (Hughey *et al.*, 2007). ENaC is composed of three subunits ( $\alpha$ ,  $\beta$ , and  $\gamma$ ). The  $\alpha$  and  $\gamma$  subunits of ENaC are processed by proteases (Hughey *et al.*, 2003). Specific proteases have been shown to activate epithelial  $\text{Na}^+$  channels by cleaving channel subunits (Kleyman *et al.*, 2009).

## 1.2.6 Pharmacology

### 1.2.6.1 Amiloride and benzamil

ASICs are reversibly inhibited by amiloride and its derivative benzamil. The concentration at which only half of the maximal current remains ( $\text{IC}_{50}$ ) is about 10 to 100  $\mu\text{M}$  depending on ASIC subunits (Kellenberger & Schild, 2002). It is supposed, based on experiments done on ENaC, that amiloride blocks ion permeation through the channel pore (Schild *et al.*, 1997).

### 1.2.6.2 Nonsteroid anti-inflammatory drugs (NSAIDs)

Nonsteroid anti-inflammatory drugs (NSAIDs) are drugs acting against inflammation and pain. Their principal mode of action is to inhibit cyclooxygenases (COXs). NSAIDs prevent the large increase of ASIC expression in sensory neurons induced by inflammation. NSAIDs such as aspirin (500  $\mu\text{M}$ ), diclofenac (200  $\mu\text{M}$ ), and flurbiprofen (500  $\mu\text{M}$ ) directly inhibit ASIC currents in sensory neurons and heterologous cell expression systems (Voilley *et al.*, 2001). It was also shown that diclofenac ( $\text{IC}_{50}$  of about 600  $\mu\text{M}$ ) and ibuprofen ( $\text{IC}_{50}$  of about 3.5 mM) inhibited proton-induced currents in hippocampal interneurons and that aspirin (500  $\mu\text{M}$ ) and salicylic acid (500  $\mu\text{M}$ ) were ineffective (Dorofeeva *et al.*, 2008). The possible differences of expression of ASICs subunits in DRG neurons and in hippocampal interneurons might explain the opposite effects of aspirin and salicylic acid on ASIC currents found by these two groups.

### 1.2.6.3 A-317567

A-317567 produced concentration-dependent inhibition of all pH 4.5-evoked ASIC currents in acutely dissociated adult rat DRG neurons with an  $\text{IC}_{50}$  ranging between 2 and 30  $\mu\text{M}$ . A-317567 blocked also the sustained phase of ASIC3-like current. With injection of Complete Freud's Adjuvant (CFA) in rat, inducing inflammatory thermal hyperalgesia, A-317567 completely inhibited the pain response at a 10-fold lower dose than amiloride (Dube *et al.*, 2005).

### 1.2.6.4 Psalmotoxin 1 (PcTx1)

Psalmotoxin 1 (PcTx1) is a 40-amino acid toxin from tarantula *Psalmopoeus cambridgei* venom. It blocks with an  $\text{IC}_{50}$  of 0.9 nM ASIC1a homomeric channels (Escoubas *et al.*, 2000). PcTx1 inhibits ASIC1a by a unique mechanism: the toxin increases the apparent affinity for  $\text{H}^+$  of ASIC1a. The toxin

shifts the inactivation curve to more alkaline pH, inactivating almost completely ASIC1a at physiological pH (Chen *et al.*, 2005).

#### 1.2.6.5 APETx2

APETx2 is a toxin from the sea anemone *Anthopleura elegantissima*, which inhibits ASIC3 homomeric channels both in heterologous expression systems and in primary cultures of rat sensory neurons. APETx2 reversibly inhibits rat ASIC3 (IC<sub>50</sub> = 63 nM), without any effect on ASIC1a, ASIC1b, and ASIC2a. APETx2 also inhibits heteromeric channels containing ASIC3 subunits, however with a lower potency. The ASIC3-like current in primary cultured sensory neurons is partly and reversibly inhibited by APETx2 (Diochot *et al.*, 2004). Recently our group showed that APETx2 inhibited the tetrodotoxin (TTX)-resistant Na<sub>v</sub> 1.8 currents of DRG neurons with an IC<sub>50</sub> of 2.6 μM, meaning that this toxin is not completely specific for ASIC3. This lack of specificity should be taken into account when using APETx2 as a pharmacological tool (Blanchard *et al.*, 2011).

#### 1.2.6.6 MitTx

Recently, it has been shown that venom from the Texas coral snake *Micrurus tener tener*, whose bite produces intense and unremitting pain, excites a large proportion of sensory neurons. The purified toxins (MitTx) act as selective agonists for ASICs, showing equal or greater efficacy compared with acidic pH. MitTx is highly selective for the ASIC1 subtype at neutral pH; under more acidic conditions (pH < 6.5), MitTx potentiates (>100-fold) proton-evoked activation of ASIC2a channels (Bohlen *et al.*, 2011).

### 1.3 ASICs in the central nervous system

#### 1.3.1 Expression pattern

All ASICs except ASIC1b and ASIC3 are expressed in the CNS. ASICs are distributed widely throughout the brain. ASIC1a, ASIC2a, and ASIC2b have a similar widespread distribution pattern in the brain. They are expressed in areas such as cortex, olfactory bulb, hippocampus, amygdala, and cerebellum (Waldmann & Lazdunski, 1998). Within cells, ASIC1 was found in almost all parts, including the soma and along the branches of axons and dendrites. In one study, ASIC1 was found not to be enriched in the microdomains where pH may reach low values, such as in synaptic vesicles or synaptic membranes (Alvarez de la Rosa *et al.*, 2003). In another study, ASIC1a was found to be enriched in areas with strong excitatory synaptic input such as the glomerulus of the olfactory bulb, whisker barrel cortex, cingulate cortex, striatum, nucleus accumbens, amygdala, and cerebellar cortex (Wemmie *et al.*, 2003). ASIC1 null mice had impaired hippocampal long-term potentiation and had reduced excitatory postsynaptic potentials during high-frequency stimulation, suggesting a

postsynaptic localisation of ASIC1a (Wemmie *et al.*, 2002). This post-synaptic localisation is in contradiction with the previous findings done by de la Rosa *et al.* ASIC2a is enriched in synaptic fractions from cerebellum (Jovov *et al.*, 2003).

ASIC4 shows strongest expression in pituitary gland. Moreover, ASIC4 expression is detected throughout the brain, in spinal cord, and inner ear (Grunder *et al.*, 2000). Reverse transcriptase-nested PCR and Western blotting showed that three ASIC isoforms, ASIC1a, ASIC2a, and ASIC2b, are expressed at a high level in dorsal horn neurons (Wu *et al.*, 2004). ASIC1a and ASIC2a are the most abundant ASICs in mouse adult spinal cord and are coexpressed by most neurons in all the laminae (Baron *et al.*, 2008). Photoreceptors and neurons of the mouse retina express ASIC2a and ASIC2b (Ettaiche *et al.*, 2004).

### **1.3.2 Role of ASIC1a in memory and fear**

ASIC1a null mice have impaired hippocampal long-term potentiation. ASIC1a null mice had reduced excitatory postsynaptic potentials and NMDA receptor activation during high-frequency stimulation. Null mice displayed defective spatial learning and eyeblink conditioning. Therefore ASIC1a has a small role in processes underlying synaptic plasticity, learning, and memory (Wemmie *et al.*, 2002). However, another study did not observe any differences in short-term plasticity upon blockade of ASIC1 with amiloride or inactivation of ASIC1 by lowering the conditioning pH to 6.7 in cultured hippocampal neurons. Protons released during intense synaptic activity did not activate postsynaptic ASIC1 currents in excitatory synapses and any activation of presynaptic ASIC currents did not alter synaptic transmission (Alvarez de la Rosa *et al.*, 2003).

ASIC1a modulates the activity of the circuits underlying innate fear (Wemmie *et al.*, 2003). Furthermore, removing the ASIC1a gene or acutely inhibiting ASIC1a suppresses fear and anxiety independent of conditioning (Coryell *et al.*, 2007). Rescue experiments, expressing ASIC1a in the basolateral amygdala of ASIC1a null mice using viral vector-mediated gene transfer pinpoint the basolateral amygdala as the site where ASIC1a contributes to fear memory (Coryell *et al.*, 2008). Inhaled CO<sub>2</sub> reduces brain pH and evokes fear behavior in mice. Using ASIC1a knock-out mice or inhibiting ASIC1a significantly reduced the effect of CO<sub>2</sub>. Rescuing ASIC1a specifically in the amygdala of ASIC1a null animals re-established the CO<sub>2</sub>-induced fear deficit. The amygdala is through ASIC1a an important chemosensor that detects hypercarbia and acidosis and initiates fear responses (Ziemann *et al.*, 2009).

### **1.3.3 Role of ASIC1a in cerebral ischemia**

ASICs in central neurons might contribute to the neuronal death associated with brain ischemia. In cell culture, cells lacking endogenous ASICs are resistant to acid injury, while transfection of Ca<sup>2+</sup>-

permeable ASIC1a establishes sensitivity to acid. In focal ischemia, intracerebroventricular injection of ASIC1a blockers (amiloride, venom containing PcTx1) or knockout of the ASIC1a gene protects the brain from ischemic injury and does so more potently than glutamate antagonism (Xiong *et al.*, 2004).

#### 1.4 ASICs in the peripheral nervous system

All ASIC subunits are found in the PNS. ASIC expression has also been found outside the nervous system in eye, ear, taste buds and bone (Wemmie *et al.*, 2006). ASICs are expressed in all DRG neuron subtypes, with the subunit composition varying among DRG neurons, producing different types of ASIC currents in different DRG neuron populations. An electrophysiological characterization performed in our group proposes the following classification (Poirot *et al.*, 2006). Small-diameter DRG neurones expressed three different ASIC current types which were all preferentially expressed in putative nociceptors. Type 1 currents are mediated by ASIC1a homomultimers and are characterized by steep pH dependence of current activation in the pH range 6.8–6.0. Type 3 currents are activated in a similar pH range as type 1, while type 2 currents are activated at pH<6. Type 1 current slowly inactivates at pH6, whereas type 2 and 3 inactivate rapidly. Within small-diameter neurones, two main subpopulations can be distinguished based on the binding of IB4. IB4-negative neurones are known to express neuropeptides and therefore IB4 is a marker for non-peptidergic neurones. There is evidence for different functions of IB4-positive and negative neurones in pain sensation (Snider & McMahon, 1998).

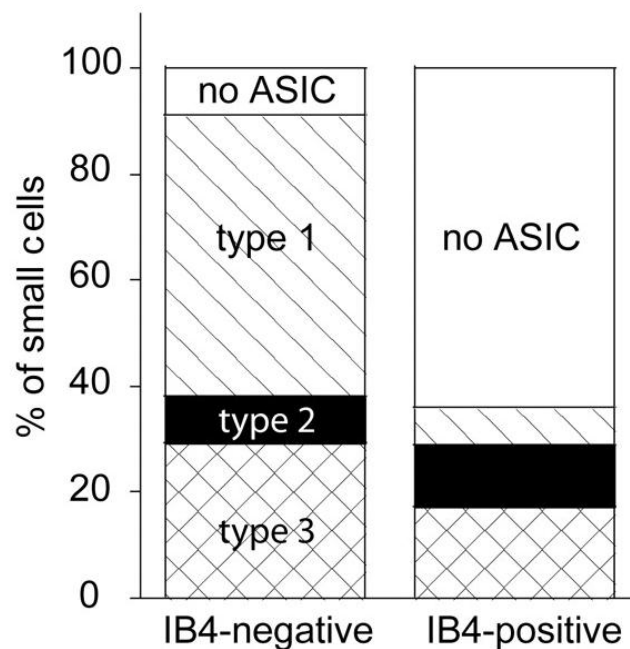


**Figure 6 : Proportion of small IB4-negative (left) and IB4-positive neurones (right) without ASIC current (white), and type 1 (hatched), type 2 (black) and type 3 (cross-hatched)**  
(Poirot *et al.*, 2006)



The correlation with ASIC currents showed first that 91% of IB4-negative, but only 36% of IB4-positive, neurones express an ASIC current. In IB4-positive neurones expressing an ASIC current, the majority of the ASIC currents (70%) are of the fast inactivating types 2 and 3. About half of IB4-negative neurones express type 1 current (Figure 6) (Poirot *et al.*, 2006).

#### 1.4.1 Mechanosensation

The similarity of ASICs to nematode proteins involved in mechanotransduction suggested that they might be involved in mechanosensation. In one study, disrupting the mouse ASIC2 gene markedly reduced the sensitivity of a specific component of mechanosensation: low-threshold rapidly adapting mechanoreceptors. In rodent hairy skin these mechanoreceptors are excited by hair movement. Consistent with this function, ASIC2 was found in the lanceolate nerve endings that lie adjacent to and surround the hair follicle. Thus, it was concluded that ASIC2 is essential for the normal detection of light touch and may be a central component of a mechanosensory complex (Price *et al.*, 2000). Interestingly, another study investigated the effect of an ASIC2 gene knockout in mice on hearing and on cutaneous mechanosensation and visceral mechanonociception. They did not find a role of ASIC2 in these aspects of mechanoperception. They performed the same experiments low-threshold rapidly adapting mechanoreceptors, but on the contrary of the previously cited study, they did not find any difference between ASIC2 null mice and wild type mice (Roza *et al.*, 2004). Using ASIC2 null mice, it has been shown that normal ASIC2 expression is required for normal pressure-induced constriction in the middle cerebral arteries (Gannon *et al.*, 2008a). ASIC2 was found to be expressed in aortic baroreceptor neurons in the nodose ganglia and their terminals. ASIC2 null mice developed hypertension, had exaggerated sympathetic and depressed parasympathetic control of the circulation, and a decreased gain of the baroreflex, all being a sign of an impaired baroreceptor reflex (Lu *et al.*, 2009).

ASIC3 was identified in several different specialized sensory nerve endings of skin, suggesting it might participate in mechanosensation. Disrupting the mouse ASIC3 gene altered sensory transduction. Loss of ASIC3 increased the sensitivity of mechanoreceptors detecting light touch (Price *et al.*, 2001).

Because functional redundancy of ASIC subunits might explain limited phenotypic alterations, it was hypothesized that disrupting multiple ASIC genes would markedly impair cutaneous mechanosensation. In a recent study, it was found the opposite. In behavioral studies, mice with simultaneous disruptions of ASIC1a, -2 and -3 genes (triple-knockouts) showed increased paw withdrawal frequencies when mechanically stimulated with von Frey filaments. In single-fiber nerve recordings of cutaneous afferents, mechanical stimulation generated enhanced activity in A-mechanoreceptors of ASIC triple-knockouts compared to wild-type mice (Kang *et al.*, 2012).

### 1.4.2 Nociception

As mentioned before, ASICs are localized in nociceptors and are activated by protons, one of the first compounds released by damaged cells during inflammation. Acidification also occurs in painful diseases like ischemia, hematoma, fracture, tumor development and incisions after a surgery. ASIC1a, -2 and -3 knockout mice have been used to elucidate the role of ASICs in different models of nociception.

ASIC3 knockout mice have been reported to have a small but significant increase of sensitivity compared to wild-type animals in a model of mechanical hyperalgesia induced with carrageenan. After injection of acidic (pH 4) saline into the gastrocnemius muscle, ASIC3 null mice had significantly less hyperalgesia compared to wild-type mice (Price *et al.*, 2001). In an animal model of long lasting mechanical hypersensitivity produced by repeated acidic saline injection in the muscle ASIC3 null mice did not develop mechanical hyperalgesia, while wild-type mice did. ASIC1 null mice were also tested and did not show any difference compared to wild type mice (Sluka *et al.*, 2003). In a rescue experiment, it has been shown that the injection into muscle, but not skin of ASIC3 null mice of ASIC3-encoding virus, which induce the expression of ASIC3 in primary afferent fibers innervating the site of injection, resulted in the development of mechanical hyperalgesia similar to that observed in wild-type mice. Heat hyperalgesia develops similarly in ASIC3 null and wild-types animals (Sluka *et al.*, 2007). The secondary mechanical hyperalgesia that develops after knee joint inflammation, induced by carrageenan injection in the knee joint cavity, was not induced in ASIC3 null mice. However, the primary mechanical hyperalgesia was still present in ASIC3 null mice (Ikeuchi *et al.*, 2008). Another study showed similar results with carrageenan-induced muscle inflammation. ASIC3 null mice develop primary muscle hyperalgesia but not secondary paw mechanical hyperalgesia after injection of carrageenan in the gastrocnemius muscle. In contrast, ASIC1 null mice did not develop primary muscle hyperalgesia but developed secondary paw hyperalgesia after carrageenan injection. The ASIC inhibitor A-317567, given locally, reverses both the primary and the secondary hyperalgesia induced by carrageenan muscle inflammation (Walder *et al.*, 2010). Recently, it has also been shown that reducing in-vivo ASIC3 using artificial miRNAs inhibits both primary and secondary hyperalgesia after muscle inflammation in wild-type mice (Walder *et al.*, 2011).

In contradiction with studies cited above, a group showed that ASIC3 null mice displayed a reduced latency to the onset of pain response, or more pain-related behaviour, when stimuli of moderate to high intensity were used. This effect seemed independent of the modality of the stimulus and was observed in the acetic-induced writhing test, in the hot plate test, and in tail-pressure test for mechanically induced pain (Chen *et al.*, 2002). Chen later found with his own group that ASIC3 null mice showed normal thermal and mechanical hyperalgesia with acute (4 hours) intraplantar CFA- or

carrageenan-induced inflammation. The hyperalgesic effects in the sub-acute phase (1-2 days) induced by carrageenan were milder in ASIC3 null mice for the mechanical hyperalgesia and normal for the thermal hyperalgesia. It was also confirmed that mechanical hyperalgesia was abolished in ASIC3 null mice in a model of carrageenan-induced inflammation in muscles (Yen *et al.*, 2009). These results of the carrageenan injection model are in contradiction with Price *et al.* (Price *et al.*, 2001) who describe opposite effects. Following hind paw inflammation with formalin injection, ASIC1 and ASIC2, but not ASIC3 null mice showed enhanced pain behaviour compared to wild type littermates, predominantly in the second phase of the test (Staniland & McMahon, 2008).

An interesting approach has been used to circumvent the heteromultimerisation of ASIC subunits which renders difficult the understanding of single ASIC subunit knock-out mice experiments. Transgenic mice expressing a dominant negative form of the ASIC3 subunit have been generated. All native neuronal ASIC-like currents were inactivated in these mice. Both wild-type and transgenic mice were equally sensitive to thermal pain and to thermal hypersensitivity after inflammation. Surprisingly, transgenic mice were more sensitive to mechanical pain, inflammatory pain after formalin injection, intraperitoneal injections of acetic acid, mechanical hypersensitivity after zymosan inflammation, and mechanical hypersensitivity after intramuscular injection of hypotonic saline (Mogil *et al.*, 2005).

Systemic administration of amiloride produces a robust, dose-dependent blockade of late phase nociceptive behaviour on the mouse formalin test in female but not male mice (Chanda & Mogil, 2006). This discrepancy between male and female has also been shown in muscle fatigue, which is associated with a number of clinical diseases, including chronic pain conditions. Enhanced muscle fatigue occurred in male but no female ASIC3 null mice (Burnes *et al.*, 2008).

Using rats, it has been shown that moderately acidic pH increased the excitability of nociceptors and that subcutaneous injections of moderately acid solutions in one of the hind paws produced pain. Both effects were suppressed by the toxin APETx2, a blocker of ASIC3. Both APETx2 and the *in vivo* knockdown of ASIC3 with a specific siRNA had potent analgesic effects against primary inflammation-induced hyperalgesia (Deval *et al.*, 2008). From studies with rats, PcTx1 has been shown to possess opioid-type analgesic properties via ASIC1a channels. This means that central inhibition of ASIC1a, acting upstream of the opiate system, might be exploited to treat any type of pain (Mazzuca *et al.*, 2007). ASIC1a was found to be the predominant ASICs in rat spinal dorsal horn neurons. Downregulation of ASIC1a by local spinal infusion with specific inhibitors or antisense oligonucleotides attenuated complete Freund's adjuvant-induced thermal and mechanical hypersensitivity. An increased ASIC activity in spinal dorsal horn neurons was shown to promote pain by central sensitization (Duan *et al.*, 2007). In a rat model of postoperative pain involving plantar

incision, ASIC3 mRNA and protein levels in lumbar DRG neurons are increased 24 h after surgery. Pharmacological inhibition of ASIC3 with APETx2 or in vivo knockdown of ASIC3 by siRNA led to a significant reduction of postoperative spontaneous, thermal, and postural pain behaviours, showing a significant role for peripheral ASIC3-containing channels in postoperative pain (Deval *et al.*, 2011).

Finally, direct injection of acidic solutions ( $\text{pH} \geq 6.0$ ) into human skin caused localized pain, which was blocked by amiloride. Under more severe acidification ( $\text{pH} 5.0$ ) amiloride was less effective in reducing acid-evoked pain (Ugawa *et al.*, 2002). In another study, iontophoresis of protons was used to investigate acid-induced pain in human volunteers. It was found that transdermal iontophoresis of protons consistently caused moderate pain that was dose-dependent. Subcutaneous injection of amiloride significantly inhibited the pain induced by iontophoresis of acid, suggesting an involvement of ASICs (Jones *et al.*, 2004).

### 1.4.3 Taste and hearing

In situ hybridisation and RT-PCR experiments revealed that ASIC2a and ASIC2b transcripts were localized in taste bud cells (Shimada *et al.*, 2006). However,  $\text{Ca}^{2+}$  imaging experiments on taste bud cells of ASIC2 knock-out mice showed that the cells had normal physiological responses to acid taste stimuli (Richter *et al.*, 2004). In human, it has been shown that ASIC1a, -1b, -2a, -2b and -3 were expressed in lingual fungiform papillae which contain taste cells. These transcripts were undetectable in two patients with an acquired sour ageusia, suggesting a role for ASICs in human sour perception (Huque *et al.*, 2009).

ASIC2 is present in the spiral ganglion neurons in the mouse adult cochlea. ASIC2 null mice showed no significant hearing deficit but were considerably more resistant to noise-induced temporary, but not permanent, threshold shifts. It suggests that ASIC2 is not directly involved in the mechanotransduction of the cochlea but could contribute to suprathreshold functions of the cochlea (Peng *et al.*, 2004). ASIC3 has been also found in the cochlea of mice by quantitative real-time polymerase chain reaction. In-situ hybridisation and immunofluorescence showed that ASIC3 was expressed in the cells and in the neural fibre region of the spiral ganglion. ASIC3 protein was also detected in cells of the organ of Corti. An ASIC3 knockout mouse model was tested for a hearing loss phenotype and was found to have normal hearing at 2 months of age but appeared to develop hearing loss early in life (Hildebrand *et al.*, 2004). It has also been shown that female ASIC3 null mice showed elevated hearing thresholds for low to ultrasonic frequency on auditory brain stem response. The response to pups' wriggling calls and ultrasonic vocalization, as well as the retrieval of pups was deficient in these mice (Wu *et al.*, 2009).

#### 1.4.4 Molecular basis of signal detection and propagation

The primary afferent nerve fiber detects thermal, mechanical or chemical environmental stimuli and transduces the information into electrical current. In the following, I describe an important class of channels which detect stimuli in sensory neurons and two classes of channels involved in the transmission of the electrical signal in the same neurons.

##### 1.4.4.1 ThermoTRP channels (TRPV1, TRPV2, TRPA1 and TRPM8)

Transient receptor potential (TRP) channels were first identified in a phototransduction mutant in *Drosophila* that showed a transient instead of a sustained response to light (Montell & Rubin, 1989). In this chapter, I will only focus on four members of this family which play an important role in stimulus detection in sensory neurons.

Four identical TRPV1 subunits, each containing six transmembrane segments with a pore loop between transmembrane segments 5 and 6, assemble to form the channel (Lee & Caterina, 2005). In heterologous systems this channel is weakly  $\text{Ca}^{2+}$ -selective, and when stimulated by capsaicin, resiniferatoxin, acid, endocannabinoids, or heat ( $>43^{\circ}\text{C}$ ), it produces outwardly rectifying cation currents (Caterina *et al.*, 1997; Tominaga *et al.*, 1998; Caterina *et al.*, 1999). TRPV1 is expressed primarily in small- to medium-diameter peptidergic and nonpeptidergic sensory neurons (from A $\delta$  and C fibers) within the dorsal root, trigeminal, and nodose sensory ganglia (Caterina *et al.*, 1997; Tominaga *et al.*, 1998). TRPV1-knockout mice have been generated and electrophysiological responses to capsaicin, acid, and heat ( $>43^{\circ}\text{C}$ ) were reduced or absent in these mutants. Inflammation-induced heat hyperalgesia was virtually abolished in TRPV1 knockout animals (Caterina *et al.*, 2000; Davis *et al.*, 2000).

TRPV2 has been found to mediate high-threshold heat sensations ( $>52^{\circ}\text{C}$ ) *in vitro*. Since it is expressed in medium- to large-diameter sensory neurons, it is thought to be associated with A $\delta$  fibers (Caterina *et al.*, 1999). Evidence that the TRPV2 channels mediate sensation to heat *in vivo* is lacking.

TRPM8 channels are activated by menthol, icilin and by reductions in temperature from cool ( $<28^{\circ}\text{C}$ ) to noxious cold ( $<15^{\circ}\text{C}$ ) (McKemy *et al.*, 2002; Peier *et al.*, 2002; Voets *et al.*, 2004). TRPM8 expression is restricted to approximately 5%–10% of adult DRG neurons. TRPM8 is expressed in small-sized neurons (from A $\delta$  and C fibers). TRPM8-positive neurons appear to belong to a subset of nociceptive or thermoceptive neurons that express tyrosine kinase receptor A (trkA), an NGF receptor, during development. TRPM8 is expressed in a small subpopulation of neurons distinct from the well-characterized heat- and pain-sensing neurons expressing the markers TRPV1, CGRP, or IB4 (Peier *et al.*, 2002). TRPM8 knock-out mice showed a reduced sensitivity to menthol in one study (Colburn *et al.*, 2007), and were in a second study completely insensitive to menthol and icilin (Bautista *et al.*,

2007). Cold analgesia after formalin injections was also evaluated on TRPM8 ko mice. On a 17°C cold plate, formalin-treated wild type mice displayed reduced responses compared to mice at room temperature during the acute and inflammatory phases of the test, demonstrating that cold is analgesic to formalin administration. This behaviour is completely ablated in TRPM8-deficient mice, suggesting that TRPM8 activation can elicit an analgesic response (Dhaka *et al.*, 2007). TRPM8 is important for thermal sensitivity and contributes to responses in the cold range; however detection of noxious cold appears to involve additional mechanisms.

TRPA1 is activated by cold temperature (<18°C), icilin, cannabinoids, mustard oil, as well as mechanical stimuli (hair cells in inner ear) (Corey *et al.*, 2004; Wang & Woolf, 2005). Submicromolar to low micromolar concentrations of menthol cause TRPA1 activation, whereas higher concentrations lead to a reversible channel block (Karashima *et al.*, 2007). TRPA1 is involved in nicotine-induced irritation. Micromolar concentrations of nicotine activated heterologously expressed mouse and human TRPA1. TRPA1 mediated the mouse airway constriction reflex to nasal instillation of nicotine (Talavera *et al.*, 2009). TRPA1 is expressed in a small population of sensory neurons expressing TRPV1, CGRP, SP, but not TRPM8 (Jordt *et al.*, 2004; Wang & Woolf, 2005). TRPA1 is not expressed with TRPM8, indicating that these channels do not coordinate at the level of individual sensory cells to integrate thermal information. Since TRPA1 is not expressed in heavily myelinated neurons, it has been suggested that it is localized to non-myelinated C- or lightly myelinated A $\delta$ -fibers. Experiments in heterologous cells have shown that TRPA1 is stimulated by formalin (McNamara *et al.*, 2007). Neurons from wild type trigeminal and dorsal root ganglia were activated also by formalin and the responses were blocked by a TRPA1 inhibitor (HC-030031), whereas neurons from TRPA1 knock-out mice were unresponsive to formalin. TRPA1 appears to mediate nociceptive responses to formalin (Wetsel, 2011). A single point mutation in TRPA1 (N855S) has been linked with an autosomal-dominant familial episodic pain syndrome characterized by episodes of debilitating upper body pain, triggered by fasting and physical stress. The mutant channel showed altered biophysical properties, with a 5-fold increase in inward current on activation at normal resting potentials. Patients carrying this gain-of-function mutation in TRPA1 displayed an enhanced secondary hyperalgesia to punctate stimuli on treatment with mustard oil compared to non-affected siblings (Kremeyer *et al.*, 2010). Cold plate and tail-flick experiments on TRPA1 null mice revealed a TRPA1-dependent, cold-induced nociceptive behaviour, showing that TRPA1 acts as a major sensor for noxious cold (Karashima *et al.*, 2009).

#### 1.4.4.2 *Na<sub>v</sub> channels*

Nine pore-forming sodium channel  $\alpha$ -subunits (Na<sub>v</sub>1.1–Na<sub>v</sub>1.9) have been identified in mammals, and their expression is spatially and temporally regulated (Catterall *et al.*, 2005a). These channels are large polypeptides that fold into four domains (DI–DIV), each domain including six transmembrane

segments, linked by three loops (Catterall, 2000). Recently, a Na<sub>v</sub> channel from *Arcobacter butzleri* has been crystallised. One of the new findings was that the arginine gating charges make multiple hydrophilic interactions within the voltage sensor, including unexpected hydrogen bonds to the protein backbone (Payandeh *et al.*, 2011).

Different channels gate with different kinetics and voltage-dependent properties, with six channels sensitive to block by nanomolar concentrations of tetrodotoxin (TTX), which are called TTX-sensitive (TTX-S), and three channels resistant to this blocker and which are called TTX-resistant (TTX-R) (Catterall *et al.*, 2005a). DRG neurons can express up to five types of sodium channels, more than in any other neuronal cell type (Black *et al.*, 1996; Dib-Hajj *et al.*, 1998). Adult DRG neurons can express the TTX-S channels Na<sub>v</sub>1.1, Na<sub>v</sub>1.6, and Na<sub>v</sub>1.7, and the TTX-R channels Na<sub>v</sub>1.8 and Na<sub>v</sub>1.9 (as well as Na<sub>v</sub>1.5 at low levels). Na<sub>v</sub>1.3 channels are present in embryonic, but not in adult DRG neurons and are re-expressed under pathological condition (Waxman *et al.*, 1994). Na<sub>v</sub>1.1 and Na<sub>v</sub>1.6 expression is common to central nervous system (CNS) and peripheral nervous system (PNS) neurons, whereas Na<sub>v</sub>1.7, Na<sub>v</sub>1.8, and Na<sub>v</sub>1.9 are specific to PNS neurons. Na<sub>v</sub>1.7 is expressed in sensory and sympathetic (Toledo-Aral *et al.*, 1997), and myenteric (Sage *et al.*, 2007) neurons, whereas Na<sub>v</sub>1.9 is expressed in sensory and myenteric neurons (Dib-Hajj *et al.*, 1998; Rugiero *et al.*, 2003), and Na<sub>v</sub>1.8 only in sensory neurons (Akopian *et al.*, 1996; Rugiero *et al.*, 2003). Na<sub>v</sub>1.7, Na<sub>v</sub>1.8, and Na<sub>v</sub>1.9 may have evolved in a specialized sensory role in mammals, including pain (Dib-Hajj *et al.*, 2010).

Inherited erythromelalgia (IEM) is characterized by intense episodic burning pain associated with redness and warmth of the affected extremities. Several groups identified point mutations in Na<sub>v</sub>1.7 of patients affected with IEM (Yang *et al.*, 2004; Dib-Hajj *et al.*, 2005). IEM mutations of Na<sub>v</sub>1.7 have been shown to cause a hyperpolarizing shift in activation and slow deactivation, decreasing the threshold for action potential generation in sensory neurons and increasing neuronal excitability (Cummins *et al.*, 2004; Fischer & Waxman, 2010).

Some members of three consanguineous families from northern Pakistan have a complete inability to sense pain. These individuals carry homozygous nonsense mutations on the Na<sub>v</sub>1.7 gene causing a loss of function of the channel, suggesting that Na<sub>v</sub>1.7 is an essential and non-redundant requirement for nociception in humans (Cox *et al.*, 2006).

Finally, from a more pharmacological point of view, residues in the inner cavity of the channel pore involving the S6 segment of domains I, III, and IV form the binding site for local anesthetic drugs such as lidocaine, meaning that lidocaine can be used as a sodium channel blocker (Liu & Wood, 2011).



#### 1.4.4.3 Voltage-gated calcium channels ( $Ca_v$ )

Certain types of voltage-gated calcium channels ( $Ca_v$ ) can trigger the release of neuropeptide-containing vesicles via an entry of calcium in DRG sensory neurons and dorsal horn neurons.  $Ca_v$  can be classified based on their voltage activation characteristics as high- or low-voltage activated channels. The  $Ca_v$ s can also be classified based on their structural similarities of the channel-forming  $\alpha_1$ -subunit ( $Ca_v1$ ,  $Ca_v2$ ,  $Ca_v3$ ) or their sensitivity to blockade by pharmacological agents (L, N, P/Q, R and T-type). The high- $Ca_v$ s include L-type ( $Ca_v1.1$ ,  $Ca_v1.2$ ,  $Ca_v1.3$ ,  $Ca_v1.4$ ), P/Q-type ( $Ca_v2.1$ ), N-type ( $Ca_v2.2$ ) and R-type ( $Ca_v2.3$ ) channels, while the low- $Ca_v$ s include T-type ( $Ca_v3.1$ ,  $Ca_v3.2$ ,  $Ca_v3.3$ ) channels. The high- $Ca_v$ s typically form heteromultimers that consist of the channel-forming  $\alpha_1$ -subunit along with auxiliary  $\beta$ -,  $\alpha_2\delta$  and  $\gamma$ -subunits. (Catterall *et al.*, 2005b). The  $\alpha_1$ -subunits have the same topology as the main  $Na_v$  subunits (Yu *et al.*, 2005).

L-type channels are widely distributed in the central nervous system. Four different isoforms exist for L-type channels ( $Ca_v1.1$ – $Ca_v1.4$ ), with  $Ca_v1.2$  and  $Ca_v1.3$  being strongly expressed in neurons (Ertel *et al.*, 2000). The 1,4-dihydropyridines are able to activate or block specifically  $Ca_v1$  (L-type channels). Nifedipine is a Dihydropyridine which inhibits L-type channels (Triggle, 2003).

N-type channels are expressed at high density on the presynaptic terminals of primary afferent neurons that terminate in the dorsal horn of the spinal cord. The modulation of both central and peripheral T-type channels results in significant alteration of the pain threshold in some animal pain models (Todorovic & Jevtovic-Todorovic, 2006). The highly N-type selective  $\omega$ -conotoxins MVIIA and CVID reduced pain behaviours in rats (Smith *et al.*, 2002). Ziconotide, a synthetic form of  $\omega$ -conotoxin MVIIA, is used for intrathecal treatment of severe chronic pain in patients (Schmidtko *et al.*, 2010).

$Ca_v2.1$  P/Q-type channels are expressed at the presynaptic terminals in the spinal dorsal horn (Catterall & Few, 2008). The involvement of P/Q-type channels in pain processing is not well understood. P/Q-type channels show little colocalization with substance P, and treatment with  $\omega$ -agatoxin IVA, a specific inhibitor of P/Q-type channels, has no effect on the release of either substance P or CGRP from peptidergic sensory neurons (Evans *et al.*, 1996; Westenbroek *et al.*, 1998).  $\omega$ -conotoxin MVIIC is also a specific inhibitor for the P/Q-type channels (Nielsen *et al.*, 2000).

In sensory pathways, T-type channels are located on primary afferent terminals and dorsal root ganglia, with  $Ca_v3.2$  being the most abundant isoform in the DRG (Bourinet *et al.*, 2005). The T-type channel subtype has one of the most prominent roles in nociception (Park & Luo, 2010). Mibefradil is a compound that blocks both T-type and L-type calcium channels. It blocks T-type calcium channel currents at a lower concentration than that needed to inhibit L-type channels (Mocanu *et al.*, 1999).

## 1.4.5 Neuropeptides and their peripheral targets

### 1.4.5.1 Calcitonin gene-related peptide (CGRP)

CGRP is a 37–amino acid peptide that is a member of the calcitonin family, which also includes calcitonin, amylin, and adrenomedullin. CGRP exists in two distinct isoforms: CGRP $\alpha$  (CGRP1), which is the product of alternative splicing of the calcitonin gene in neurons, and CGRP $\beta$  (CGRP2), which is encoded by a separate gene (Poyner, 1992). These two CGRP peptides differ from each other by three amino acids and are not distinguishable in their biological activities. CGRP is widely expressed in the central and peripheral nervous systems. CGRP is expressed in a subset of small neurons in the DRG, trigeminal, and vagal ganglia. These CGRP-containing neurons are polymodal nociceptors that are activated by chemical, thermal and high-threshold mechanical stimuli (Tsukagoshi *et al.*, 2006). These peptidergic neurons have small myelinated (A $\delta$ ) and unmyelinated (C) axons that innervate essentially all peripheral tissues and send primary afferent input to nociceptive and viscerosensitive neurons in the dorsal horn (Gu & Yu, 2007).

CGRP and substance P are released from large dense-core vesicles. In rat trigeminal ganglia CGRP was found to be co-expressed with the three exocytotic SNAREs (SNAP25, syntaxin 1 and the synaptobrevin isoforms) and synaptotagmin. Ca<sup>2+</sup>-dependent CGRP release was evoked with K<sup>+</sup>-depolarisation and, to lower levels, by capsaicin or bradykinin from neurons that contain TRPV1, respectively bradykinin receptor 2 (Meng *et al.*, 2007).

### 1.4.5.2 The CGRP Receptor

The functional CGRP receptor consists of the assembly of a 7-transmembrane domain G protein–coupled receptor known as calcitonin receptor-like receptor (CLR) and an associated single transmembrane domain protein called receptor activity-modifying protein 1 (RAMP1) (Walker *et al.*, 2010) (Figure 7) (Benarroch, 2011). RAMP1 is required to transport CLR to the plasma membrane, to present the receptor at the cell surface as a mature glycoprotein, and is essential for CGRP receptor signalling (McLatchie *et al.*, 1998). The primary signal transduction pathway for the CGRP receptor is mediated by G $\alpha$ s, which activates adenylyl cyclase, leading to the production of cyclic adenosine monophosphate (cAMP) and activation of protein kinase A (PKA). The CGRP-triggered cAMP-PKA pathway regulates the activity of various downstream signaling components, including K<sup>+</sup> channels, L-type Ca<sup>2+</sup> channels, and cAMP response element binding protein. These effector mechanisms mediate numerous actions of CGRP, including vasodilation, neurotransmitter release, increased neuronal excitability, and synaptic plasticity (Walker *et al.*, 2010). In general, the distribution of CGRP receptors overlaps with that of CGRP in peripheral tissues (particularly blood vessels), dorsal horn, trigeminal nucleus, parabrachial nuclear complex, thalamus, amygdala, striatum, and cerebellum (Tschopp *et al.*, 1985; Henke *et al.*, 1987).

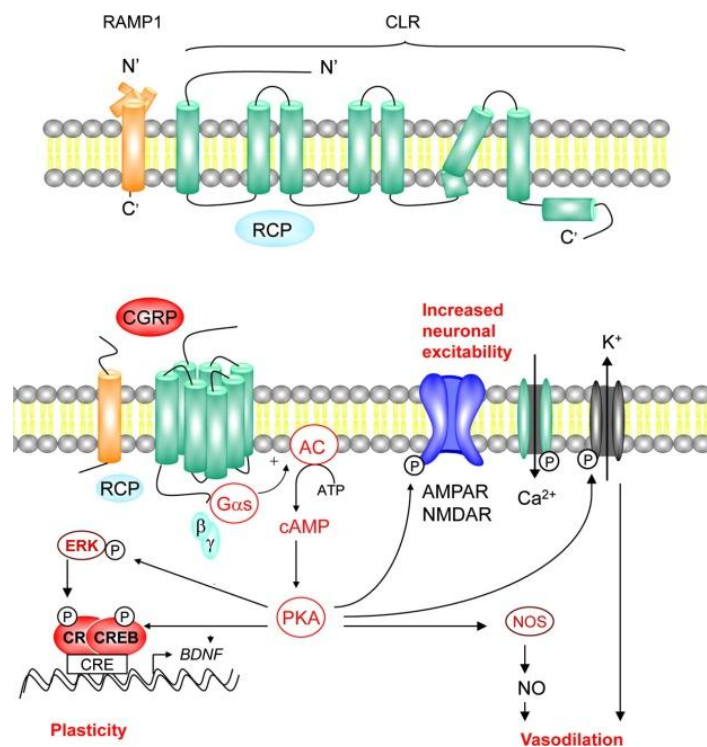


**Figure 7 : Calcitonin gene-related peptide (CGRP) receptor and transduction pathways.**

The upper panel shows the topology of RAMP1 and CLR which form the CGRP receptor. The lower panel shows the transduction pathway of the CGRP receptor at a neuronal plasma membrane (Benarroch, 2011).

### 1.4.5.3 Substance P (SP)

SP is a neuropeptide that has, among others, a crucial role in nociceptive signal transmission. The history of this neuropeptide began in 1931, when Von Euler and Gaddum isolated a substance from the brain and gut of horses, which caused hypotension (V. Euler & Gaddum, 1931). In the spinal cord, SP is found in abundance in terminals of primary afferent nerves in the dorsal horn, and in the dorsal roots of the spinal nerves. In the dorsal horn, high concentrations of substance P are present in the synaptic vesicles of primary afferent nerve fibres (Cuello *et al.*, 1977). Due to the size and hydrophilic nature of SP, it crosses the biological membranes poorly, and its release requires the process of exocytosis (Persson *et al.*, 1995). SP and CGRP are co-expressed in the peptidergic neurons.

The release of SP has already been described in chapter 1.4.5.1.

### 1.4.5.4 NK1 Receptor

The tachykinin peptide family certainly represents one of the largest peptide families described in the animal organism. SP may be considered as a prototype of the tachykinins. The tachykinins differ in their receptor affinity. Substance P binds preferentially to the neurokinin 1 (NK1) receptor. NK1 receptors are found both in central nervous tissue (mainly in the striatum and in the spinal cord) and in peripheral organs. The NK1 receptor is the major mediator of plasma protein extravasation produced

by both exogenous and endogenous tachykinins (Abelli *et al.*, 1991; Xu *et al.*, 1992). SP induces clathrin-dependent internalization of the NK1 receptor. The complex formed by SP and its receptor dissociates in acidified endosomes. SP is degraded and the NK1 receptor is recycled to the cell surface (Grady *et al.*, 1995). After binding to its NK1 receptor, substance P modifies  $Ca^{2+}$  and  $K^+$  currents at the cellular level (Snijdelaar *et al.*, 2000).

#### **1.4.5.5 Role of CGRP and SP in the CNS**

CGRP participates in mechanisms of central sensitization that contribute to the development and maintenance of chronic pain. In the spinal cord, CGRP increases responses of dorsal horn neurons by increasing synaptic transmission and neuronal excitability (Seybold, 2009). In the brain, periaqueductal grey (PAG) is an important relay in the descending pathway of analgesia from brain to dorsal horn of the spinal cord. CGRP, as well as its receptor, is present in the nerve fibers in PAG. The CGRP receptor is involved in the CGRP-induced antinociception in PAG. Other regions of the brain, which are known to play important roles in pain modulation, like the nucleus raphe magnus, the nucleus accumbens and the central nucleus of amygdala also demonstrate an antinociceptive effect of CGRP. CGRP and its receptor are also involved in learning, memory, opioid tolerance and addiction (Yu *et al.*, 2009). As CGRP is released from activated trigeminal sensory nerves, dilates intracranial and extracranial blood vessels and centrally modulates vascular nociception, CGRP plays an important role in the pathophysiology of migraine (Villalon & Olesen, 2009).

SP and the NK1 receptor have been found within brain areas known to be involved in the regulation of stress and anxiety responses. Emotional stressors increase SP efflux in specific limbic structures such as amygdala. Depending on the brain area, an increase in intracerebral SP concentration produces mainly anxiogenic-like responses in various behavioural tasks (Ebner & Singewald, 2006).

#### **1.4.5.6 Role of CGRP and SP in the PNS**

Neurogenic inflammation increases vasodilatation, capillary permeability, and activation of inflammatory cells. It results from the antidromic (toward the periphery) release of CGRP, substance P, and neurokinin A (NKA) from C-afferent terminals of primary sensory neurons distributed to almost all the tissues and organs, particularly around the blood vessels. Pharmacological evidence shows that CGRP is the primary neuropeptide responsible for neurogenic vasodilation (Benemei *et al.*, 2009). CGRP causes endothelium and nitric oxide (NO) independent vasodilation through a direct action on the smooth muscle cells mediated both by cAMP and activation of ATP-dependent  $K^+$  channels. PKA can also directly activate endothelial production of NO, which contributes to CGRP-triggered vasodilation (Brain & Grant, 2004; Benarroch, 2011). The vascular reaction most clearly related to SP release via stimulation of NK1 receptors is an increase in postcapillary venular permeability leading to extravasation of plasma proteins. It has been observed that exogenous SP

increases vascular permeability in the same regions of the body where plasma protein extravasation is elicited by capsaicin (Lembeck & Holzer, 1979).

## **1.5 Aims of the Thesis**

During my thesis, I have mainly worked on the two following projects:

### **1.5.1 Role of ASICs in neuropeptide secretion**

We hypothesized that some neurons expressing ASIC current types 1 and 3 may mediate neuropeptide secretion in DRG neurons. This hypothesis was formulated from the discovery that most of the neurons expressing ASIC current type 1 were also IB4 negative, in other words, were expressing neuropeptides (Poirot *et al.*, 2006). The aim of the study was to determine whether the activation by extracellular acidification of ASICs in DRG neurons induces the release of neuropeptides CGRP and SP, and to determine the implication of other relevant ion channels in this process. To test this hypothesis, we have measured the co-expression of ASICs with CGRP and SP with immunocytochemistry and in-situ hybridization. We have also measured with calcium imaging the Ca<sup>2+</sup> entry in DRG neurons due to ASIC activation. We have finally measured the CGRP secretion from DRG neurons after an extracellular acidification.

### **1.5.2 Role of ASICs in neuropathic pain**

We hypothesized that ASICs could have a role in neuropathic pain. This hypothesis was formulated from the observation that in a model of neuropathic pain performed on rat, the relative expressions of the different ASICs subunits in DRG neurons were modified by the nerve injury (Poirot *et al.*, 2006). To test this hypothesis, we decided to perform the same model on three different mouse strains deficient of ASIC1a, -2 or -3. The mechanical hyperalgesia induced by the nerve injury in the left hindpaw of the mice was assessed with Von Frey filaments.

## 2. Materials and methods

### 2.1 DRG neuron isolation and culture

Rats were killed using CO<sub>2</sub>. Lumbar DRGs (L1–L8) were removed bilaterally and collected in PBS (137 mM NaCl, 2.7 mM KCl, 10 mM Na<sub>2</sub>HPO<sub>4</sub>, 2 mM KH<sub>2</sub>PO<sub>4</sub>, pH 7.4) containing 50 U ml<sup>-1</sup> penicillin and 50 µg ml<sup>-1</sup> streptomycin (Invitrogen, Basel, Switzerland). DRGs were then incubated for 120 min at 37°C in 2 ml Neurobasal A medium (Invitrogen) completed with 10% heat-inactivated fetal calf serum (FCS) (Invitrogen), and 22 mM glucose (named here NeuroA medium) to which collagenase type P (Roche, Basel, Switzerland) was added to a final concentration of 0.125%. Osmolarity was adjusted to 320 mosmol l<sup>-1</sup> with sucrose. Then, DRGs were washed two times with PBS, treated with trypsin 0.25% (Invitrogen) for 30 min at 37°C, washed with NeuroA and taken up in 2 ml NeuroA, complemented with 50 µg ml<sup>-1</sup> DNase and soybean trypsin inhibitor (Sigma, Buchs, Switzerland). The ganglia were triturated 4–6 times with a fire-polished Pasteur pipette or a blue tip to obtain the cell suspension. DRG neurones were plated either on glass coverslips (12 mm diameter for labelling, 22 mm x 40 mm for the calcium imaging), or in 24-wells plate (for the secretion assay), previously coated with a high molecular weight (>300'000 Da) poly-l-lysine (Sigma) solution (0.2 mg ml<sup>-1</sup>). The neurones were maintained in NeuroA at 37°C, 5% CO<sub>2</sub> and 90% humidity for 3 h. Next, neurones were maintained at 4°C in Leibovitz's L15 medium supplemented with 10% FCS and 5 mM HEPES. Osmolarity and pH were adjusted, respectively, to 320 mosmol l<sup>-1</sup> using sucrose and pH 7.4 using NaOH.

### 2.2 Immunocytochemistry

Cells on coverslips were washed three times for five minutes with PBS. Then they were fixed with freshly prepared 4% paraformaldehyde in PBS for 20 minutes. Cells were then washed three times in PBS containing 0.5% BSA (protease free, Acros Organics). The cells were permeabilized with 0.4% Triton X-100 (Sigma) in PBS for 10 minutes. Subsequently, cells were incubated with the first antibody or antibodies (if they are raised in different species) in PBS containing 2% BSA, 0.1% Triton X-100, for two hours at RT. Cells were washed three times in PBS containing 0.5% BSA. The cells were then incubated with secondary antibodies, directed against the primary antibody used before, in PBS with 2% BSA, 0.1% Triton X-100, one hour at RT. Cells were washed three times in PBS with 0.5% BSA. The coverslips were finally mounted on a glass microscope slide with a drop of Vectashield medium (Reactolab, Servion, Switzerland).

When two primary antibodies were used that had been raised in the same species (here rabbit), the protocol was modified in the following way. During the first antibody incubation step, only one rabbit antibody was used. A Fab fragment secondary antibody against the first primary antibody was then

used. A second step of primary and secondary antibody incubation was then performed, using the second primary and secondary antibodies, as shown in Figure 8.

Cross reactions between the second secondary antibody and the first primary antibody were blocked with the Fab fragment secondary antibody. The role of this fragment was to block the epitopes of the primary antibody to avoid any interference with the secondary antibody of the second step. The monovalent nature of Fab fragments furthermore avoided an interaction with the primary antibody of the second step (Negoescu *et al.*, 1994).

In order to block all the epitopes of the first antibody of the first step, a saturating concentration of Fab fragments was reached by adding unconjugated Fab fragments (twice the concentration of the conjugated fragment) to the Fab fragments conjugated with a fluorescence probe after the incubation with the conjugated Fab fragments (Dou *et al.*, 2004).

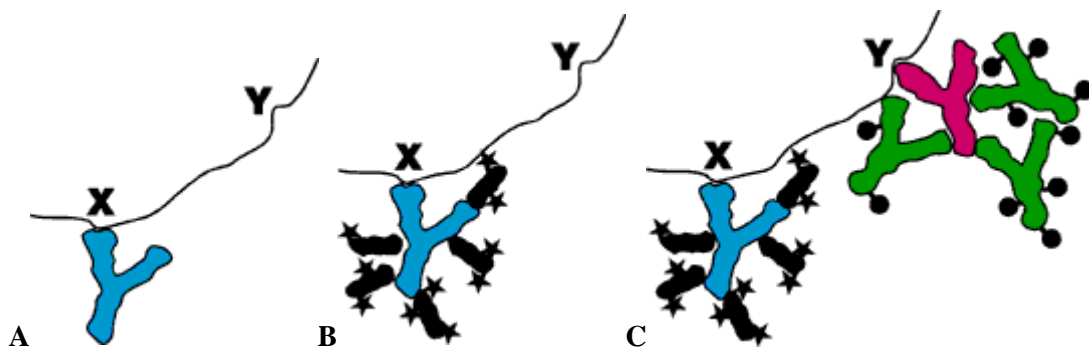


**Figure 8: Use of Fab fragments for labelling and blocking**

A: Incubation with the first primary antibody, in this example rabbit anti-antigen X (blue Y-shape). B: Incubation with excess Fab fragments antibody against the host species of the primary antibody, in this example Cy3(\*)-Fab fragment goat anti-rabbit IgG (H+L)(black Y-shape). C: Incubation with the second primary antibody, rabbit anti-antigen Y (pink Y-shape), followed by conjugated divalent secondary antibody, in this example FITC(●)-goat anti-rabbit IgG (H+L)(green Y-shape). To simplify the scheme, only the conjugated Fab fragments were depicted, avoiding the unconjugated Fab fragments. Adapted from: <http://www.jireurope.com/technical/examplea.asp>

### 2.2.1 Test of ASIC2 antibody

The ASIC2 antibody was a generous gift from Heather A. Drummond (Gannon *et al.*, 2008b). It was tested here for its specificity on mouse DRG neurons. Figure 9 shows that the antibody is specific, as it stained the DRG from wild type mice, but not from ASIC2 knock-out mice.



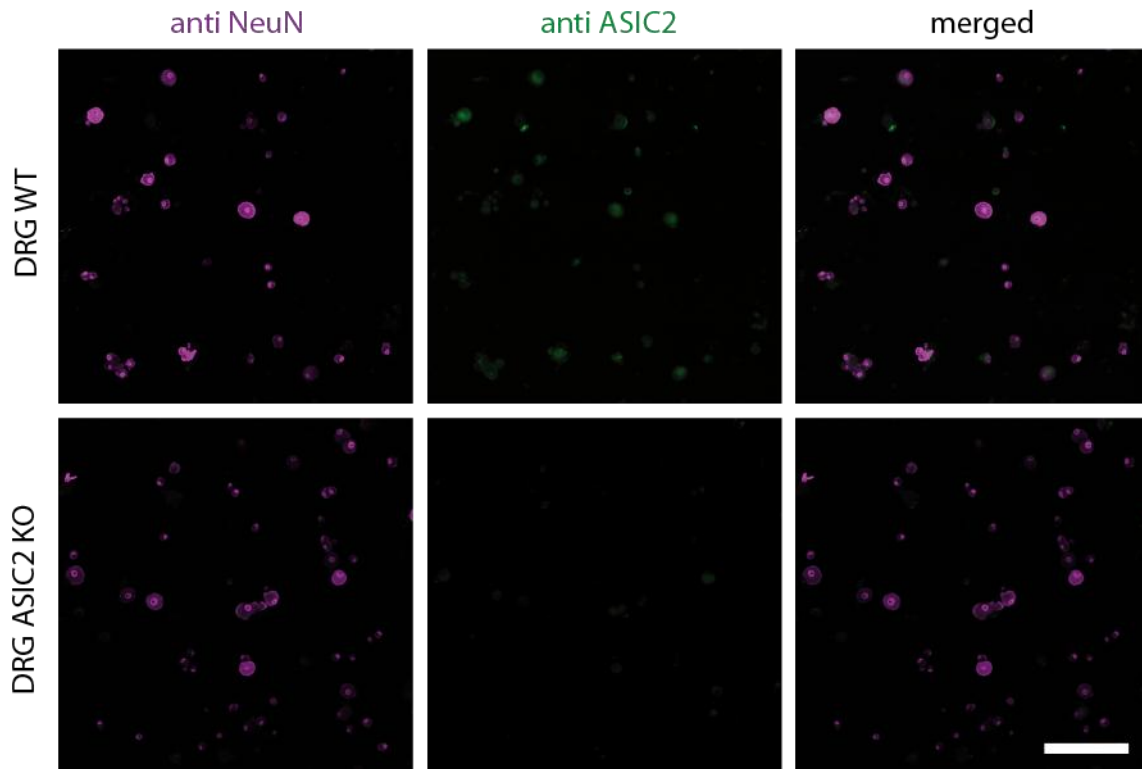


**Figure 9: Test of ASIC2 antibody on ASIC2 knock-out DRG**  
The antibody dilution was 1/200. Scale bar: 200  $\mu$ m

## 2.3 In-situ hybridization

For the in-situ hybridization the general protocol described by Zaal Kokaia was followed (Kokaia, 2001).

### 2.3.1 Preparation of cells

The cells were rinsed twice in PBS, two min each, at RT. Then the cells were fixed in 4% paraformaldehyde solution for 10 min at RT. The cells were again rinsed twice in PBS, for two min each, at RT. They were permeabilized in PBS, 0.1% Triton X-100, 5% vanadyl ribonucleoside complex (VRC; New England Biolabs, Ipswich, USA) for five minutes at RT (Bobrow & Moen, 2001).

### 2.3.2 Labelling of oligonucleotides

The oligonucleotides were labelled with digoxigenin-ddUTP with the DIG Oligonucleotide 3'-End Labelling Kit (Roche), following the manufacturer's protocol. Briefly, 100 pmol oligonucleotide were added to a reaction vial, along with sterile double distilled water to make a final volume of 10  $\mu$ l. Then 4  $\mu$ l reaction buffer 5x, 4  $\mu$ l  $\text{CoCl}_2$  solution, 1  $\mu$ l DIG-ddUTP solution and 1  $\mu$ l terminal transferase were added to the vial. The content of the vial was then mixed, centrifuged briefly and incubated at 37  $^\circ\text{C}$  for 15 min, then put on ice. The reaction was stopped by adding 2  $\mu$ l 0.2 M EDTA (pH 8.0). The final concentration of the oligonucleotides was 2.5 pmol/ $\mu$ l. The labelling efficiency was then estimated via a direct detection method. A series of dilutions of DIG-labeled oligonucleotide was

bound to a small strip of positively charged membrane (Amersham Hybond-ECL nitrocellulose membrane, GE Healthcare, Glattbrugg, Switzerland). A part of the membrane was preloaded with known concentrations of provided DIG-labelled control oligonucleotide. The oligonucleotides were cross-linked on the membrane with UV light. The labelled nucleotides on the membrane were detected with an anti-DIG-alkaline phosphatase (AP)-labelled antibody (1:500, Roche) and an AP substrate (BCIP/NBT Liquid Substrate System, Sigma). The intensity of the dots was compared between the labelled nucleotides and the controls to evaluate the efficiency of the labelling. The dots were still visible at 1-3 fmol/ $\mu$ l dilutions. As there were no significant differences between the different labelled oligonucleotides and the labelled control oligonucleotide, all the nucleotides were considered as labelled.

### **2.3.3 Hybridization and detection of the oligonucleotides**

2  $\mu$ l (5 pmol) of DIG-labeled probe was added to 1 ml of hybridization buffer (see section 2.3.4) to form the hybridization mix. Hybridization mix was applied on the cells on coated coverslips (high molecular weight poly-l-lysine (Sigma)). The cells were incubated in a humidified chamber sealed with tape and placed in a 37°C incubator for 16 to 18 hours. The coverslips were then rinsed quickly in dishes with 1x SSC (see section 2.3.4), at 48°C to remove the hybridization mix. The dishes were filled with 1X SSC, preheated to 48°C, on top of a water bath at 48°C. The 1X SSC solution was changed three times, once every 30 minutes. For the last wash, 1X SSC at 48°C was added, then the dishes were removed from the water bath and allowed to cool to room temperature. The coverslips were washed twice, each time for five minutes in binding buffer (see section 2.3.4) at RT. The coverslips were incubated in binding buffer containing either the anti-DIG-alkaline phosphatase-conjugated antibody (1:500, Roche), or the anti-DIG-fluorescein-conjugated antibody (1:10, Roche), 1% normal sheep serum (Invitrogen) and 0.3% Triton X-100 (Sigma) for three hours in a humidified chamber at RT. When the incubation was completed, the coverslips were briefly rinsed in binding buffer. Then, the slides were washed three times, each time for 10 min, in binding buffer at room temperature. The coverslips were rinsed briefly in wash buffer (see section 2.3.4) and washed for five minutes in wash buffer. For the alkaline phosphatase conjugated antibody, an AP substrate (BCIP/NBT Liquid Substrate System, Sigma) producing a blue-purple precipitate was applied for 12 to 24 hours in the dark at RT. The reaction was stopped by washing the slides twice, each time for five minutes in stop buffer (see section 2.3.4). Finally, with both alkaline phosphatase- or fluorescein-conjugated antibodies, coverslips were washed twice for five min with water at room temperature and were mounted with a drop of Vectashield medium (Reactolab).

#### 2.3.4 Solutions

All the solutions of this section were prepared with DEPC-treated water (250 µl/l (v/v) DEPC), autoclaved.

**Hybridization buffer** (50% (v/v) deionized formamide (Sigma), 4× SSC, 1× Denhardt solution, 1% sarkosyl, 10 ml 30 mM phosphate buffer, pH 7.0, 0.55 mg/ml (v/v) salmon testes DNA (Sigma), 100 g/l (w/v) dextran sulphate (Sigma))

**SSC, 20×, pH 7.0** (3 M NaCl, 300 mM sodium citrate dihydrate (C<sub>6</sub>H<sub>5</sub>Na<sub>3</sub>O<sub>7</sub>×2H<sub>2</sub>O)) The pH was adjusted to pH7.0 with NaOH or concentrated HCl.

**Denhardt solution, 50×** (10 g/l polyvinylpyrrolidone (Sigma), 10 g/l BSA (proteases free, Acros Organics), 10 g/l Ficoll (Sigma))

**Sarkosyl, 20% (w/v)** (200 g/l (w/v) N-laurylsarcosine (Sigma))

**Phosphate buffer, 0.2 M** (50 mM NaH<sub>2</sub> PO<sub>4</sub> × H<sub>2</sub>O, 150 mM Na<sub>2</sub> HPO<sub>4</sub>)

**Binding buffer** (150 mM NaCl, 100 mM Tris) The pH was adjusted pH 7.5 with HCl.

**Wash buffer** (100 mM NaCl, 100 mM Tris, 50 mM MgCl<sub>2</sub>×6H<sub>2</sub>O) The pH was adjust to pH 9.5 with HCl.

**Stop buffer** (150 mM NaCl, 10 mM Tris, 1 mM EDTA) The pH was adjust to pH 7.5 with HCl.

#### 2.3.5 Oligonucleotides sequences

The oligonucleotides were selected to match the sequence (sense probe) or the complementary sequence (antisense probe) of the cDNA of the different ASIC subunits. The following parameters were used to select the oligonucleotides. The desired GC content had to be between 48 and 62%. The oligonucleotide length had to be between 42 and 54 nucleotides. The calculated melting point of the oligonucleotide had to be between 100°C and 106°C. The oligonucleotide had not to contain hairpins with free energy more negative than -4.7 kcal. Finally, the sequence of the oligonucleotide had to avoid runs of more than five identical nucleotides in series (Erdtmann-Vourliotis *et al.*, 1999).

The designed oligonucleotides were tested as described in section 2.3.6. When the negative control experiments were not negative, the oligonucleotide was redone.

	sense probes
ASIC1a	5'-GATGAAAAGCAGCTAGAGATATTGCAGGACAAGGCCAACTTCCGGAGCTTC-3'
ASIC1b	5'-AGAGGAAGAGAAGGAAATGGAGGCAGGGTTCGGAGTTGGATGAGGGTGATGA-3'
ASIC2a	5'-CATCAGCGCTGCCTTCATGGACCGTTTGGGCCACCAGCTGGAGGATATGCT-3'
ASIC2b	5'-CAGCCTGCAACCTTCCAGTATCCAGATCTTCGCCAATACCTCCACTCTCCA-3'
ASIC3	5'-GCTGTGCTCCTGTCGCTGGCGGCCTTCCTCTACCAGGTGGCTGAGCGG-3'

**Table 1 : List of ASIC subunits sense oligonucleotides**

	antisense probes
ASIC1a	5'-GAAGCTCCGGAAGTTGGCCTTGTCTGCAATATCTCTAGCTGCTTTTCATC-3'
ASIC1b	5'-TCATCACCTCATCCAACCTCCGACCCTGCCTCCATTTCCTTCTCTTCTCT-3'
ASIC2a	5'-AGCATATCCTCCAGCTGGTGGCCCAAACGGTCCATGAAGGCAGCGCTGATG-3'
ASIC2b	5'-TGGAGAGTGGAGGTATTGGCGAAGATCTGGATACTGGAAGGTTGCAGGCTG-3'
ASIC3	5'-CCGCTCAGCCACCTGGTAGAGGAAGGCCGCCAGCGACAGGAGCACAGC-3'

**Table 2 : List of ASIC subunits anti-sense oligonucleotides**

### 2.3.6 Test of in-situ hybridization probes against ASIC subunits

The probes against ASIC1a, -1b, -2a, -2b, and 3 mRNA were tested on CHO cells expressing stably or transiently one of the five ASIC subunits. ASIC1a, -1b and -2a were stably expressed in CHO cells, ASIC2b and -3 were transiently co-expressed with eGFP (the eGFP staining is shown in the images showing green fluorescence) (Figure 10).

For each subunit, a specific antisense probe was designed, as well as the complementary sense probe as a negative control. As a supplementary negative control, each antisense probe was also tested on CHO cells either expressing no ASICs or another ASIC. Figure 10 shows that the antisense probes are specific. On the left panels, representing the specific staining of each probe for the corresponding ASIC subunit, cells were dark stained with BCIP/NBT precipitate. This dark precipitate indicated that the probes recognised the mRNA of the corresponding subunits. In the middle panels, the sense probes were used as negative controls. On most cells, there was no, or background staining, showing that the sense probes did not recognise ASIC mRNAs. On the right panels, the antisense probes were used on CHO cells that were not expressing the corresponding ASIC subunit. These negative controls had no or basal staining, meaning that the probes seemed to be specific to their corresponding ASIC subunit.

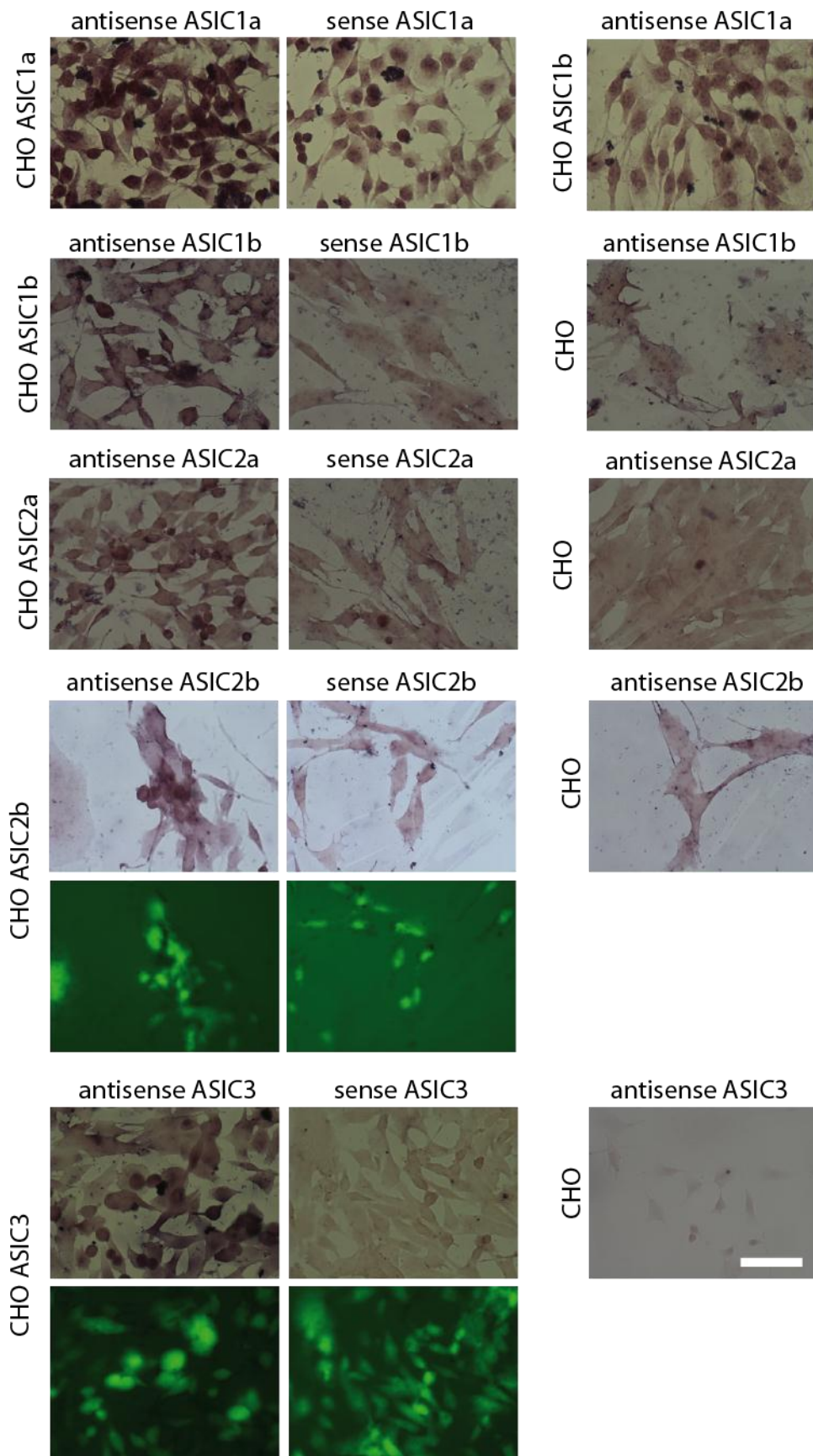


Figure 10 : Test of in-situ hybridization probes (antisense and sense) for ASIC1a, -1b, -2a, -2b and -3 in CHO cells. Scale bar: 100  $\mu$ m.

## 2.4 Microscopy and cell counting

Both immunocytochemistry and/or in-situ hybridization experiments slides were imaged using a confocal microscope (LSM 710, Zeiss, Feldbach, Switzerland), with an EC Plan-Neofluar 40x/1.30 Oil DIC M27 objective. The confocal microscope was operated with the LSM Software ZEN 2009 (Zeiss). The “smart setup” tool was used to select the appropriate dyes and the “Fastest” acquisition mode was selected. For counting purposes, large images were taken by using “tile scan”. The large image was done by imaging seven x seven 512 x 512 pixels images at a resolution of 0.45  $\mu\text{m}$  / pixel, resulting in a 3584 by 3584 pixels image. The confocal “.lsm” images files were converted to “.jpg” files with Axiovision LE (Zeiss). To count the positive cells for a given fluorescent dye, the ImageJ software was used. Briefly, the grey scale images for each fluorescent dye were opened in the software. For each experiment, a mouse primary monoclonal antibody against NeuN, a neuronal marker, followed by an anti-mouse cy5 secondary antibody was used to stain all neurons. The cy5 image was used to create regions of interest (ROI). Each region delimited a neuron. The average grey scale value was then measured for each region of interest for each fluorophore (except for the cy5). For each set of experiment and each type of antibody or oligonucleotide, a threshold value was then chosen, above which a neuron was counted as positive.

## 2.5 Calcium imaging

The cells were plated on large 22 mm x 40 mm coverslips coated with high molecular weight poly-l-lysine (Sigma) solution ( $0.2 \text{ mg ml}^{-1}$ ). Cells were washed with 1x PBS. Coverslips were mounted in the perfusion chamber (Warner Instruments, Hamden, USA), using grease to seal the coverslip to the bottom of the chamber. For CHO cells, cells were incubated with 5  $\mu\text{M}$  Fura2-AM in 1ml of pH 7.4 Tyrode solution directly in the perfusion chamber for 30 min in the dark in a 37°C water bath. For neurons, the time of incubation was reduced to 20 minutes. After incubations, cells were perfused for a few minutes with pH 7.4 Tyrode to rinse the Fura2-AM. Up to eight different solutions were perfused on the cells with the Solution Changer Manifold MSC-200 (Bio-Logic, Claix, France). The solutions were exchanged with a CFlow flux controller (Cell MicroControls, Norfolk, USA). The imaging solution was the VisiFluor system (Visitron Systems, Puchheim, Germany) with a CoolSnap HQ camera, VisiChrome polychromator and Metafluor software (Molecular Devices, Sunnyvale, USA). Briefly, for each time point, two images were taken at excitation wavelengths of 340 and 380 nm. The emitted fluorescence at 520 nm was recorded through an emission filter. A ROI was drawn on images to select regions which correspond to cells. The average grey scale level for each ROI was calculated for each 340 and 380 nm image at each time point. A region empty of cells was also selected to have a measure of the background fluorescence. The background values for each time point at 340 and 380 nm wavelengths were subtracted for each value. The ratio between the fluorescence at 340 nm and 380 nm (340/380) was then plotted as a function of the time.



## 2.6 In vitro CGRP secretion assay with DRG neurons

Freshly dissociated neurons were plated into 24 well dishes, coated with a high molecular weight poly-L-lysine (Sigma) solution ( $0.2 \text{ mg ml}^{-1}$ ). Neurons were maintained during ~18 hours in NeuroA at  $37^\circ\text{C}$  and 5%  $\text{CO}_2$ . The cells were then first washed one time with PBS, then a second time with PBS containing protease inhibitors (Leupeptin ( $1\mu\text{g/ml}$ ), Pepstatin ( $1\mu\text{g/ml}$ ), Aprotinin( $1\mu\text{g/ml}$ ), PMSF (1 mM) (Roche, Rotkreuz, Switzerland)) and 0.3 % bovine serum albumin (BSA) (proteases free, Acros Organics part of Fisher Scientific, Wohlen, Switzerland). Protease inhibitors and 0.3 % BSA were added to all the solutions used in this this assay. In this assay, secretion was measured during a 20 min period. For some pharmacological compounds a preincubation was necessary. In these cases, the compounds were incubated for 5 min at room temperature (RT) in 200  $\mu\text{l}$  Tyrode (140 mM NaCl, 4 mM KCl, 2 mM  $\text{CaCl}_2$ , 1 mM  $\text{MgCl}_2$ , 10 mM MES, 10 mM Hepes, 10 mM glucose) at pH 7.4. The corresponding negative controls were preincubated with 200  $\mu\text{l}$  Tyrode at pH 7.4. The preincubation solutions were then removed. Subsequently, 200  $\mu\text{l}$  Tyrode solution adjusted to the desired pH with or without pharmacological compounds were added to each well. The wells were incubated for 20 min on top of a water bath at  $37^\circ\text{C}$ . After the incubation, the supernatant of each well was transferred into a polyethylene tube (Nunc-Immuno™ Tubes MiniSorp, Fisher Scientific, Wohlen, Switzerland) and kept on ice. Tubes were centrifuged for 10 min at 500 rpm at  $4^\circ\text{C}$ . The supernatants were transferred into new polyethylene tubes and then frozen at  $-80^\circ\text{C}$ . In each well, the cells were incubated for 5 min with 100  $\mu\text{l}$  lysis buffer (50 mM Tris pH7.5, 5 mM EDTA, 1% Triton X-100), then harvested. The lysates were then transferred to polyethylene tubes, sonicated a few seconds at  $4^\circ\text{C}$  and then frozen at  $-80^\circ\text{C}$ . They were used to determine the cellular content in CGRP in order to normalize the secretion of each well. The CGRP content of the supernatants and the lysates were subsequently measured using an enzyme immunoassay kit, as described in the next section.

## 2.7 CGRP enzyme immunoassay

CGRP content of the supernatants and the lysates samples were measured using a rat CGRP enzyme immunoassay (EIA) kit (SPI-bio, Montigny le Bretonneux, France). This kit was used according to the manufacturer's recommendations. Briefly, the lyophilised CGRP of the standard vial was reconstituted with 1 ml of experimental solution (Tyrode solution adjusted to pH 7.4, supplemented with 0.3% BSA, protease inhibitors). A serial dilution of the standard was performed to obtain the following concentrations: 500 (S1), 250 (S2), 125 (S3), 62.5 (S4), 31.25 (S5), 15.6 (S6), 7.81 (S7),  $3.91 \text{ pg ml}^{-1}$ . The lyophilised CGRP of the quality control vial was reconstituted with 1 ml of the experimental solution. The lysates were diluted fifty times with experimental solution, to ensure that the measured CGRP concentration was in the detection range of the kit. Wells of the 96 well plate, precoated with a CGRP mouse monoclonal antibody, were washed five times with the provided wash buffer. 100  $\mu\text{l}$  of sample (supernatant or diluted lysate), quality control or standard solution were pipetted into each



well. Each measurement was performed in duplicate. The blank (B) wells were kept empty and 100  $\mu$ l of experimental solution were pipetted into the non-specific binding (NSB) wells. The plate was then covered with a plastic film and incubated 16 to 20 hours at 4°C without shaking. The anti-CGRP-AChE tracer was then reconstituted with 10 ml of the provided EIA buffer. 100  $\mu$ l of the tracer was pipetted into each well, except the blank wells and briefly mixed. The plate was again covered with a plastic film and incubated 16 to 20 hours at 4°C. The plate was then emptied by turning over and shaking. Each well was washed three times with the wash buffer (300  $\mu$ l per well), slightly shaken for 2 minutes with an orbital shaker and then rewashed three times with the wash buffer. A few minutes before use, the Ellman's reagent was reconstituted with 49 ml of deionized water and 1 ml of concentrated wash buffer. 200  $\mu$ l of Ellman's reagent was added to each well. The plate was incubated in the dark, covered with an aluminium sheet at room temperature. The plate was read with a spectrophotometer plate reader at 405 nm between 30 to 60 minutes after adding the Ellman's reagent. To analyse the data, first of all, the average of the blank wells was subtracted from the absorbance reading of the rest of the plate. The average absorbance for each NSB, standard and sample well was calculated. The absorbance for each standard versus the concentration was plotted. The concentration for each sample was determined using the equation of the fit of the standard curve.

## 2.8 Animal surgery

All experiments were approved by the Committee on Animal Experimentation of the Canton de Vaud, Switzerland, in accordance with Swiss Federal law on animal care and the guidelines of the International Association for the Study of Pain (IASP) (Zimmermann, 1983). 8-10 week-old C57BL/6 male mice were housed in the same room, one per cage, at constant temperature ( $21 \pm 2$  °C) and a 12/12 dark/light cycle. No other animals were housed in that room. Mice had ad libitum access to water and food.

The spared nerve injury (SNI) model consists of sparing the sural nerve, while two other terminal branches of the sciatic nerve are injured (common peroneal and tibial nerves). Intense, reproducible and long-lasting mechanical allodynia-like behaviour is measurable in the non-injured sural nerve skin territory (Decosterd *et al.*, 2004). The surgery was performed as previously described (Bourquin *et al.*, 2006). SNI surgery was performed under general anaesthesia by 1.5–2.5% isoflurane. The left hindlimb was immobilized in a lateral position and slightly elevated. Incision was made at mid-thigh level using the femur as a landmark and a section was made through the *biceps femoris* in the direction of point of origin of the vascular structure. At that stage, the surgery continued with the help of a stereomicroscope. The three peripheral branches (sural, common peroneal, and tibial nerves) of the sciatic nerve were exposed without stretching nerve structures. Both tibial and common peroneal nerves were ligated and transected together. A micro-surgical forceps with curved tips was delicately placed below the tibial and common peroneal nerves to slide the thread (6.0 silk) around the nerves. A

tight ligation of both nerves was performed and a 1–2 mm section of the two nerves was removed. The sural nerve was carefully preserved by avoiding any nerve stretch or nerve contact with surgical tools. Muscle and skin were closed in two distinct layers with silk 6.0 sutures.

## **2.9 Behaviour**

The following behavioural experiments, as well as the previously described SNI model surgery, were performed in collaboration with the group of Isabelle Decosterd. The surgery was performed by technicians of Isabelle Decosterd's group (Marie Pertin, Guylène Magnin). I learned the behavioural experiments procedures with Marie Pertin for the Von Frey experiments and with Guylène Magnin for the hot plate and tail-flick experiments.

### **2.9.1 Von Frey monofilaments**

Testing procedures started with one week of acclimatization of the animals to the testing room environment, with handling reduced to a minimum. For another week, mice were habituated to the testing material. The experimenter placed each mouse on an elevated platform with a 20 mm soft wire mesh floor, in a transparent Plexiglas box (10 × 10 × 13 cm) for a 15-min session every two days. During the last session, mice were familiarized with the application of von Frey monofilaments under the paw. Recordings of mechanical sensitivity were then performed before and after surgery. Two sets of baseline measurements were taken, baseline 1 at 4 days before surgery and baseline 2 at 2 days before surgery. Measurements were also taken 3, 9, 15 and 21 days after SNI. The investigator was blinded to the genotype of the mice. The plantar side of the hindpaw ipsilateral or contralateral to the surgery was stimulated with calibrated von Frey monofilaments (Stoelting Co, Wood Dale, USA). Monofilaments were applied perpendicularly to the glabrous skin with sufficient force to cause filament bending. Ten stimuli were made with each of a series of Von Frey hairs comprised of the first 11 monofilaments supplied by the manufacturer (0.008, 0.02, 0.04, 0.070, 0.16, 0.40, 0.60, 1.0, 1.4, 2.0, and 4.0 g). We measured the number of positive withdrawal responses in ten applications for each monofilament of the series. The 11 monofilaments were tested in ascending order to determine the relative frequency of paw withdrawal. The number of hindpaw withdrawal after 10 stimulations is a measure of the sensitivity of the animal to the stimulations. Classically, with wild type mice, the number of withdrawal of the ipsilateral hindpaw increases after the SNI surgery, for a given filament. On the contrary, the number of withdrawal of the contralateral hindpaw does not change after SNI surgery.

### **2.9.2 Hot plate**

Mice were habituated to the testing material for four days before the measurements. Mice were placed in a transparent acrylic box without bottom which was placed on a cold and hot plate analgesia meter

(Bioseb, Paris, France) maintained at 49, 52, or 55°C. The reaction time was scored when the animal licked its paws or jumped. The maximal time of exposure was set to 40 s to avoid any paw damage. Three measurements for each mouse were taken and averaged for a single temperature each day, leaving a couple minutes between each measurement. The three different temperatures were assessed on three different days, first 49, then 52 and finally 55°C.

### **2.9.3 Tail flick**

Mice were habituated to the testing material the day before the experiment. The tail flick procedure was carried out as previously described (Dewey *et al.*, 1970). Mice were immobilized in a cone shape tissue, leaving the tail out of the tissue. The tail was then placed on the light beam path of the Tail-Flick Analgesia Meter (Columbus Instruments, Columbus, USA). In order to avoid tissue damage, a maximum latency of 10 s was imposed. The intensity of the light falling on the tail of the mouse was adjusted such that each reaction time fell within the 10 s range. This intensity was then maintained for the entire experiment. Three measurements, taken 30 minutes apart, were averaged and constituted the time of reaction.

### 3. Results

#### 3.1 Distribution of ASICs, TRPV1 and neuropeptides in rat DRG neurons

We have analysed the distribution of ASICs, TRPV1 and neuropeptides (CGRP and SP) in the rat DRG neurons in culture, more specifically the coexpression of the different ASIC subunits with the neuropeptides, and also the coexpression of different ASIC subunits. In order to test for these coexpressions, two different approaches were used. First, immunocytochemistry was performed on the cells for ASIC1 (antibody recognising both ASIC1a and ASIC1b subunits), ASIC2 (antibody recognising both ASIC2a and ASIC2b subunits), TRPV1, CGRP and SP. To distinguish between the different isoforms of ASIC1 and ASIC2, and to show the distribution of ASIC3, in-situ hybridization was used.

##### 3.1.1 ASIC1, -2 and TRPV1 are preferentially localised in peptidergic neurons

Immunocytochemistry was performed on dissociated rat DRG neurons. In each immunostaining experiment, the neurons were also stained for NeuN, a neuronal marker, to mark each neuron and distinguish them from non-neuronal cells in the preparation. Double staining experiments were carried out (see Methods). Each neuron was then assigned as positive or negative for the expression of neuropeptides (CGRP or SP, red, in Figure 11), or ASICs/TRPV1 (green). The different subpopulations were then counted and represented in concentric pie charts. Figure 11 shows in panels A and B the immunostaining and the proportion of subpopulations of neurons expressing respectively CGRP or SP and ASIC1. Panel C shows the proportion of subpopulations of neurons expressing respectively CGRP or SP and ASIC2; panel D the proportion of subpopulations of neurons expressing respectively CGRP or SP and TRPV1. All DRG neurons, not only small diameter neurons, were included in the experiments shown in this figure.

On average CGRP and SP were found to be present in about half of the neurons. ASIC1 and CGRP are co-expressed in 45% of the neurons, whereas ASIC1 and SP are co-expressed in 39% of the neurons. The staining thus showed that ASIC1a and/or ASIC1b (the antibody labels both isoforms) are preferentially co-expressed with neuropeptides. ASIC2 and CGRP are co-expressed in 57% of the neurons and ASIC2 and SP are co-expressed in 41% of the neurons. Therefore ASIC2a and/or ASIC2b (the antibody labels both isoforms) are preferentially co-expressed with neuropeptides. TRPV1 and CGRP are co-expressed in 46% of the neurons and TRPV1 and SP are co-expressed in 39% of the neurons. It showed that TRPV1 are preferentially co-expressed with neuropeptides.

No subtype specific antibodies for ASIC1a/b or ASIC2a/b are available and all ASIC3 antibodies tested are not good enough for immunocytochemistry in neurons. In order to have a better view on the expression of the five different ASIC subunits, we decided to carry out in-situ hybridization

experiments to have a better understanding of the expression of ASIC subunits in the peptidergic and non-peptidergic population of nociceptors.

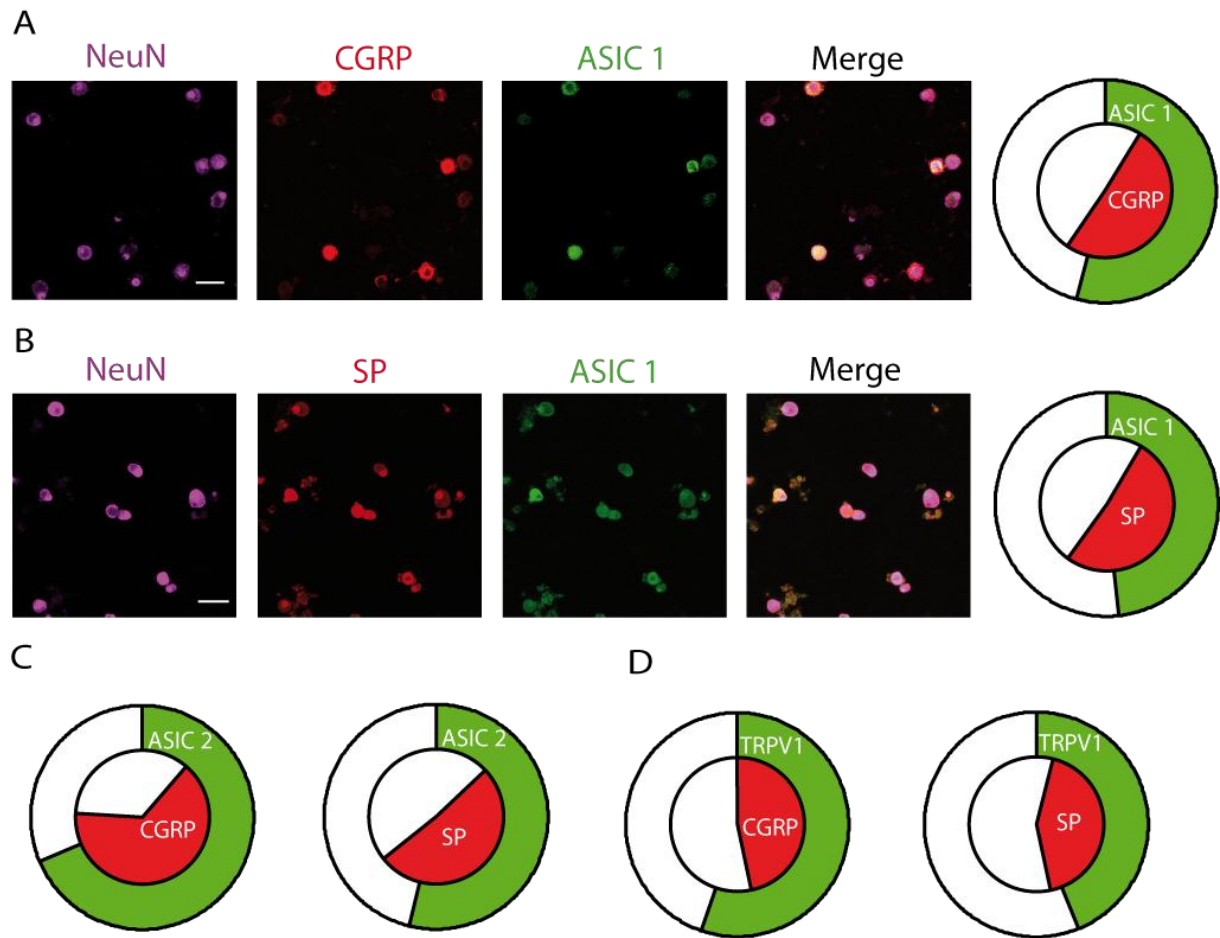


**Figure 11 : Co-expression of ASIC1, -2, and TRPV1 with neuropeptides in DRG neurons**

Panels A and B show immunostaining for ASIC1, CGRP and SP respectively. The bar is 100  $\mu$ m. The proportions of subpopulations expressing ASIC1 and CGRP or SP are shown in a concentric pie chart on the right. Panel C shows the proportions of subpopulations expressing ASIC2 and CGRP or SP. Panel D shows the proportions of subpopulations expressing TRPV1 and CGRP or SP. The total number of cells are respectively 661 for ASIC1/CGRP staining, 471 for ASIC1/SP staining, 124 for ASIC2/CGRP staining, 311 for ASIC2/SP staining, 58 for TRPV1/CGRP and 75 for TRPV1/SP.

### 3.1.2 In situ hybridization experiment confirm that ASIC subunits are preferentially expressed in the peptidergic population of small neurons

As in the previous experiments, anti-NeuN antibodies were used to label the neurons and anti-CGRP and anti-SP antibodies were used to detect the neuropeptides CGRP and SP. Prior to this standard immunostaining, in-situ hybridization was performed on DRG neurons with the probes previously tested, as described in section 2.3.6.

In Figure 12, only the conditions with antisense probes are shown, as the sense probes showed no or very faint staining compared to antisense probes. Confocal images of staining with ASIC1a antisense probes are shown (green), along with immunostaining by anti-NeuN (pink) and anti-CGRP (red). Figures for the analogous analyses for ASIC1b, -2a, -2b and -3 are shown in Annexes (pp.78-80).

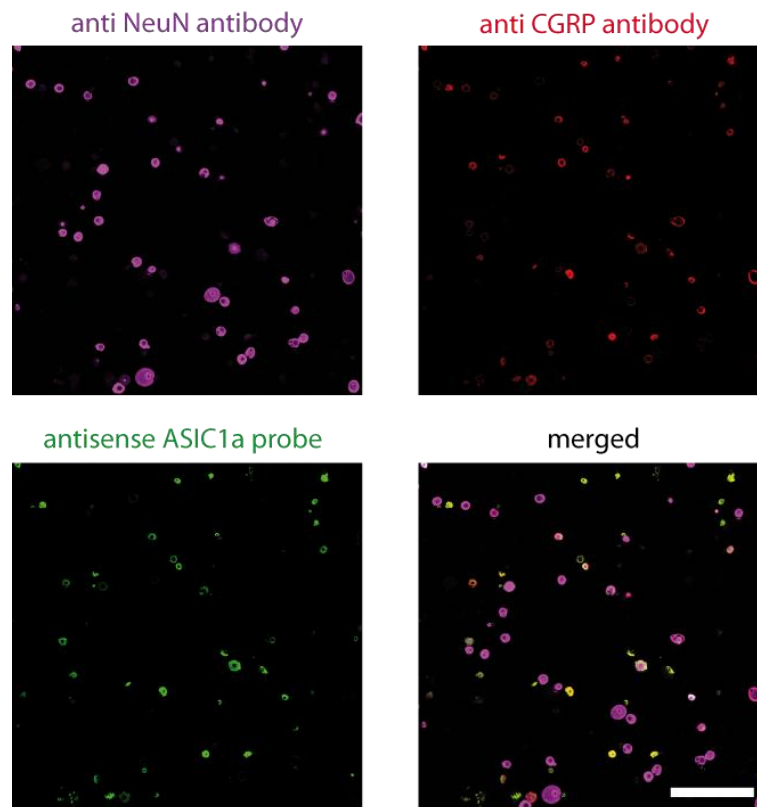


**Figure 12 : Example of staining of ASIC1a with in-situ hybridization on DRG neurons**

ASIC1a antisense probe, shown in green, and anti CGRP antibody, shown in red are used. Scale bar: 100  $\mu$ m. In the merged image, cells which are positive for NeuN, CGRP and ASIC1a appear yellow.

In Figure 13, the proportion of subpopulations of neurons expressing for each ASIC mRNA probe and neuropeptides CGRP or SP are shown in pie charts. Only the neurons whose apparent diameters were smaller or equal to 30  $\mu$ m were used for this analysis. The diameters of the neurons were estimated using the area of the NeuN staining for each cell. The area of the neuron was converted as a diameter, by approximating the area of the neuron as a disc.

ASIC1a mRNA was expressed in about 60% of small diameter DRG neurons. ASIC1a mRNA was co-expressed with CGRP peptide in 43% of the small diameter neurons and with SP peptide in 49% of the small neurons, as seen in the first two charts of the first row in Figure 13. A large part of the neurons that expressed ASIC1a also expressed CGRP and SP. The last two charts of the first row show that ASIC1b mRNA was less expressed (36-37% of small diameter neurons) than ASIC1a mRNA. Most of neurons expressing ASIC1b also expressed CGRP (74%) and SP (91%). Almost all neurons expressing ASIC1b were also expressing neuropeptides, but about 44% of CGRP-positive neurons and 44% of the SP-positive neurons did not express ASIC1b. The first two charts of the second row show that about 26-27% of the small diameter neurons expressed ASIC2a. Almost all small neurons expressing ASIC2a also expressed CGRP (87%) and SP (100%). About half of the neuropeptide-positive neurons expressed ASIC2a.

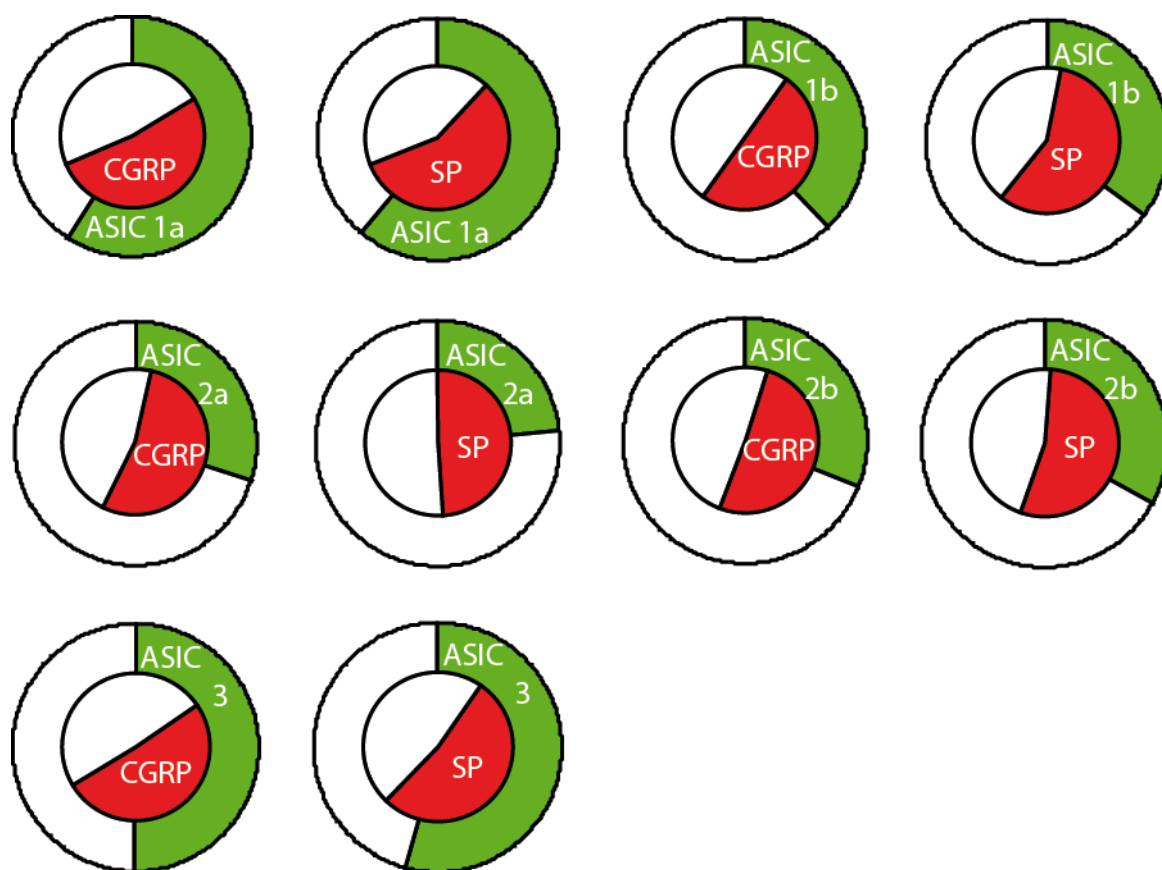


**Figure 13 : ASIC subunits are preferentially expressed in the peptidergic population of small DRG neurons**

Each pie chart shows the proportion of subpopulation of neurons expressing ASIC1a, 1b, 2a, 2b, 3 and CGRP or SP, respectively, on small (< 30  $\mu$ m diameter) DRG neurons. ASIC staining (green) was determined by in situ hybridization and neuropeptides staining (CGRP/SP, red) by immunostaining. The total number of cells are respectively 214 for ASIC1a/CGRP staining, 133 for ASIC1a/SP staining, 177 for ASIC1b/CGRP staining, 213 for ASIC1b/SP staining, 226 for ASIC2a/CGRP staining, 278 for ASIC2a/SP staining, 357 for ASIC2b/CGRP staining, 267 for ASIC2b/SP staining, 334 for ASIC3/CGRP staining, 281 for ASIC3/SP staining.

The last two charts of the second row show that the results for ASIC2b were similar to ASIC2a. About 32% of the small diameter neurons expressed ASIC2b. Almost all small neurons expressing ASIC2b also expressed CGRP (84 %) and SP (97%). About half of the neuropeptide-positive neurons did not express ASIC2b. The last row shows results for ASIC3 which are similar to the ASIC1a results. About 52% of the neurons expressed ASIC3 mRNA. ASIC3 and CGRP were co-expressed in 35% of the small diameter neurons, and ASIC3 and SP were co-expressed in 44% of the small diameter neurons.

To summarize, these results clearly show that all ASICs subunits are preferentially expressed in the peptidergic population of small diameter neurons. The most widely distributed ASIC subunits are ASIC1a and -3. ASIC1b, -2a, and -2b are expressed in a smaller population of small diameter DRG neurons.

In order to investigate the co-expression of ASICs subunits, immunocytochemistry with either anti-ASIC1 or anti-ASIC2 antibodies was performed after the in-situ hybridization. In Figure 14, the top-left chart shows the co-expression between ASIC1 (ASIC1a and -1b) proteins and the ASIC1a mRNA



in small DRG neurons. 39 % of the small neurons were both positive to ASIC1 protein and ASIC1a mRNA. Interestingly 16% of ASIC1a mRNA positive neurons were negative to ASIC1 antibody, either showing a differential expression between the protein and the mRNA, or a difference of sensitivity between the immunostaining and the in-situ hybridization techniques. The left-bottom chart shows that 49% of the small neurons expressing ASIC1 proteins also expressed ASIC3 mRNA. Even if, as mentioned before, the immuno- and the in-situ hybridization-staining cannot be directly compared, it showed that a rather large population of neurons expressed both ASIC1a or -1b together with ASIC 3. The right charts showed that ASIC1a and ASIC3 mRNA have only a slight co-expression with ASIC2 proteins (10% and 18 % respectively). The quantification of ASIC2 immunostaining was different in this figure compared to Figure 11. This difference was certainly due to the fact that in this figure, only the small diameter DRG neurons were taken into account, whereas all DRG neurons were taken into account in Figure 11. It means that there was less staining of ASIC2 in small neurons. This hypothesis is confirmed by evidences that most ASIC2-positive neurons were medium-to-large neurons (Kawamata *et al.*, 2006).

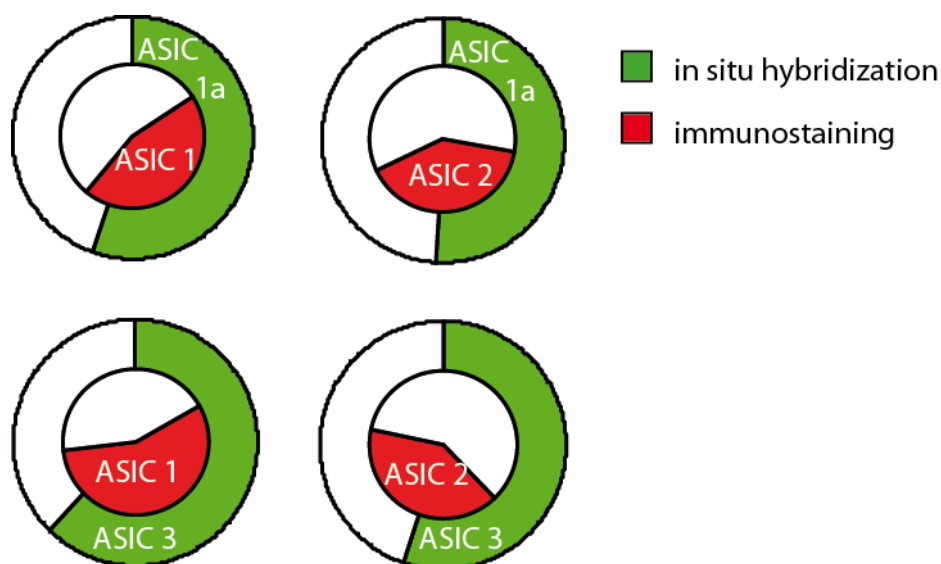


**Figure 14 : A large population of neurons express both ASIC1a/1b and ASIC 3**

The pie charts show the expression of ASIC1 and 2 proteins (red) with ASIC1a and 3 mRNA (green). The total number of cells are respectively 119 for ASIC1a/ASIC1 staining, 149 for ASIC1a/ASIC2 staining, 95 for ASIC3/ASIC1 staining, 85 for ASIC3/ASIC2 staining.

ASIC1a, which can form a  $\text{Ca}^{2+}$ -conducting homomeric channel and ASIC3 were expressed in a large proportion of the small peptidergic neurons. Considering their pH50 (see section 1.2.4), activation of these ASICs occurs at mildly acidic pH and would mediate an entry of  $\text{Na}^+$  and  $\text{Ca}^{2+}$  into the peptidergic neurons. To investigate the increase of calcium in the DRG neurons, calcium imaging experiments were performed.

## 3.2 Functional experiments with calcium imaging on cells in culture

### 3.2.1 Heterologous expressed ASIC1a and TRPV1 are activated by extracellular acidification

In a first series of experiments we tested whether the activation of ASIC1a or TRPV1 increases the ratio of intracellular fluorescence, which would indicate an increase of the intracellular calcium concentration. Human ASIC1a (hASIC1a) and rat TRPV1 (rTRPV1) were separately stably expressed in CHO cells. In Figure 15, panel A, a typical fluorescence trace from a cell expressing ASIC1a is shown. A brief (30 s) extracellular acidification to pH 6 increased the intracellular fluorescence.

N-(4-Tertiarybutylphenyl)-4-(3-cholorpyridin-2-yl)tetrahydropryazine-1(2H)-carbox-amide (BCTC) is an inhibitor of capsaicin- and acid-mediated currents in rat TRPV1 (Pomonis *et al.*, 2003).

Co-perfusion of an extracellular solution at pH 6 with increasing concentrations of amiloride (100, 200 and 500  $\mu\text{M}$ ) showed a concentration-dependent reduction of the induced fluorescence. The fluorescence amplitude obtained in the presence of amiloride was normalized to the fluorescence amplitude of the pH6 condition and plotted in panel B ( $n = 8$ ). A paired t-test showed that the decrease of fluorescence was significant for the condition with 200 and 500  $\mu\text{M}$  amiloride ( $p\text{-value} = 0.020$  and  $0.0004$ , respectively). Amiloride at a concentration of 500  $\mu\text{M}$  reduced the increase in intracellular calcium by 87%. This concentration of amiloride was chosen for all the following experiments. The estimated  $\text{IC}_{50}$  for amiloride in these experiments was  $272 \pm 40 \mu\text{M}$ .

Panels C and D show that an acidification to pH 5 produced an increase of fluorescence in TRPV1-expressing cells. 500  $\mu\text{M}$  amiloride increased non-significantly the pH 5-induced fluorescence change (paired t-test,  $p\text{-value} = 0.103$ ,  $n = 3$ ). Panels E and F show that 1  $\mu\text{M}$  and 5  $\mu\text{M}$  BCTC decreased the fluorescence induced by an extracellular acidification to pH 5 by respectively 72 and 88 % (paired t-test,  $p\text{-value} = 0.002$ ,  $n = 4$ ,  $p\text{-value} = 0.009$ ,  $n = 8$ , respectively). BCTC showed no significant effect on ASIC1a (data not shown).

We conclude that activation of both ASIC1a and TRPV1 can increase the intracellular calcium concentration in cells, that amiloride inhibits ASIC1a, but not TRPV1, and that BCTC inhibits TRPV1, but not ASIC1a. The effect of amiloride on TRPV1 was not significant, but as the number of  $n$  is very low ( $n = 3$ ), it is possible that increasing the number of experiment could give significant differences. It means that amiloride could affect TRPV1 by increasing the conductivity of the channel.

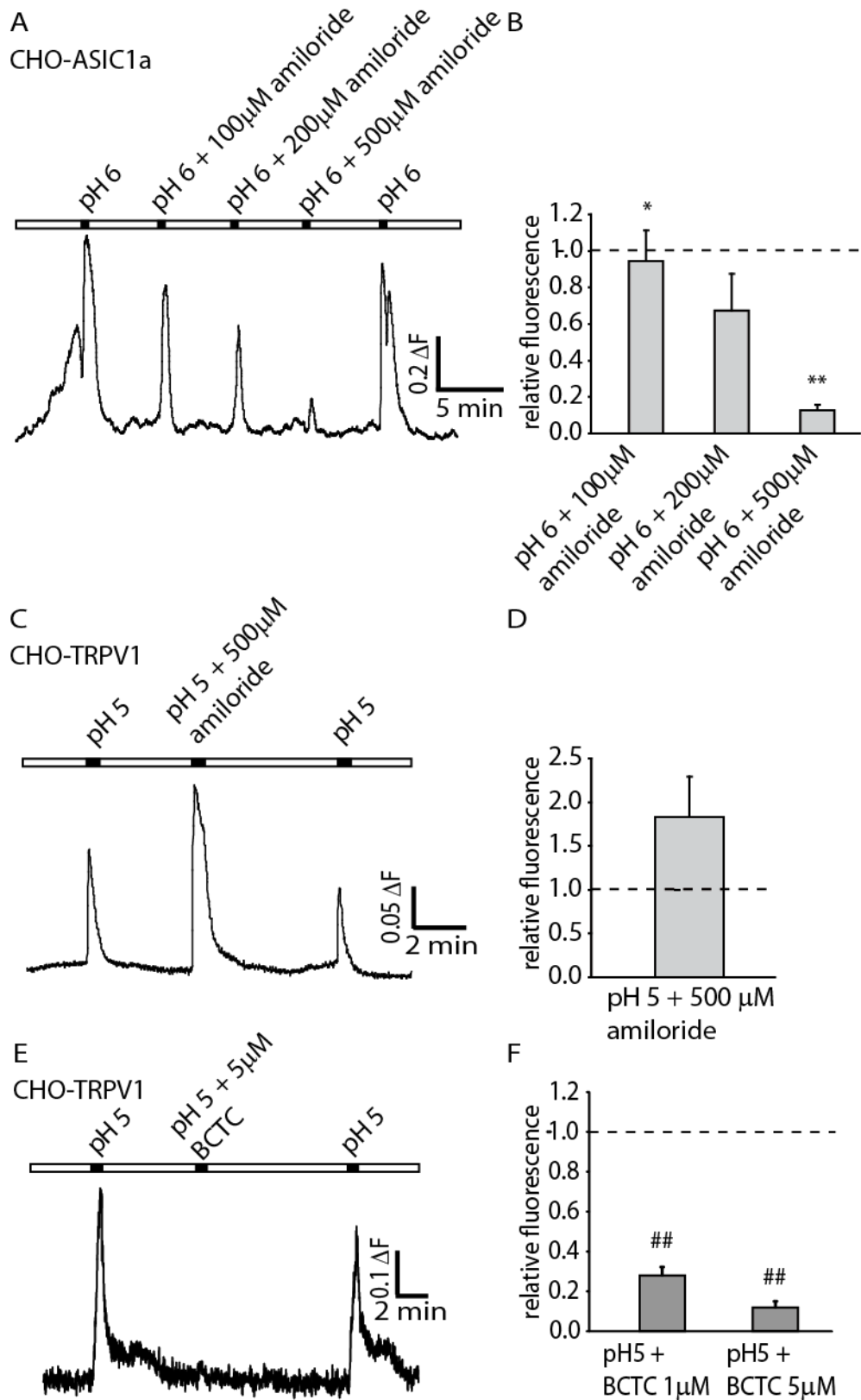


**Figure 15 : Effect of amiloride and BCTC on ASIC1a and TRPV1 stably expressed in CHO cells**

Panels A and B show the effect of increasing concentrations of amiloride on the amplitude of the pH6-induced fluorescence change in CHO cells expressing ASIC1a, n = 8. Panels C and D show that amiloride had no significant effect on TRPV1, n = 3. Panels E and F show the inhibition by BCTC of H<sup>+</sup>-induced intracellular Ca<sup>2+</sup> concentration increase in TRPV1 expressing CHO cells, n = 4 for 1 μM BCTC, n = 8 for 5 μM BCTC. \*: p-value < 0.05 compared with "pH 6" value, \*\*: p-value < 0.01 compared with "pH 6" value, ##: p-value < 0.01 compared with "pH 5" value

### 3.2.2 Amiloride prevents the ASIC-induced $\text{Ca}^{2+}$ entry in a population of DRG neurons

Calcium imaging experiments were performed on dissociated rat DRG neurons. First of all, amiloride was used to identify among the neurons responding to extracellular acidification at two pH values (pH 6 and pH 5), those in which ASICs mediated the  $\text{Ca}^{2+}$  entry.

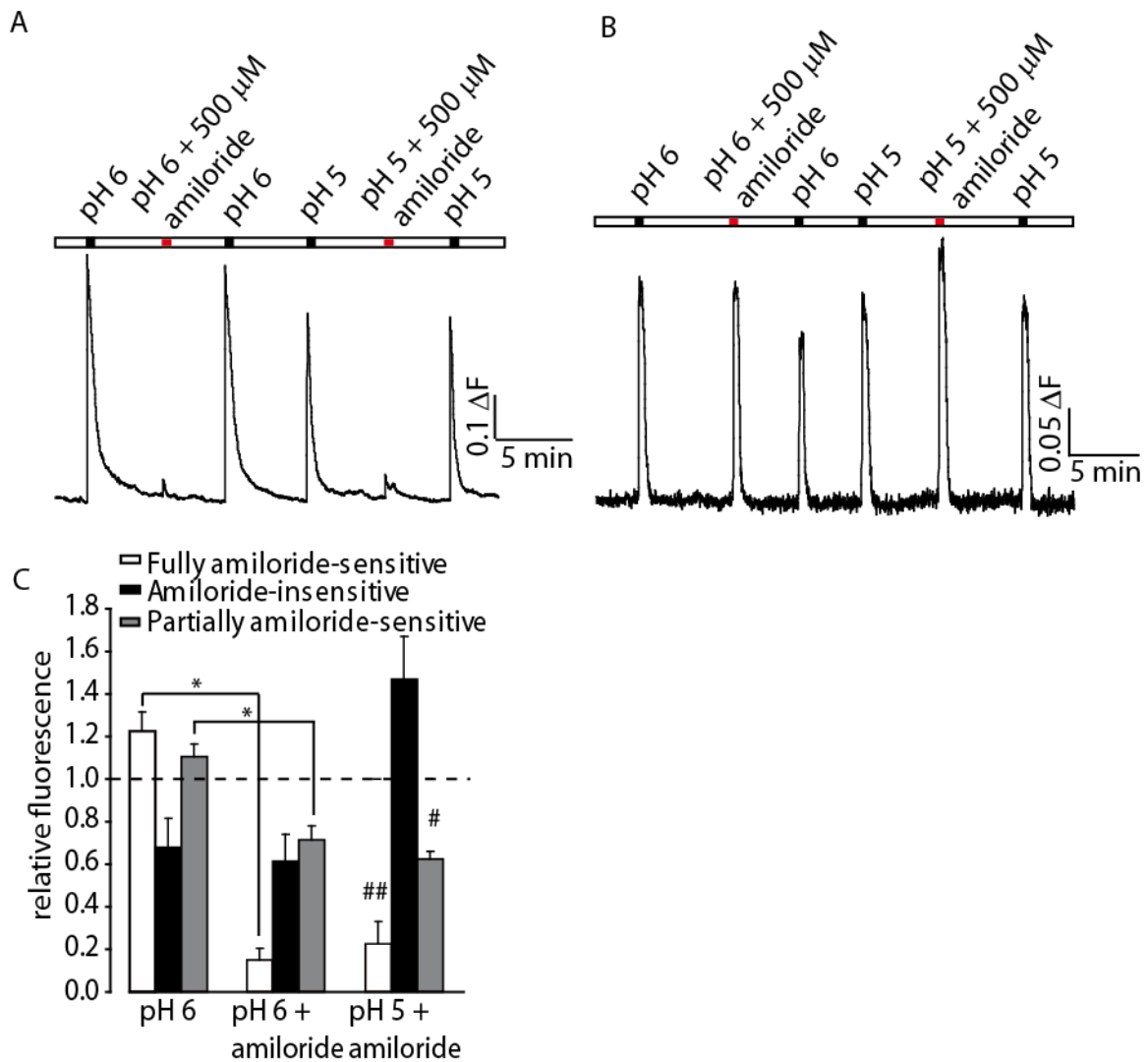


**Figure 16 : Amiloride inhibits the acid-induced  $\text{Ca}^{2+}$  entry in a sub-population of DRG neurons**

Panel A shows a representative trace from an experiment in which amiloride inhibited the increase of fluorescence at pH 5 and pH 6. Panel B shows a representative trace from an experiment in which amiloride had no effect on fluorescence at pH 5 and pH 6. These effects are summarized in panel C. n = 4-5 for each group. \*: p-value < 0.05 compared with “pH 6” value, \*\*: p-value < 0.01 compared with “pH 6” value, #: p-value < 0.05 compared with “pH 5” value, ##: p-value < 0.01 compared with “pH 5” value

In Figure 16, panel A, a representative trace shows that amiloride inhibited the increase in fluorescence at pH 5 and pH 6 in a population of cells. As amiloride acts on ASICs, this population of DRG neurons expressed mainly ASICs, and did almost not express TRPV1. The kinetics of the fluorescence were also compatible with ASICs, as the signal started to decrease still in presence of

acidification, reflecting the inactivation of ASICs. This population of neurons in which 500  $\mu\text{M}$  amiloride inhibited  $\geq 70\%$  of the pH 5 induced  $\text{Ca}^{2+}$  increase was named “Fully amiloride-sensitive”.

On panel B, a typical trace of a amiloride-insensitive neuron is shown. In contrast to panel A, the fluorescence remained high during the extracellular acidification and decreased only when the pH was changed back to pH 7.4. In this population of neurons, the increase in intracellular calcium concentration was mediated by another channel than ASIC, probably TRPV1. In neurons of this population, the pH5-induced increase of intracellular  $\text{Ca}^{2+}$  concentration was not inhibited ( $< 0\%$ ) by 500  $\mu\text{M}$  amiloride. These neurons were named “Amiloride-insensitive”. In some cells, amiloride was partially effective. This partial effectiveness showed that in these cells, ASICs are only partially responsible for the increase of intracellular calcium concentration. In neurons of this population, the pH5-induced increase of intracellular  $\text{Ca}^{2+}$  concentration was inhibited between 50% and 70% by 500  $\mu\text{M}$  amiloride. These neurons were named “Partially amiloride-sensitive”. We did not find any neuron in which the pH5-induced increase of intracellular  $\text{Ca}^{2+}$  concentration was inhibited by 0% - 50% by 500  $\mu\text{M}$  amiloride.

On panel C, the quantification for the three populations is shown. Statistical analysis showed that concerning the “fully amiloride-sensitive” population of neurons, amiloride reduced significantly fluorescence at pH 5 and 6, compared to their control (paired t-test, p-value = 0.019 and 0.004, respectively). For the “Amiloride-insensitive” population of neurons, there was no significant differences between the groups (paired t-test, p-value = 0.461 and 0.078 respectively). The “Partially amiloride-sensitive” population of neurons, showed a significantly reduced fluorescence with amiloride at pH 5 and 6, compared to their control (paired t-test, p-value = 0.042 and 0.013, respectively).

In this experiment, we counted that 31% of the neurons were fully amiloride-sensitive, 38% were amiloride-insensitive and 31% were partially amiloride-sensitive (n=13). It means that 62% of the neurons were expressing ASICs and that 69 % of the neurons were expressing TRPV1, as we believe that the partially amiloride-sensitive neurons express both ASICs and TRPV1. These proportions are comparable with the proportions we observed with immunostaining and in-situ hybridization.

When looking at the traces of the amiloride-sensitive neurons (Figure 16A) and of the amiloride-insensitive neurons (Figure 16B), it is clearly visible that the acid-induced fluorescence of the amiloride-insensitive neurons desensitizes less than the fluorescence of the full amiloride-sensitive neurons. To quantify this desensitization, the ratio of fluorescence after 20 sec of stimulation and peak fluorescence at pH5 was measured for the full amiloride-sensitive and the amiloride insensitive population. The desensitization is measured as the ratio between the fluorescence 20 s after the beginning of the pH5 stimulation and the maximum fluorescence during the stimulation. The Figure 17

shows that the full amiloride-sensitive neurons mainly expressing desensitize significantly faster than and the amiloride insensitive population (unpaired t-test, p-value = 0.003).

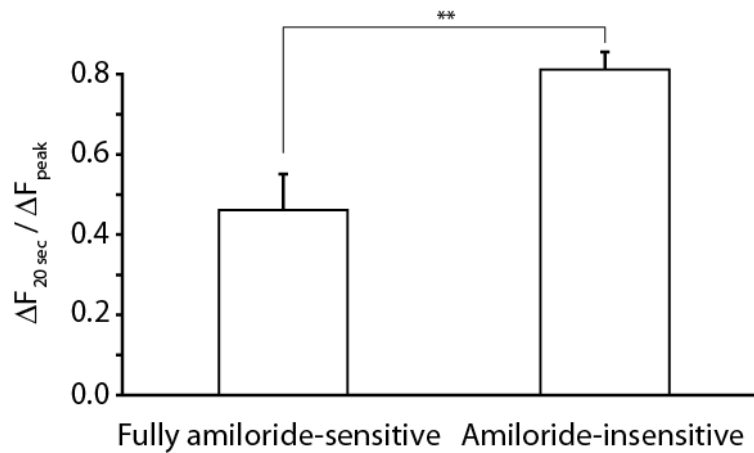


**Figure 17 : Acid-induced fluorescence of the amiloride-insensitive neurons desensitizes less than the fluorescence of the full amiloride-sensitive neurons.**

The ratio of fluorescence after 20 sec of stimulation and peak fluorescence at pH5 was measured for the full amiloride-sensitive and the amiloride insensitive population. The desensitization is measured as the ratio between the fluorescence 20 s after the beginning of the pH5 stimulation and the maximum fluorescence during the stimulation. n = 7 for each group. \*\*: p-value < 0.01, unpaired t-test

### 3.2.3 Psalmotoxin inhibits the activation of ASICs in a population of DRG neurons

In order to analyse the contribution of homomeric ASIC1a channels to the  $\text{Ca}^{2+}$  entry, PcTx1 was used. As mentioned in section 1.2.6.4, PcTx1 blocks homomeric ASIC1a at nanomolar concentrations.

In Figure 18, panel A, a representative trace of the PcTx1-sensitive neuron population is shown. Amiloride abolished almost completely the response at pH 6, indicating that ASICs were responsible for the increase of the intracellular calcium concentration. In the same experiment, 10 nM PcTx1 also abolished the response at pH 6. This shows that in this population of neurons, homomeric ASIC1a channels were responsible for the increase of the intracellular calcium concentration.

Panel B shows a representative trace of a neuron whose response to pH6 was also completely abolished by amiloride. In this experiment, however, PcTx1 was ineffective inhibiting the response to pH 6. This shows that in this population of neurons, different homomeric or heteromeric ASICs were likely responsible for the increase of intracellular calcium concentration.

Panel C shows a typical trace of a neuronal population in which neither amiloride, nor PcTx1 affected the response at pH6, indicating that in these neurons ASICs were not involved in the extracellular acid-induced increase of intracellular calcium concentration, as seen in Figure 16, panel C.

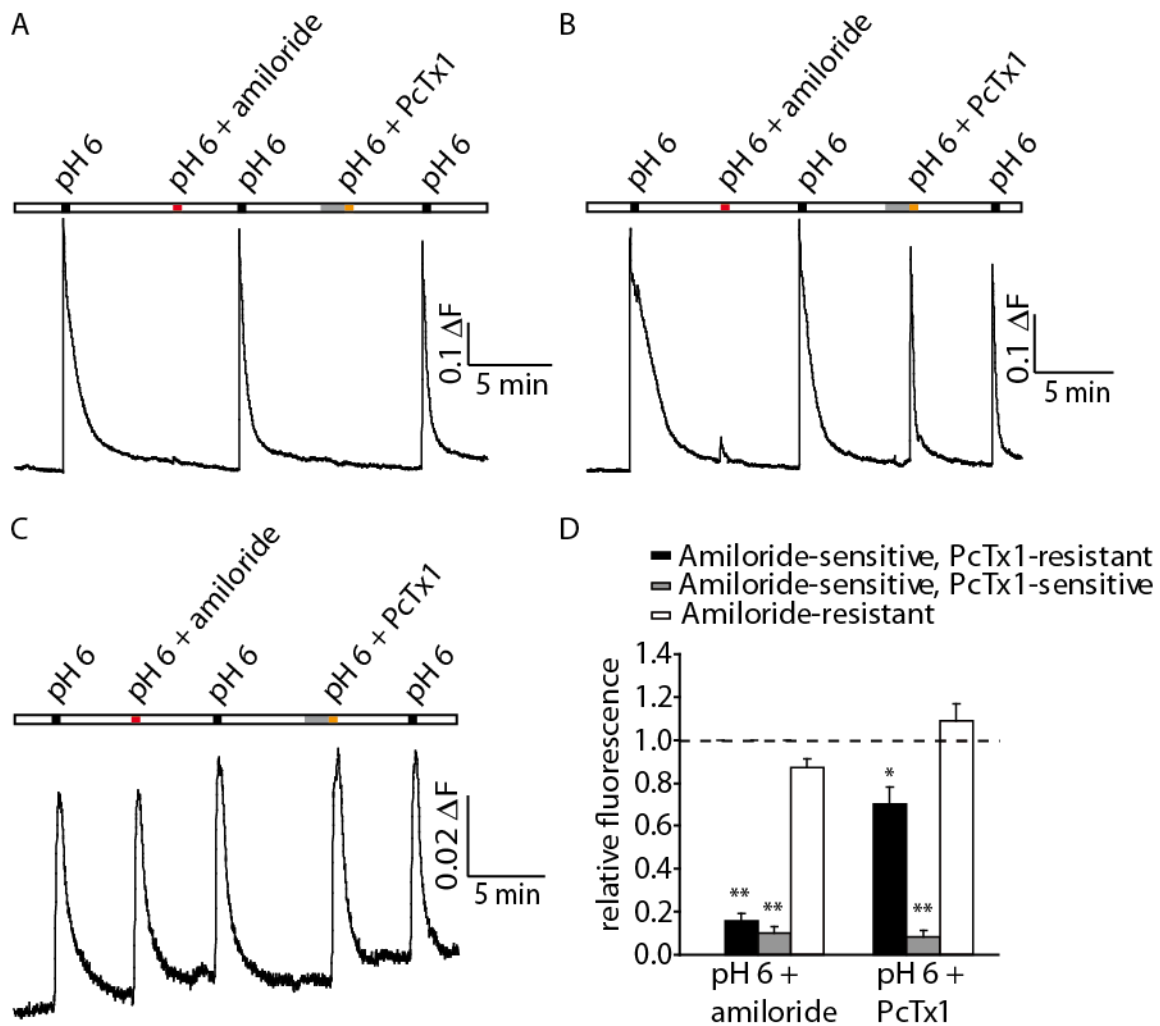


**Figure 18 : PcTx1 inhibits ASIC1a in a population of DRG neurons**

Panel A shows an experiment in which both amiloride and PcTx1 inhibited the increase of fluorescence at pH 6 in a representative neuron. Panel B shows an experiment in which PcTx1 had no effect on fluorescence at pH 6 in a representative neuron which was sensitive to amiloride. Panel C shows an experiment in which both PcTx1 and amiloride had no effect on fluorescence at pH 6 in a representative neuron. These effects are summarized in panel D. n = 5-9 for each group. \*: p-value < 0.05 compared with "pH 6" value, \*\*: p-value < 0.01 compared with "pH 6" value

In panel D, the quantification for the three populations is shown. A paired t-test showed that in the PcTx1-resistant population, amiloride (p-value = 0.006), and PcTx1 (p-value = 0.016) produced a significant decrease of the fluorescence, compared to the values at pH 6. The small (< 30%) decrease of fluorescence in the PcTx1 condition was statistically significant. It reflected a mixed population with homomeric ASIC1a and other ASICs. In the PcTx1-sensitive population (i.e. >70% of the pH6-response inhibited by 10 mM PcTx1), both amiloride (p-value =  $4.19 \times 10^{-5}$ ) and PcTx1 (p-value =  $1.90 \times 10^{-4}$ ) produced a significant decrease of the fluorescence, compared to the values at pH 6. In the amiloride-resistant population, there were no significant difference between the groups (paired t-test, p-value = 0.059 and 0.389).



In this experiment, we counted that 64% of the amiloride-sensitive neurons were also PcTx1-sensitive ( $n = 14$ ). This result is comparable with the previous experiments done in our lab showing that the type 1 current was present in about half of the total neurons (Poirot *et al.*, 2006).

### 3.2.4 $Ca_v$ inhibitors reduce the amplitude of ASIC-mediated $Ca^{2+}$ increase in DRG neurons

Calcium can enter the cell via the homomeric ASIC1a in the population of neurons which are sensitive to PcTx1. In the amiloride-sensitive, but PcTx1-insensitive DRG neuron population, calcium impermeant ASICs are likely involved in the increase of the intracellular calcium concentration showing that ASICs mediated indirectly the entry of calcium. We hypothesized that the entry of sodium through ASICs could depolarize the plasma membrane and that this depolarization could activate  $Ca_v$ . Nifedipine (10  $\mu$ M), Mibefradil (10  $\mu$ M) and  $\omega$ -conotoxin MVIIC (300 nM) were used together as pharmacological tools to inhibit a wide range of  $Ca_v$  (see section 1.4.4.2). The three inhibitors had been tested in patch-clamp experiments on dissociated DRG neurons. It had been shown that these inhibitors at the concentrations mentioned above inhibited the endogenous  $Ca_v$  currents (experiments performed by Maxime Blanchard,  $n=2$ , data not shown). The combination of these three inhibitors is thereafter named as “the  $Ca_v$  inhibitors”.

In Figure 19, panel A, a typical trace of a neuron sensitive to amiloride is shown. In most of the amiloride-sensitive cells, the  $Ca_v$  inhibitors also inhibited a large part of the acid-induced increase of intracellular calcium concentration. At the end of the experiment, the effectiveness of the  $Ca_v$  inhibitors was assessed with KCl-induced (70 mM) depolarisation. Experiments in which the  $Ca_v$  inhibitors were ineffective to block the response to KCl (i.e. inhibition < 60 %) were not taken into account for the analysis.

Panel B shows that the  $Ca_v$  inhibitors were ineffective in blocking the response to an extracellular acidification in a population of cells which was insensitive to amiloride.

In Panels C and D, the quantification of these responses is shown. A paired t-test performed on the results of the amiloride-sensitive population showed that both amiloride and  $Ca_v$  inhibitors were able to significantly reduce the response to an extracellular acidification at pH 6 (p-value = 0.006 and 0.014 respectively). For the amiloride-resistant population a paired t-test showed that the  $Ca_v$  inhibitors did not significantly prevent  $Ca^{2+}$  entry (p-value = 0.322 and 0.384). For both populations, the  $Ca_v$  inhibitors prevented the increase of intracellular  $Ca^{2+}$  concentration after KCl-induced depolarisation (paired t-test, p-value = 0.004 and 0.008 for the amiloride-sensitive and resistant population, respectively).

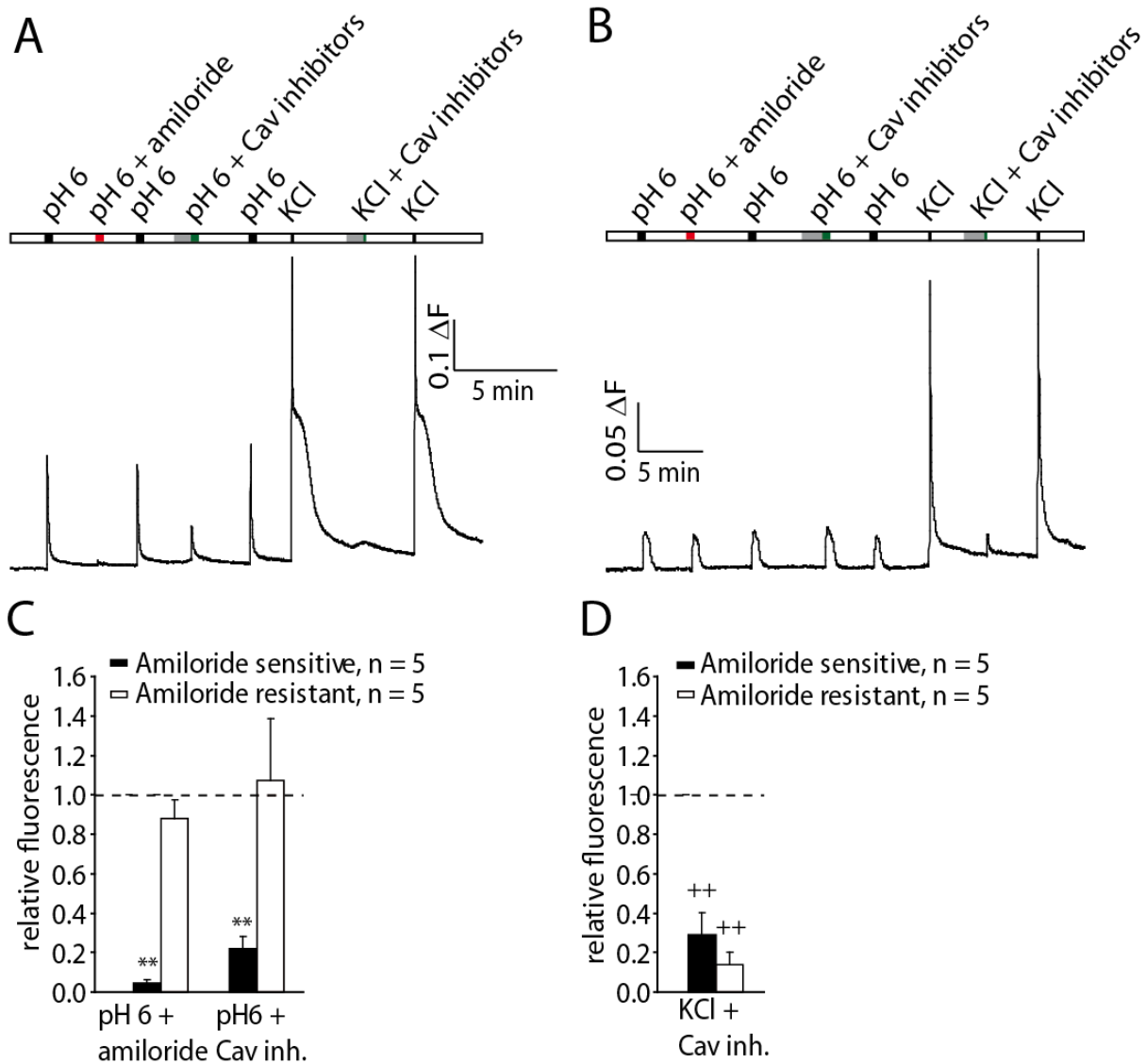


**Figure 19 :  $Ca_v$  inhibitors reduced the pH6-induced increase of  $Ca^{2+}$  concentration in an amiloride-sensitive population of neurons**

Panel A shows an experiment in which the  $Ca_v$  inhibitors reduced the pH6-induced increase of  $Ca^{2+}$  concentration in an amiloride-sensitive neuron. Panel B shows an experiment in which the  $Ca_v$  inhibitors had no effect on the pH6-induced increase of  $Ca^{2+}$  concentration in an amiloride-resistant neuron. These effects are summarised in Panel C. Panel D shows that the  $Ca_v$  inhibitors were able to inhibit the increase of  $Ca^{2+}$  concentration in neurons after a KCl-mediated depolarization of the plasma membrane. \*\*: p-value < 0.01 compared with “pH 6” value, ++: p-value < 0.01 compared with “KCl” value

These experiments confirmed our hypothesis. They indicate that in the amiloride-sensitive population, ASIC channels mediate  $Ca^{2+}$  entry via the activation of the  $Ca_v$  channels and thus do not mediate themselves a sufficiently high  $Ca^{2+}$  entry. In the amiloride-insensitive population, the  $Ca_v$  inhibitors were ineffective. In these cells TRPV1 presumably allowed the entry of calcium.

### 3.2.5 $\text{Ca}_v$ inhibitors do not affect PcTx1-sensitive $\text{Ca}^{2+}$ entry

In the experiments described in Figure 20, PcTx1 was used to identify neurons in which the pH6-induced  $\text{Ca}^{2+}$  entry was mainly due to the activity of homomeric ASIC1a. In the typical trace shown in panel A, the  $\text{Ca}_v$  inhibitors were ineffective to inhibit the pH6-induced increase of intracellular calcium concentration. The  $\text{Ca}_v$  inhibitors prevented partially the increase of intracellular  $\text{Ca}^{2+}$  concentration after KCl-induced depolarisation.

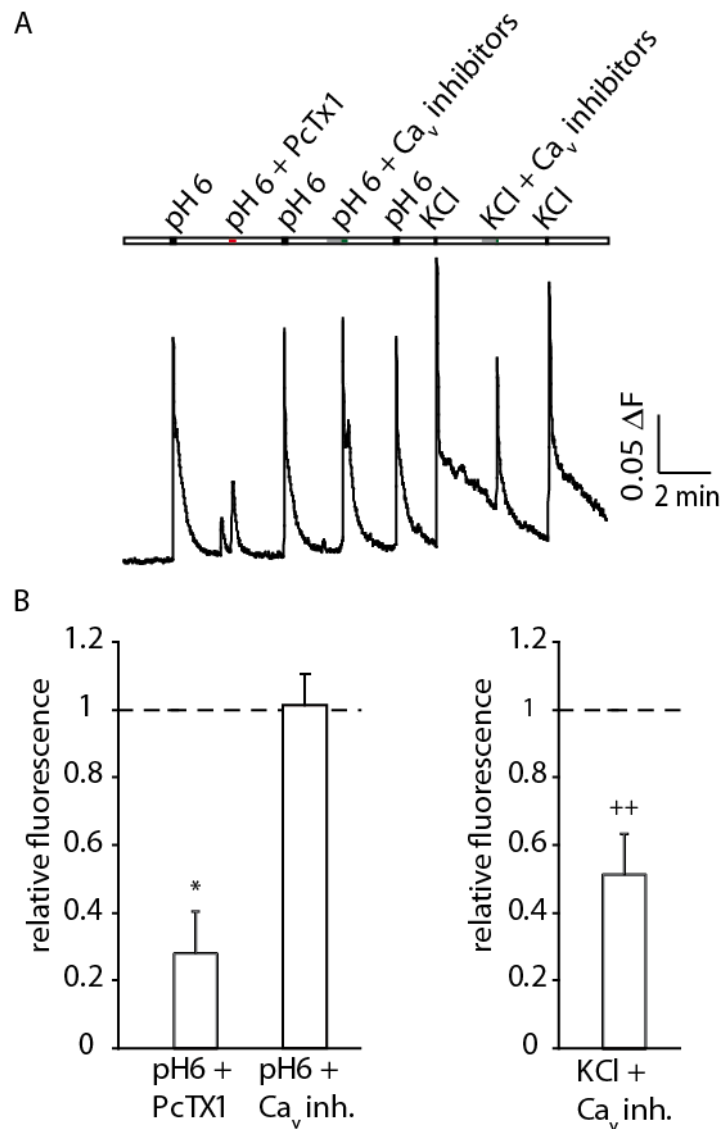


**Figure 20 :  $\text{Ca}_v$  inhibitors had no effect on the pH6-induced increase of  $\text{Ca}^{2+}$  concentration in an PcTx1-sensitive population of neurons**

Panel A shows that  $\text{Ca}_v$  inhibitors did not affect the pH6-induced increase in PcTx1 sensitive neurons. The data are summarized in panel B.  $n = 3$  for each group. \*: p-value < 0.05 compared with “pH 6” value, ++: p-value < 0.01 compared with “KCl” value

In these experiments, only the PcTx1-sensitive neurons (i.e. >60% of the pH6-response inhibited by 10 mM PcTx1) were used. PcTx1 concentration was 10 nM. The  $\text{Ca}_v$  inhibitor concentrations were as

before 10  $\mu$ M for Nifedipine and Mibefradil and 300 nM for  $\omega$ -conotoxin MVIIC. KCl was used at a concentration of 70 mM. Experiments in which the  $\text{Ca}_v$  inhibitors were ineffective to block the response to KCl (i.e. inhibition < 40 %) were not taken into account for the analysis. Unfortunately, in this set of experiments, the  $\text{Ca}_v$  were less effective to inhibit the KCl-induced increase of  $\text{Ca}^{2+}$  concentration, that why we had to choose a lower threshold (40% instead of 60%). That's why the results shown in this figure must be taken with caution. Panel B shows the quantification of the responses. As a population of PcTx1-sensitive neurons was selected, it is obvious that PcTx1 significantly decreased the pH6-induced  $\text{Ca}^{2+}$  entry (paired t-test, p-value = 0.020). The  $\text{Ca}_v$  inhibitors were effective on the KCl responses (paired t-test p-value = 0.005), showing that even if the inhibition of the KCl-mediated depolarisation by  $\text{Ca}_v$  inhibitors was only partially effective, the inhibition was still statistically significant. The  $\text{Ca}_v$  inhibitors did not inhibit the pH6-induced increase of intracellular  $\text{Ca}^{2+}$  concentration (paired t-test, p-value = 0.324). We can conclude that in the population of neurons expressing only ASIC1a homomeric channels and no TRPV1 (i.e. PcTx1-sensitive neurons) activation of homomeric ASIC1a allowed the entry of calcium directly into the cells, as  $\text{Ca}_v$  inhibitors were unable to inhibit the pH6-activated increase of intracellular  $\text{Ca}^{2+}$  concentration.

In Figure 19, we showed that in most of the amiloride-sensitive cells, the  $\text{Ca}_v$  inhibitors also inhibited a large part of the acid-induced increase of intracellular calcium concentration. On the contrary, we showed here that in a population of PcTx1-sensitive neurons, the  $\text{Ca}_v$  inhibitors did not inhibit the pH6-induced increase of intracellular  $\text{Ca}^{2+}$  concentration. As the PcTx1-sensitive neurons population is a subpopulation of the amiloride-sensitive neurons population, it is possible that none or 1 of the 5 amiloride-sensitive cells averaged in Figure 19C were PcTx1-sensitive. A combined experiment with both amiloride and PcTx1 should be made to further understand the role of  $\text{Ca}_v$  in ASIC-mediated increase of intracellular  $\text{Ca}^{2+}$  concentration.

To summarize, in this section we have shown that amiloride prevent  $\text{Ca}^{2+}$  entry through ASICs in a population of DRG neurons; that PcTx1 inhibits the activation of ASICs in another population of DRG neurons; that  $\text{Ca}_v$  inhibitors reduced the amplitude of ASIC-mediated  $\text{Ca}^{2+}$  increase in DRG neurons; and finally that  $\text{Ca}_v$  inhibitors did not affect pH6-mediated  $\text{Ca}^{2+}$  entry into PcTx1-sensitive population of DRG neurons.

### **3.3 CGRP secretion assay on dissociated DRG neurons**

#### **3.3.1 BCTC reduces CGRP secretion induced by an extracellular acidification in DRG neurons**

In order to measure directly the secretion of CGRP from DRG neurons, an *in vitro* assay was used to compare the secretion from neurons in a medium at physiological pH of 7.4 and from neurons exposed

to a more acidic pH. The duration of the secretion experiment was 15 min at 37°C. The amount of secreted CGRP is expressed as a percentage of the total CGRP content of the cells, named “relative CGRP secretion”.

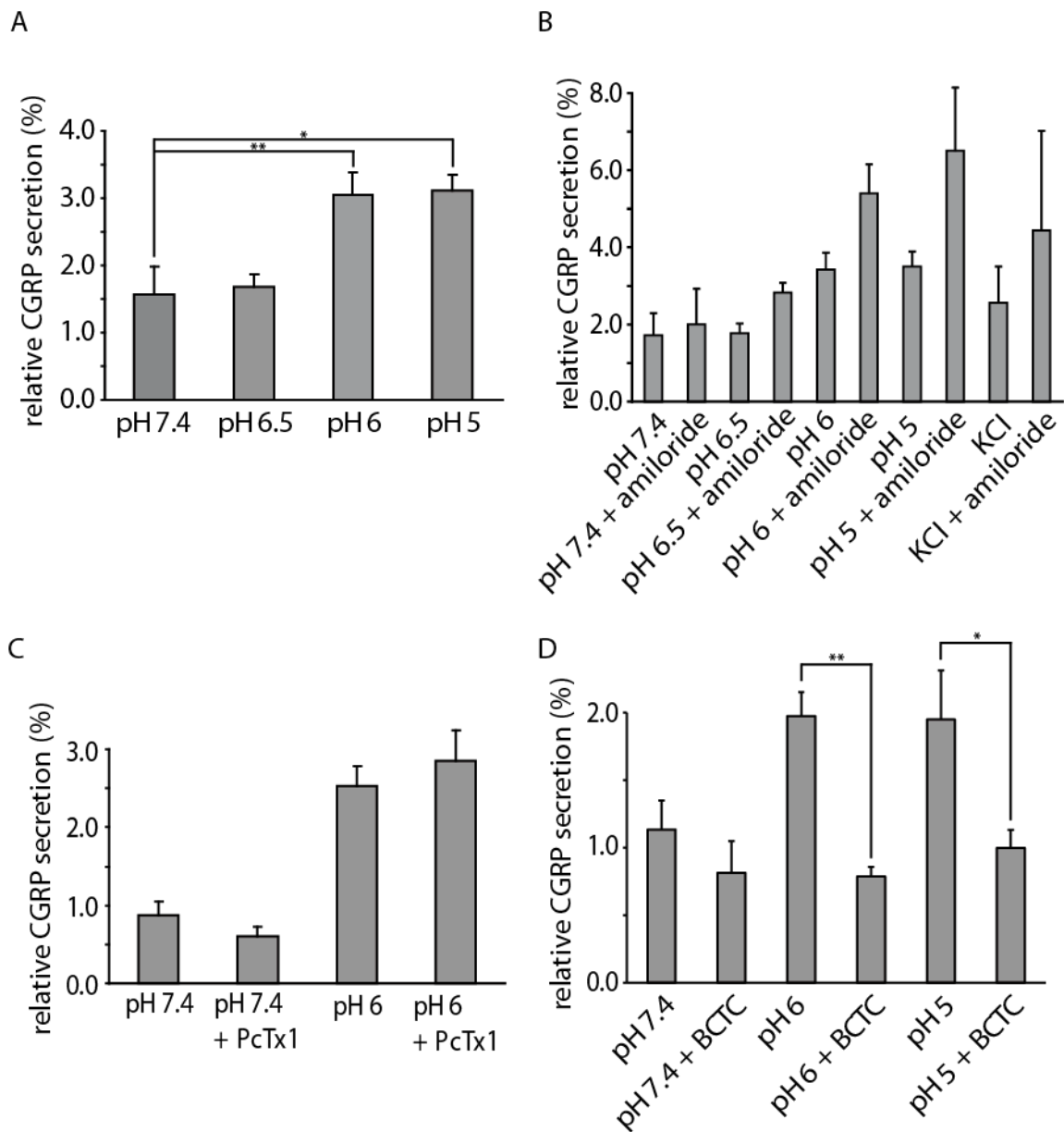


**Figure 21 : Effect of extracellular acidification on CGRP secretion**

The duration of the secretion experiment was 15 min at 37°C. The relative secreted CGRP is expressed as a % of the secreted CGRP to the total CGRP content of the cells. Panel A shows the increase of CGRP secretion at pH6 and pH5. Panel B shows no significant effect of amiloride on acid-induced CGRP secretion. Panel C shows no significant effect of PcTx1 on CGRP secretion. Panel D shows that BCTC reduced the secretion at acidic pH back to pH7.4 secretion. n = 6-12 for panel A, n = 2-5 for panel B, n = 3-5 for panel C, n = 5-9 for panel D. \*: p-value < 0.05, \*\*: p-value < 0.01

Figure 21A shows that extracellular acidification to pH 6 or 5 both significantly increased the neuronal secretion of CGRP compared to the basal level at pH 7.4 (one-way ANOVA, followed by a Tukey post-hoc test, p-values = 0.012 and 0.045, respectively). An acidification to pH 6.5 did not increase the secretion, compared to the basal level at pH 7.4 (Tukey post-hoc test, p-value = 0.991).

In experiments presented on panels B and C, amiloride (500  $\mu\text{M}$ ) and PcTx1 (10 nM) were used as ASICs inhibitors to test for an involvement of ASICs in CGRP secretion. There were no significant differences between conditions with or without inhibitors (one-way ANOVA, followed by a Tukey post-hoc test). There was even a tendency for amiloride to increase the CGRP release, perhaps caused by non-specific effects of amiloride. In this context, amiloride is probably not an ideal inhibitor (see Discussion).

In the experiments presented in panel D, the TRPV1 inhibitor BCTC (1  $\mu\text{M}$ ) was able to significantly reduce the CGRP secretion at pH 6 and 5 (one-way ANOVA, followed by a Tukey post-hoc test, p-value = 0.007 and 0.03 respectively). These experiments show that TRPV1 is involved in the CGRP secretion triggered by an extracellular acidification. Even if these experiments were not able to demonstrate a role for ASICs in this secretion, we cannot totally exclude such a role (see Discussion).

In Figure 22 effects of  $\text{Ca}_v$  and  $\text{Na}_v$  inhibitors on CGRP secretion are shown. On panel A,  $\text{Ca}_v$  inhibitors (Nifedipine (10  $\mu\text{M}$ ), Mibefradil (10  $\mu\text{M}$ ) and  $\omega$ -conotoxin MVIIC (300 nM)) had no significant effects on the secretion induced by an acidic extracellular solution (one-way ANOVA, followed by Tukey post-hoc tests). The inhibitors reduced however the secretion induced by 70 mM extracellular KCl (one-way ANOVA, followed by a Tukey post-hoc test, p-value = 0.009). At the same time this experiment indicates that the  $\text{Ca}_v$  are not involved in the extracellular acid-induced CGRP secretion.

In experiments presented on panel B, the  $\text{Na}_v$  inhibitors TTX (1  $\mu\text{M}$ ) and lidocaine (10 mM) were used. TTX or lidocaine separately had no significant effect on the CGRP secretion (one-way ANOVA, followed by a Tukey post-hoc test, p-value = 0.41 and 0.83). If applied together, lidocaine and TTX induced a small inhibition of secretion (Tukey post-hoc test, p-value = 0.007). These experiments do therefore indicate that  $\text{Na}_v$ -mediated depolarization play a role in the secretion of CGRP.

To conclude, the only effective and strong inhibitor in these experiments was BCTC. This indicates that TRPV1 is a major component of the detection of acidification that leads to CGRP secretion in these DRG neurons.  $\text{Na}_v$  channel also play a role in these secretion. The exact mechanism which mediate the  $\text{Na}_v$ -dependant CGRP secretion would necessitate more investigation to be elucidated. Likely, the  $\text{Na}_v$ -induced depolarization potentiates the  $\text{Ca}_v$  activation.

The Na/Ca exchanger (NCX) could also play a role in the secretion of CGRP. Na/Ca exchange is a mechanism that allows  $\text{Ca}^{2+}$  extrusion from the cell against its gradient without energy consumption. It is the entry of  $\text{Na}^+$  along its electrochemical gradient that provides the energy for  $\text{Ca}^{2+}$  extrusion. As NCX is electrogenic and voltage sensitive, it can reverse during cellular activation and contribute to  $\text{Ca}^{2+}$  entry into the cell (Blaustein & Lederer, 1999). As NCX are expressed in rat DRG neurons

(Verdru *et al.*, 1997), we cannot exclude that NCX could play a role in  $Ca^{2+}$  entry after an acid-induced depolarization, and therefore been implicated in an acid-induced CGRP secretion. Further experiments involving NCX inhibitors would be needed to assess the exact role of NCX in neuropeptides secretion.

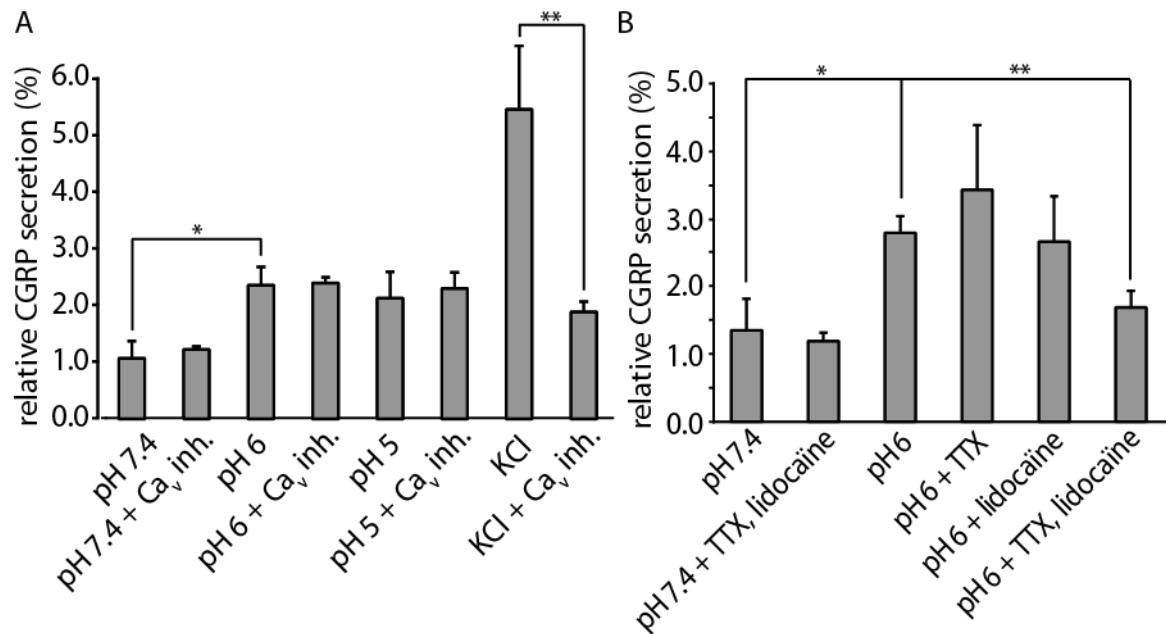


**Figure 22 : Co-application of TTX and lidocaine reduce acid-mediated CGRP secretion**

Panel A shows that Cav inhibitors had no significant effects on acid-induced CGRP secretion. Panel B shows that co-application of Nav inhibitors TTX and lidocaine reduced acid-mediated CGRP secretion. n = 2-7 for panel A, n = 2-8 for panel B \*: p-value < 0.05, \*\*: p-value < 0.01

### 3.4 Behavioural experiments on ASIC1, ASIC2 and ASIC3 null mice.

#### 3.4.1 Mechanical allodynia-like behaviour induced by spared nerve injury (SNI) is not different from wild type in ASIC1a, -2 and 3 null mice

We hypothesized that ASICs could have a role in neuropathic pain. This hypothesis was formulated based on the observation that in the SNI model of neuropathic pain performed on rats, the expression and function of different ASIC subunits in DRG neurons was changed (Poirot *et al.*, 2006). To test this hypothesis, we applied the SNI model to three different mouse strains deficient of ASIC1a, -2 or -3. The mechanical allodynia induced by the nerve injury in the ipsilateral hindpaw was assessed with von Frey filaments. The ipsi- and the contralateral paw were stimulated 10 times each with filaments of increasing forces (see Methods for details). The number of response (i.e. the mouse withdraws its paw) out of 10 was recorded for each mouse, at different time points before and after the surgery. The selected time points in the following experiments are two baseline values and measurements taken at 3, 9, 15 and 21 days after SNI surgery. As illustrated in Figure 23 for ASIC3 null mice and wild type



littermates, it has been previously shown that for wild type mice, the SNI model increases the allodynia over time until a plateau phase is reached (Bourquin *et al.*, 2006). ASIC1a, -2 and -3 null mice were compared to wild type littermates. The experimenter did not know the genotype of the mice during the experiment.

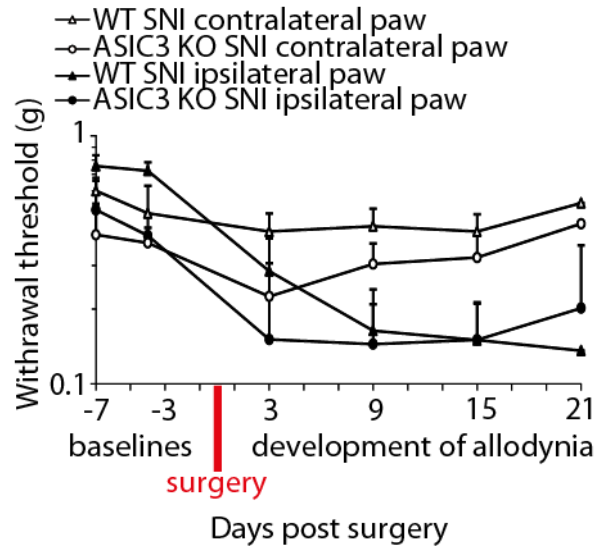


**Figure 23 : Mechanical withdrawal threshold decreases significantly in ipsilateral paws after SNI for both ASIC3 knockout mice and wild type mice**

The relative frequency of paw withdrawal at two different time points, one before and one after the surgery, is shown in Figure 24. For all mice, there was a significant difference between the ipsi- and contralateral paw starting from the third to the ninth post-operative day and persisting for the duration of the experiment (two-way analysis of variance (ANOVA), with time treated as a repeated measure), indicating that the mechanical allodynia was induced by the SNI model (data not shown).

On panel A, results for ASIC1a null mice (n=10) and wild type littermates (n=10) are shown. There were no differences between the wild-type and the ASIC1a null mice at baseline 2 and at 21 days after SNI.

On panel B, results for ASIC2 null mice (n = 19 for baseline 2, n = 9 for 21 day SNI) and wild type littermates (n = 18 for baseline 2, n = 8 for 21 day SNI) are shown. There were no differences between the wild-type and the ASIC2 null mice at baseline 2 and at 21 days after SNI.

On panel C, results for ASIC3 null mice (n = 8) and wild type littermates (n = 7) are shown. There were no differences between the wild-type and the ASIC3 null mice at baseline 2. There was however a significant difference between the wild-type and the ASIC3 null mice at 21 day after SNI (p-value < 0.0001). ASIC3 null mice were less sensitive than wild type littermates.

Panel D shows that mechanical withdrawal threshold decreases significantly in ipsilateral paws after SNI.

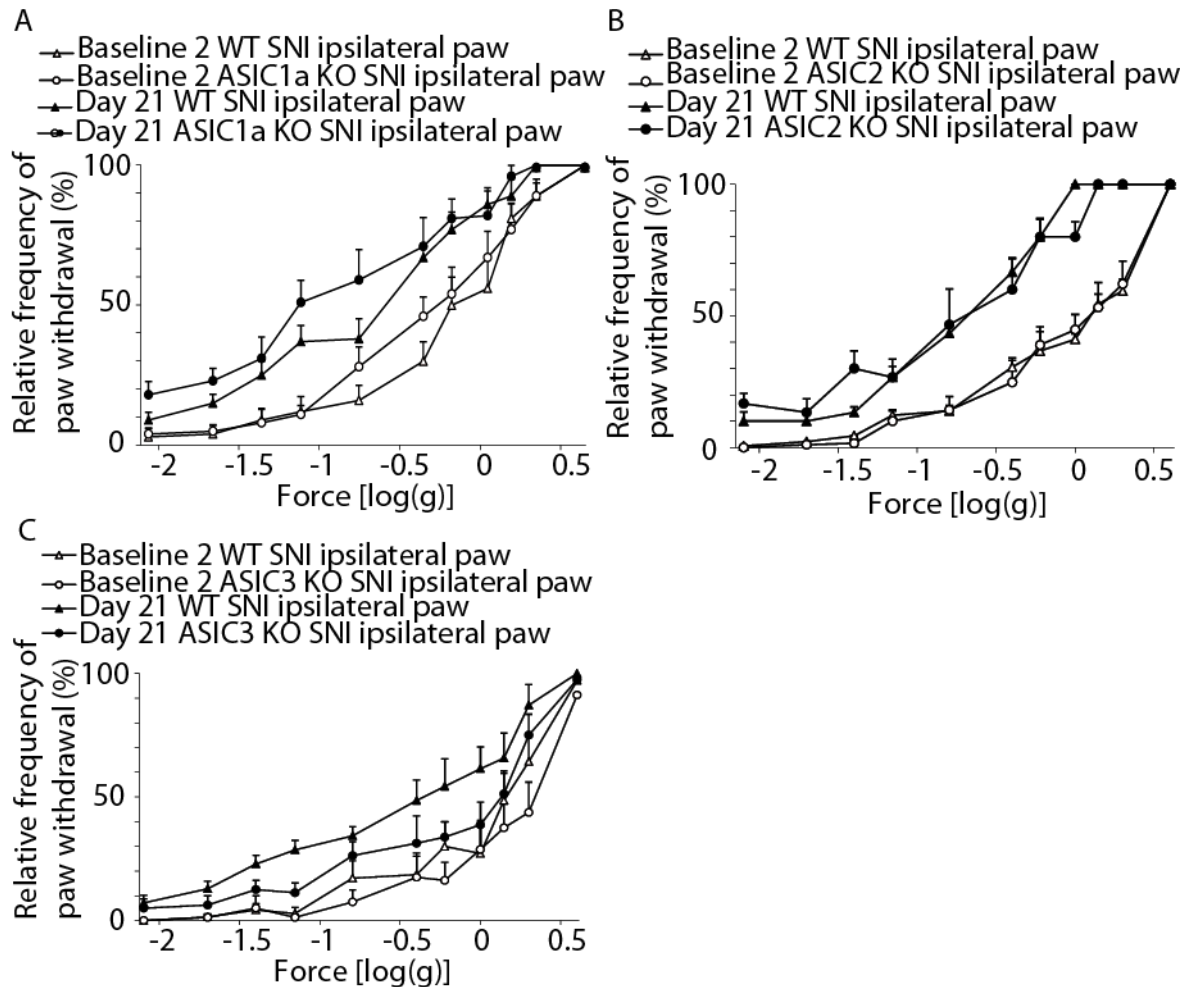


**Figure 24 : Relative frequencies of paw withdrawal are not significantly different in both wild type and null mice following SNI**

Mechanical allodynia-like behaviour induced by spared nerve injury (SNI) is not different in ASIC1a (panel A), -2 (panel B) and 3 (panel C) null mice, compared to their respective wild type littermates. n = 10 mice per group for panel A, n = 8-19 mice per group for panel B, n = 7-8 mice per group for panel C and D.

To summarize, our study shows that there were no differences between the wild-type and the ASIC1, or ASIC2, null mice at baseline 2 and at 21 days after SNI. There was a significant difference between the wild-type and the ASIC3 null mice at 21 day SNI. ASIC3 null mice were less sensitive than wild type littermates. This shows that ASIC3 must be important in the development of allodynia after a nerve injury.

### 3.4.2 ASIC2 null mice exhibit a reduced thermal allodynia-like behavior in the hot plate test

We then decided to investigate the role of ASICs in thermal sensitivity, as it is almost unknown for ASIC1 and ASIC2. Figure 25 shows thermal allodynia assessed with tail flick and hot plate apparatus.

The tail flick test measures spinal nociception and it is based on the sensitivity of the mouse to temperature. Panels A, C and E show the results for the Tail Flick experiments. There were no significant differences between ASIC1a null mice (n = 10) and wild type littermates (n = 10), between ASIC2 null mice (n = 20) and wild type littermates (n = 20), nor between ASIC3 null mice (n = 10) and wild type littermates (n = 10) (t-test, p-value = 0.34, 0.16 and 0.37 respectively).

The hot plate test is widely used to determine supraspinal nociception. Panels B, D and F show the results for the hot plate experiments at 49, 52, and 55°C for respectively ASIC1a, ASIC2 and ASIC3 null mice. There was a significant difference at each temperature between ASIC1a and wild-type littermates (t-test, p-value = 0.041, 0.001, 0.003, respectively), and between ASIC2 null mice and wild-type littermates (t-test, p-value = 0.0002, 0.005, 0.0006, respectively). ASIC1a null mice had increased thermal allodynia behaviours with the hot plate compared to wild type littermates. On the contrary, ASIC2 null mice had reduced thermal allodynia behaviours with the hot plate compared to wild type littermates. There was no significant differences at each temperature between ASIC3 null mice and wild-type littermates (t-test, p-value = 0.26, 0.35, 0.72, respectively).

To summarize, there was no difference between the different null mice and their littermates in the tail-flick test. ASIC1a null mice were more sensitive and ASIC2 null mice were less sensitive to hot temperature in the hot plate test, compared to wild type littermates. ASIC3 null mice were no different from their wild type littermates in the Hot Plate test. These results indicate that ASIC1a and ASIC2 must play a role in thermal sensation. As the effects were opposite in ASIC1a and in ASIC2 null mice, ASIC1a and ASIC2 should be involved in different mechanisms.

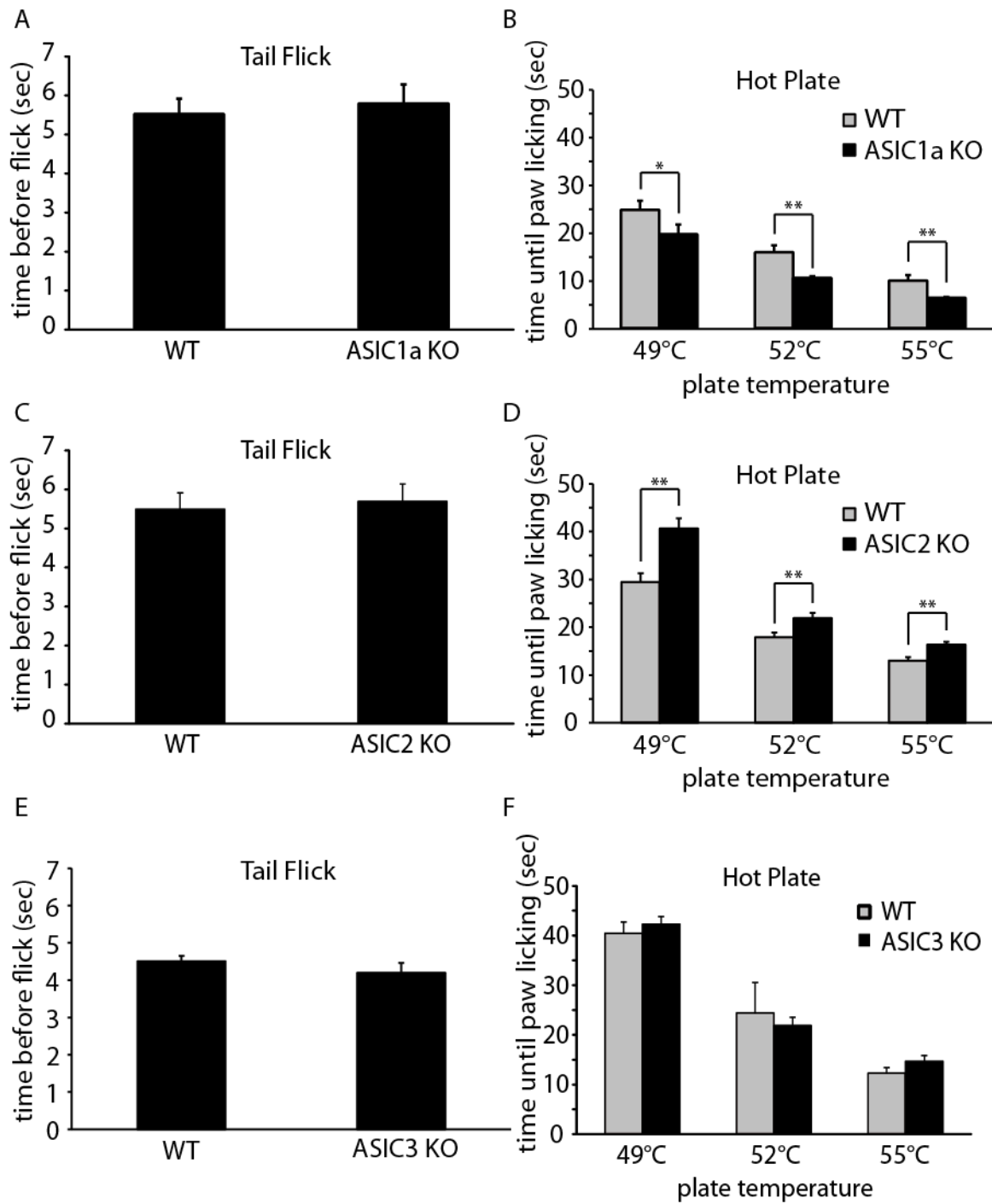


**Figure 25 : ASIC1a and ASIC2 null mice showed a significant difference in thermal with the hot plate test**

Panels A, C and E show no difference between ASIC1a, ASIC2 and respectively ASIC3 null mice and their wild type littermates with the tail flick test. Panel B shows increased thermal allodynia behaviour with the hot plate test between ASIC1a null mice and wild type littermates. Panel D shows reduced thermal allodynia behaviour with the hot plate test between ASIC2 null mice and wild type littermates. Panel F shows no difference for thermal allodynia behaviour with the hot plate test between ASIC3 null mice and wild type littermates. \*: p-value < 0.05, \*\*: p-value < 0.01

## 4. Discussion

### 4.1 Expression of the different ASIC subunits and of neuropeptides

#### 4.1.1 Advantages and limitations of immunocytochemistry and in-situ hybridization

Immunocytochemistry and in-situ hybridization were used to determine the distribution of the different ASIC subunits in two populations of DRG neurons, the peptidergic and the non-peptidergic neurons. The main aim was to identify populations of DRG neurons which expressed different ASICs subunits, and to test for a possible correlation or co-expression between ASICs subunits and neuropeptides, and also between two different ASICs subunits. The main limitation of this technique is that it is only possible to measure the distribution of one ASIC subunit with one neuropeptide or one other ASIC subunit.

The advantage of immunocytochemistry is that it detects the proteins. There are some limitations of this technique. The first limitation is that the available antibodies are not able to distinguish the splice variants (ASIC1a vs -1b, ASIC2a vs -2b). The second limitation is the quality of the antibodies. Most antibodies against ASICs are more or less efficient in recognising the proteins in a heterologous expression system, but most of them fail to specifically recognise ASICs in DRG neurons, except the two antibodies against ASIC1 and ASIC2, respectively, that were used in this study. Among all the antibodies we tested, we were only able to use one anti-ASIC1 and one anti-ASIC2 which were previously correctly tested, i.e. tested on tissues or neurons from knock-out mice.

In order to detect the different splice variants ASIC1a, -1b, -2a, -2b and the ASIC3 isoform, we decided to switch to another method; the in-situ hybridization. The main advantage is, as previously mentioned, that all ASICs subunits can be distinguished. The main limitation of the technique is that it measures mRNA levels, thus it allows to detect cells expressing the mRNA of the different isoforms of ASICs, and not the proteins. Generally, the presence of a specific mRNA in a cell is a good indication that the corresponding protein is expressed, but regulation of the translation cannot be excluded.

As already mentioned in the introduction, C-fiber nociceptors can be divided into two groups in which one class depends on NGF during postnatal development and contains neuropeptides, and the second class depends on GDNF during postnatal development and contains few neuropeptides but binds IB4 (Basbaum *et al.*, 2009). In our study, all ASICs were expressed in a higher fraction of the peptidergic population than the non-peptidergic population.

#### 4.1.2 Comparison between the labelling of ASICs and the different types of ASIC currents

Previously, an electrophysiological characterization of the different ASICs currents in dissociated rat DRG neurons was done by our group. The results showed that small-diameter DRG neurones expressed three different ASIC current types. Type 1 currents were mediated by ASIC1a homomultimers and characterized by steep pH dependence of current activation in the pH range 6.8–6.0. Type 3 currents were activated in a similar pH range as type 1, while type 2 currents were activated at pH<6. PcTx1-sensitive ASIC1a current was predominantly found in IB4 negative, thus peptidergic neurons (Poirot *et al.*, 2006). Staining done on dissociated DRG neurons confirmed that the ASIC1a subunit was predominantly expressed in peptidergic neurons.

For ASIC1a, the electrophysiological experiments had identified a large population of DRG neurons which expressed only ASIC1a homomeric channels (type 1 current). In a different sub-population, ASIC1a likely participated in forming heteromeric channels with ASIC3 and probably other subunits giving rise to type 3 currents (Poirot *et al.*, 2006). It should be noted that electrophysiological and biochemical experiments are not directly comparable. Our immunocytochemistry and in-situ hybridization showed that there are few neurons that express only ASIC1a. These results are in contradiction with the large population of expressing a type 1 current. Electrophysiological experiments give information on functional ASIC complexes present at the surface of the cell. Biochemical experiments give information on the whole cellular expression of ASICs protein or mRNA. Immunocytochemical and in situ hybridization experiments provide information about the expression of ASIC1a in a neuron, but not on the multimerization of the channel. Nevertheless, as we have shown that most ASIC subunits are expressed in the peptidergic neurons, it seems difficult to be compatible with the presence of pure homomeric ASIC1a current, as these neurons likely only express ASIC1a subunits at the cell surface.

#### 4.1.3 Comparison of the results of expression of ASICs, TRPV1, CGRP and SP with the literature

In the following I compare our results with previous studies. One study involved an electrophysiological characterization of dissociated DRG neurons from adult rats. The DRG neurons were classified in nine different types according to their immunoreactivity to CGRP or SP and their patterns of capsaicin-, proton-, and ATP-activated currents. Out of these nine types, five were analysed. They formed distinct populations of capsaicin sensitive, ATP sensitive and proton sensitive cells with uniform current kinetics, pharmacology and histochemistry. Interestingly, a type of neuron expressed CGRP and TRPV1 and another one expressed fast desensitizing ASICs with a non-desensitizing component. Two other populations did not express neuropeptides, but either ASICs or TRPV1 (Petruska *et al.*, 2000). In a follow-up study, they discovered that the four other populations of

neurons formed distinct populations of medium sized capsaicin-sensitive and -insensitive cells that all expressed amiloride-sensitive, ASIC currents. The presence of ASIC currents was associated with the expression of neuropeptides SP and/or CGRP (Petruska *et al.*, 2002). These results are consistent with our immunocytochemical and in-situ hybridization results that showed that ASIC1a, -1b, -3 and TRPV1 are preferentially expressed in neuropeptides neurons. It is difficult to compare our proportion of expression of the different ASICs and TRPV1 with neuropeptides with the proportion of the different cluster described in these studies, as it is not possible to calculate the proportions of neurons in their second study. The first study shows that ASICs and CGRP/SP are co-expressed in the cluster 7 which represent 7 % of all neurons described in the study neurons of cluster 3 express ASICs but does not express neuropeptides in a proportion of 20 %. In the second study, the 4 remaining clusters express all neuropeptides and ASICs. As the neurons of these 4 clusters were the only ones to be measured in this study, it is impossible to calculate the proportion of each cluster. Nevertheless, the co-expression of ASICs and neuropeptides in 5 of the cluster likely shows a relatively high level of coexpression of ASICs with neuropeptides. These results were also confirmed in mice. It was found that IB4-negative neurons are the major class of unmyelinated neurons that responds to protons and capsaicin. IB4-negative unmyelinated neurons selectively expressed transient proton currents and these transient currents were reversibly blocked by amiloride, i.e. were mediated by ASICs. Furthermore, the authors think that a likely candidate for the sustained-only proton current was the capsaicin receptor TRPV1 (Dirajlal *et al.*, 2003). A study demonstrated with a double immunofluorescence method that many ASIC3-immunoreactive neurons co-expressed CGRP in the jugular (about 80%) and petrosal ganglia (about 60%), confirming our results. It must be noted here that this result should be taken with caution, as the anti-ASIC3 antibody they were using was not working in our hands, and they did not carry out the necessary controls (Fukuda *et al.*, 2006). In-situ hybridization on ASIC1a, -1b, -3 and TRPV1 has also been performed by a research group. They found that ASIC1a transcripts were expressed in 20-25% of the small diameter rat DRG neurons. ASIC1b was expressed in about 10% of neurons and ASIC3 in 30-35% of the neurons (Ugawa *et al.*, 2005). We also found that ASIC1b was less expressed than ASIC1a and ASIC3. The striking difference is that our results show more neurons expressing ASICs than in this paper (about 60 % for ASIC1a, 35-40% for ASIC1b and about 50 % for ASIC3). The most likely explanation is that they used radioactive probes which were less sensitive than our DIG-labelled probes detected with an anti-DIG antibody coupled to a fluorophore which amplified the signal. They found that TRPV1 was expressed in 35-40% of neurons, which was not so different from what we found with immunocytochemistry (45-55%).

For this part, we conclude that our results showing that ASIC1a, -1b, -3 and TRPV1 are preferentially expressed in the peptidergic population are confirmed in the literature by similar or completely



different methods (electrophysiology). We show here an interesting complete characterization of the expression of all ASIC subunits (except the non-conducting ASIC4) and TRPV1 and of their expression with neuropeptides CGRP and SP.

## **4.2 Increase of intracellular calcium concentration via ASICs and TRPV1**

### **4.2.1 Effect of amiloride on the intracellular $\text{Ca}^{2+}$ concentration of CHO cells expressing ASIC1a**

Amiloride induced a concentration dependent reduction of the increase of intracellular calcium concentration during an acidification. This demonstrates that ASIC1a homomeric channels are able to allow a significant increase of intracellular calcium concentration. This experiment was not able to show us the exact mechanism of increase of intracellular concentration. Obviously, calcium entered the cell via ASIC1a. It is not known if the totality of the calcium enters via ASIC1a, or if a small amount of calcium entering the cell via ASIC1a could trigger intracellular mechanisms that could release  $\text{Ca}^{2+}$  from intracellular stores.

### **4.2.2 Effect of amiloride on the intracellular $\text{Ca}^{2+}$ concentration of DRG neurons**

Calcium imaging experiments were then performed on dissociated rat DRG neurons to understand how the intracellular calcium concentration of the neurons changes during an extracellular acidification. We showed that 500  $\mu\text{M}$  amiloride prevented the increase of fluorescence at acidic pH by  $\geq 70\%$  in a population of cells that we named “Fully amiloride-sensitive”. As amiloride acts on ASICs and not TRPV1, this population of DRG neurons likely expressed mainly ASICs, and almost did not express TRPV1. The kinetics of the fluorescence were also compatible with ASICs, as the signal started to decrease still in presence of the acidification, reflecting the inactivation of ASICs. The kinetics would certainly be different if TRPV1 was involved, as TRPV1 does not inactivate. The calcium concentration remained high during the extracellular acidification and decreased only when the pH came back to pH 7.4. Likely this increase of calcium was mediated by a channel which does not inactivate, probably TRPV1 (see Figure 17). In the last population of cells which we named “Partially amiloride-sensitive” the amiloride was partially effective. This partial effectiveness showed that in these cells, as amiloride was only able to inhibit partially the increase of intracellular calcium concentration, ASICs were only partially responsible for this increase.

### **4.2.3 Effect of PcTx1 on the intracellular $\text{Ca}^{2+}$ concentration of DRG neurons**

In order to further analyse the “Amiloride-sensitive” population, in other words the population expressing ASIC channels responsible for the increase of intracellular calcium concentration, PcTx1, a toxin that inhibits homomeric ASIC1a channels, was used. It is useful here to remind that it has been extensively described in the literature that all ASIC channels are permeable for sodium but not for

divalent cations, except for ASIC1a homomeric channels which are permeable to sodium and calcium. The contribution of homomeric ASIC1a channels to the increase of intracellular  $\text{Ca}^{2+}$  concentration in neurons expressing ASICs but no TRPV1 was tested. PcTx1 abolished in a subpopulation the response to extracellular acidification. This indicates that in this subpopulation of neurons, ASIC1a homomeric channels were responsible for the increase of intracellular calcium concentration. There was also a neuronal population in which neither amiloride, nor PcTx1 affected the  $\text{Ca}^{2+}$  concentration at pH6, indicate that in these cells that ASICs were not involved in the extracellular acid-induced increase of intracellular calcium concentration. Considering that the “Partially amiloride-sensitive” population of neurons express both ASICs and TRPV1, 62% of the measured neurons expressed ASICs, 69% expressed TRPV1 and 20% only ASIC1a homomeric channels (31% of fully amiloride-sensitive neurons \* 64% of the amiloride-sensitive neurons which were also PcTx1-sensitive). The proportions for ASICs and TRPV1 are compatible with our results of the immunocytochemistry and in situ hybridization experiments. As previously mentioned, the immunocytochemistry and in situ hybridization experiments do not allow to know the oligomerization state of a channel, it is therefore difficult to discuss the ratio of ASIC1a homomeric channels. As PcTx1 is highly specific for homomeric ASIC1a, there is no doubt that the inhibition of increase of intracellular calcium concentration by this toxin reflects the inhibition of homomeric ASIC1a channels in our experiments. Nevertheless, we cannot exclude here that the entry of  $\text{Na}^+$  via ASIC1a could indirectly trigger the increase of intracellular calcium concentration by activating voltage-gated  $\text{Ca}^{2+}$  channels.

#### 4.2.4 Effect of $\text{Ca}_v$ s on the intracellular $\text{Ca}^{2+}$ concentration of DRG neurons

As previously mentioned, calcium can enter the cell via the homomeric ASIC1a in the population of neurons which are sensitive to PcTx1. In the amiloride-sensitive, but PcTx1-insensitive DRG neuron population, calcium impermeant ASICs were involved in the increase of intracellular calcium concentration, thus the ASICs mediated indirectly the entry of calcium. Since we know that the entry of  $\text{Na}^+$  through ASICs can depolarize the plasma membrane, our hypothesis is that this depolarization can activate  $\text{Ca}_v$ s.

In order to evaluate the role of  $\text{Ca}_v$  channels, three inhibitors (“the  $\text{Ca}_v$  inhibitors”) Nifedipine, Mibefradil and  $\omega$ -conotoxin MVIIC were used together as pharmacological tools to inhibit a wide range of  $\text{Ca}_v$ . In most of the amiloride sensitive cells, the  $\text{Ca}_v$  inhibitors also blocked a large part of the acid-induced increase of intracellular calcium concentration. This result is consistent with the pathway depicted at the right of the Figure 26. The  $\text{Ca}_v$  inhibitors were ineffective to block the response to an extracellular acidification in a population of cells which were insensitive to amiloride. As previously mentioned, this population expresses TRPV1 as the main sensor of extracellular acidification. TRPV1 being highly permeant to calcium (Caterina *et al.*, 1997; Mohapatra *et al.*, 2003; Samways *et*

*al.*, 2008),  $Ca_v$  are not necessary to allow an increase on the intracellular calcium concentration. It cannot be excluded that the  $Ca_v$  played a role in the increase of intracellular calcium concentration in those cells.

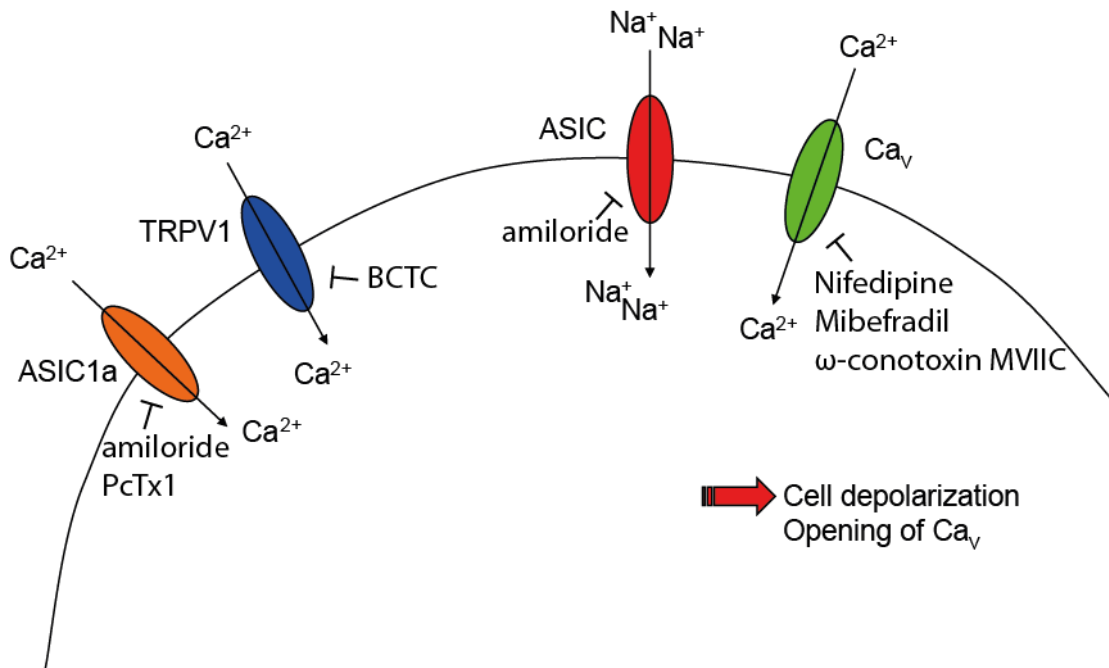


**Figure 26: Schematic drawing of a neuron expressing ion channels**

The drawing shows on the left homomeric ASIC1a channels which can be inhibited with PcTx1 and TRPV1 which can be inhibited by BCTC. On the right, it shows that an entry of Na<sup>+</sup> through amiloride-sensitive ASICs can depolarize the cell. In our hypothesis, this depolarization could activate Cav<sub>s</sub> and allow an entry of calcium, even in absence of homomeric ASIC1a or TRPV1. This depolarization is inhibited by Cav<sub>s</sub> antagonists Nifedipine, Mibefradil and ω-conotoxin MVIIC.

PcTx1 was used to isolate the population of cells which expressed homomeric ASIC1a. In this population, the  $Ca_v$  inhibitors were ineffective in blocking the increase of the intracellular calcium concentration. The KCl-induced depolarization was partially blocked by  $Ca_v$  inhibitors in these experiments. In the PcTx1-sensitive neurons,  $Ca_v$  inhibitors failed to decrease the response at pH6. This set of experiment suggests that  $Ca^{2+}$  is able to enter the cells via homomeric ASIC1a, but it cannot be excluded that the  $Ca_v$  also played a role in this population of neurons, as the inhibition of  $Ca_v$  by their inhibitors was not completely effective.

#### 4.2.5 Comparison of our results on ASICs and TRPV1 function in DRG neurons with the literature

Previously, calcium imaging has been performed on cultured DRG neurons from mice. A study has found that experiments performed with antagonists for P2X, ASIC, and TRPV1 receptors suggested that these three receptors act together to detect protons, ATP, and lactate when presented together in physiologically relevant concentrations (Light *et al.*, 2008). Even if many groups show that the

homomeric ASIC1a are calcium permeant (Waldmann *et al.*, 1997; Chu *et al.*, 2002; Yermolaieva *et al.*, 2004), a paper claims that ASIC1a channels conduct only negligible  $\text{Ca}^{2+}$  (Samways *et al.*, 2009). They were unable to record any difference of fluorescence after activation of native and recombinant homomeric ASIC1a channels in calcium imaging experiments. As it is the only study that showed that homomeric ASIC1a were impermeant to  $\text{Ca}^{2+}$  and as I and others showed the contrary, I believe they are wrong. A study on rat DRG neurons demonstrated the expression of  $\text{Ca}^{2+}$ -permeable ASICs, with simultaneous whole-cell recording and ratiometric imaging techniques, in peptidergic nociceptive neurons. The simultaneous recording of ASICs currents and increases of intracellular  $\text{Ca}^{2+}$  concentration, which was prevented by the absence of extracellular  $\text{Ca}^{2+}$ , show strong evidences for the presence of a  $\text{Ca}^{2+}$  permeable ASIC. Sensitivity to PcTx1 indicated the presence of  $\text{Ca}^{2+}$ -permeable ASIC1a (Jiang *et al.*, 2006). Another study also performing calcium imaging on mouse neurons showed that extracellular acidosis opened ASIC1a channels, which provided a pathway for  $\text{Ca}^{2+}$  entry and elevated intracellular  $\text{Ca}^{2+}$  concentration in wild type, but not ASIC1a knockout mouse hippocampal neurons. It shows that ASIC1a subunits are necessary for  $\text{Ca}^{2+}$  permeability of the ASICs, but it does not show that only homomeric ASIC1a are  $\text{Ca}^{2+}$  permeant. Acid application also raised  $\text{Ca}^{2+}$  concentration and evoked  $\text{Ca}^{2+}$  currents in heterologous cells expressing ASIC1a. They demonstrated that although ASIC2a is also expressed in central neurons, neither ASIC2a homomultimeric channels nor ASIC1a/2a heteromultimers showed  $\text{H}^{+}$ -activated  $\text{Ca}^{2+}$  concentration elevation or  $\text{Ca}^{2+}$  currents, confirming the  $\text{Ca}^{2+}$  permeability of homomeric ASIC1a channels (Yermolaieva *et al.*, 2004). A study on the mechanism by which toxic  $\text{Ca}^{2+}$  loading of cells occurs in the ischemic brain also shows an implication of ASIC1a homomeric channels in the increase of intracellular calcium concentration. They showed that acidosis activates  $\text{Ca}^{2+}$ -permeable ASICs, inducing  $\text{Ca}^{2+}$ -dependent, neuronal injury inhibited by ASIC blockers (Xiong *et al.*, 2004).

All these studies confirm what we observed with our own calcium imaging experiments. We showed that a population of neuron expressed ASICs which are important for the increase of intracellular calcium concentration. We also confirm, in a population of neurons, the importance of ASIC1a homomeric channels for the entry of calcium into the cell. The presence of a population of neurons insensitive to amiloride is compatible with the presence of the  $\text{Ca}^{2+}$  permeable TRPV1.

### **4.3 Secretion of CGRP from DRG neurons**

#### **4.3.1 Extracellular acidification induces CGRP secretion**

In order to measure directly the secretion of CGRP from DRG neurons, we have used an *in vitro* assay to compare the secretion from neurons in a medium at physiological pH of 7.4 and from neurons in a more acidic pH. Extracellular acidification to pH 6 and 5 both significantly increased the neuronal secretion of CGRP compared to the basal level at pH 7.4. An acidification at pH 6.5 did not increase

the secretion, compared to the basal level at pH 7.4. This shows that an extracellular acidification was able to trigger the secretion of CGRP. It is surprising that an acidification at pH6.5 had no effect on the secretion, as ASICs currents at pH6.5 are already almost maximal. A possible explanation could be that secretion of CGRP is not induced by ASICs, but rather by TRPV1, as TRPV1 is not activated at pH 6.5.

#### 4.3.2 Role of ASICs in acid-induced CGRP secretion

Amiloride and PcTx1 were used as ASICs inhibitors to test if ASICs were involved in CGRP secretion. There were no significant differences in CGRP secretion between conditions with or without amiloride or PcTx1. PcTx1 has only an effect on the population of neurons which express mainly homomeric ASIC1a. All the other DRG neurons expressing other ASICs or TRPV1 are not affected by PcTx1. Therefore, it was not really a surprise that PcTx1 had no effect on the secretion of CGRP, as a large part of the small diameter neurons was not affected by the toxin (more than about 79%). More surprisingly, amiloride had no inhibitory effect on the secretion of CGRP by DRG neurons. Amiloride even had the tendency to increase the secretion of CGRP. The main difference between the secretion assay and the calcium imaging experiments was the duration of the exposition to amiloride, or to other inhibitory compounds. For the calcium imaging experiments, the cells were exposed to amiloride only a few seconds, while for the secretion assay experiments, the cells were exposed to amiloride for 15 min. Although there is no doubt that amiloride act on ASICs during a brief exposition, as shown with calcium imaging experiments, it certainly also act on transporters. During a brief stimulation, the effect on the transporters has certainly no consequences. On the contrary, during a prolonged exposition, amiloride could inhibit transporters for several minutes and therefore the inhibition of these transporters could have effects on the neurons and their viability. It is known that amiloride act on many sodium channels/transporters, as for example the  $\text{Na}^+/\text{H}^+$  exchanger (Masereel *et al.*, 2003). It is possible that inhibiting such channels/transporters for min can stress the cells and allows unspecific release of CGRP.

#### 4.3.3 Role of $\text{Ca}_v$ s in acid-induced CGRP secretion

We also wanted to know if  $\text{Ca}_v$ s were necessary for the release of CGRP.  $\text{Ca}_v$  inhibitors had no significant effects on the secretion induced by an acidic extracellular solution. The inhibitors efficiently inhibited  $\text{Ca}_v$ s in control experiments, as they reduced the secretion induced by KCl-induced depolarization. We can conclude that  $\text{Ca}_v$  were not involved in the extracellular acid-induced CGRP secretion. As our hypothesis was that  $\text{Ca}_v$  were activated by the entry of  $\text{Na}^+$  by ASICs, and that as mentioned before, we were not able to show an effect of ASICs on the secretion of CGRP, this result show that ASICs seems to play no or only a small role in the secretion of CGRP in this assay.  $\text{Ca}_v$  inhibitors were able to inhibit the increase of intracellular  $\text{Ca}^{2+}$  concentration in calcium imaging

experiments in a population of neurons sensitive to amiloride. On the contrary the  $Ca_v$  inhibitors were unable to inhibit this increase in a population which was resistant to amiloride. As the secretion is dependant of an increase of intracellular calcium concentration and as the secretion of CGRP was not inhibited by  $Ca_v$  inhibitors, we can conclude that the neurons secreting CGRP probably belong to the amiloride-resistant population.

#### 4.3.4 Role of TRPV1 in acid-induced CGRP secretion

The TRPV1 blocker BCTC was able to significantly reduce the CGRP secretion at pH 6 and 5. This showed that TRPV1 activity was regulated for the CGRP secretion triggered by an extracellular acidification. Even if these experiments were not able to demonstrate a role for ASICs in this secretion, we cannot totally exclude such a role. As the sensibility of the EIA assay used to measure the amount of secreted CGRP was limited, neurons were incubated for 15 min. In physiological conditions, the nerve endings could be in presence of extracellular acidification for a shorter period. This could influence the mechanisms of CGRP secretion even if experiments in which the period of incubation was shorter (2 min) showed no difference of CGRP secretion compared to the situation after 15 min of incubation (data not shown), as 2 min might already be too long. One of the main differences between ASICs and TRPV1 are kinetics of inactivation. ASICs inactivate fast; most of the subunits, except those containing ASIC3 subunits, are completely inactivated after few seconds of exposition to an extracellular acidification. On the contrary, TRPV1 does not inactivate. It results, as we have shown in our group (Blanchard & Kellenberger, 2011), that even if during the first seconds of activation, ASICs transfer more charges than TRPV1, the situation is inverted in the case of a prolonged stimulation, as in our secretion experiments.

#### 4.3.5 Role of $Na_v$ s in acid-induced CGRP secretion

$Na_v$ s inhibitors TTX and lidocaïne were applied with an acidic pH to investigate the potential roles of  $Na_v$ s in CGRP secretion. TTX or lidocaïne separately had no visible effect on the CGRP secretion. Together, lidocaïne and TTX had a significant effect. The role of  $Na_v$ s is not very clear here, as in this cellular system, as mentioned earlier, TRPV1 seems to be able to trigger the secretion of CGRP. It is possible that inhibiting  $Na_v$ s prevent a depolarization of the neuron which could be required for the CGRP secretion. It has already been shown that  $Na_v$ 1.8 channels play a role in SP secretion. The SP released from cultured DRG neurons of  $Na_v$ 1.8 knock-out mice exposed to either capsaicin or KCl was significantly lower than that from wild-type mice based on a radioimmunoassay. The SP level of L6 DRG in  $Na_v$ 1.8 knock-out mice was also lower than that in wild-type mice. These results suggest that  $Na_v$ 1.8 is involved in the regulation of the release and synthesis of SP in the DRG neurons of wild-type mice (Tang *et al.*, 2008). Even if Nav1.8 is TTX-resistant, other  $Na_v$ s could also mediate neuropeptide secretion. A study investigated mechanisms that mediate CGRP release from the rat

colon in vitro. It is even surprising that lidocaine had either no significant or an inhibitory effect, when applied with TTX, on the CGRP secretion, as it has been reported that lidocaine can activate TRPV1 and can induce a TRPV1-dependant CGRP secretion (Leffler *et al.*, 2008).

#### 4.3.6 Comparison of our results on CGRP secretion from DRG neurons with the literature

Capsaicin and low pH induced significant increases in CGRP release which was shown to be mediated by TRPV1 activation. The TRPV1 antagonists (2R)-4-(3-chloro-2pyridinyl)-2-methyl-N-[4-(trifluoromethyl)phenyl]-1 piperazonecarboxamide (CTPC) and capsazepine inhibit this increase (Kaur *et al.*, 2009). It has already been shown that TRPV1 is important for the release of CGRP. TRPV1 knockout mice were employed to assess the TRPV1 contribution to tracheal responsiveness. Heat-induced CGRP release depended entirely on extracellular calcium and partly on TRPV1 as knockout mice showed 60% less CGRP release at 45°C than wild types. Proton stimulation resulted in a maximum secretion at pH 5.7. Acid-induced secretions of CGRP were greatly reduced but not abolished in TRPV1 knockout mice. It was also found that amiloride at 30 µm, was ineffective in TRPV1 knockout mice and wild type mice (Kichko & Reeh, 2009). This is not a surprise as we neither found an inhibitory effect of amiloride at much higher concentrations (500 µm). Another study using a model of colonic inflammation showed that desensitization of colonic TRPV1 receptors prior to inflammation abolished SP increase in the urinary bladder but did not affect CGRP concentration in the urinary bladder. However desensitization caused a reduction in CGRP release from lumbosacral DRG neurons during acute phase of inflammation. This demonstrates that colonic inflammation triggers the release of pro-inflammatory neuropeptides SP and CGRP in the urinary bladder via activation of TRPV1 signaling mechanisms (Pan *et al.*, 2010). The aim of a study was to investigate some receptors possibly involved in the proton-mediated CGRP release from the heart. Acidification at pH 5.7 and 5.2 caused significant increases in CGRP release in wild type mice but not in mice lacking the TRPV1 receptor. The same acid stimuli caused no significant differences in CGRP release between wild type and ASIC3 knockout. Capsaicin caused massive CGRP release in all mouse genotypes with the exception of TRPV1 knockout (Strecker *et al.*, 2005). An acid-induced neuropeptide secretion can also in some situations not depend on TRPV1, or ASIC3 activation. In the stomach, Proton concentrations in the range of pH 2.5-0.5 stimulated the release of CGRP and substance P. Both TRPV1 and ASIC3 are expressed in the sensory neurons innervating the stomach walls. However, the proton-induced gastric CGRP release in mice lacking the TRPV1 or the ASIC3 channels was the same as in corresponding wild-type mice (Auer *et al.*, 2010).

To conclude, the only effective inhibitors in the CGRP secretion experiments were BCTC and a combination of TTX and lidocaine. It seems that TRPV1 is a major component of the detection of acidification that leads to CGRP secretion in these DRG neurons. As described above, it has been



shown in many studies that TRPV1 plays a role in neuropeptide secretion. Some  $\text{Na}_v$ s (as  $\text{Na}_v 1.8$ ) could also play a role in the secretion of CGRP. We cannot exclude that ASICs play a role in the CGRP secretion, as we did not find an inhibitor of all ASICs which was more specific than amiloride. To our knowledge, no study showed a role for ASICs in neuropeptide secretion.

## 4.4 Behavioural experiments with mice

### 4.4.1 Mechanical allodynia-like behaviour induced by SNI

Mechanical allodynia behaviour was induced by SNI in mice. For all mice, there was a significant difference of paw responses between the ipsilateral and the contralateral paw starting from third to the ninth post-operative day and persisting for the duration of the experiment, showing that the mechanical allodynia was induced by the SNI model. There were no differences between the wild-type and the ASIC1, or ASIC2, null mice at baseline 2 and at 21 days after SNI. There was a significant difference between the wild-type and the ASIC3 null mice at 21 day SNI. ASIC3 null mice were less sensitive than wild type littermates.

Our hypothesis was that ASICs could have a role in neuropathic pain, as it has been previously observed in our group that in a model of neuropathic pain performed on rat, the relative expressions of the different ASIC subunits in rat DRG neurons were modified by the SNI model. In rat, type 1 and type 3 current densities were reduced in injured neurons after SNI (Poirot *et al.*, 2006). As type 3 current is formed of ASIC1a- and ASIC3- containing heteromers, this current must be absent in ASIC3 knockout animals, which could reduce the development of allodynia, as a possible role for this modulation of ASICs expression after the SNI injury could be to develop allodynia.

ASIC3 knockout mice were reported to have a small but significant increase of sensitivity compared to wild-type animals in a model of mechanical hyperalgesia induced with carrageenan. (Price *et al.*, 2001). The secondary mechanical hyperalgesia that develops after knee joint inflammation was abolished in ASIC3 null mice. (Ikeuchi *et al.*, 2008). Similar results were obtained with carrageenan-induced muscle inflammation. ASIC3 null mice develop primary muscle hyperalgesia but not secondary paw hyperalgesia (Walder *et al.*, 2010). Recently, it has also been shown that reducing in-vivo ASIC3 using artificial miRNAs inhibits both primary and secondary hyperalgesia after muscle inflammation in wild-type mice (Walder *et al.*, 2011). Following hind paw inflammation with formalin injection, ASIC1 and ASIC2, but not ASIC3 null mice showed enhanced pain behaviour compared to wild type littermate, predominantly in the second phase of the test (Staniland & McMahon, 2008).

It is necessary to remind here that our hypothesis was based on observations made on rat DRG neurons. In rat DRG neurons, ASIC1a/b and -3 are the predominant isoforms as ASIC2a/b are less expressed (Poirot *et al.*, 2006). On the contrary, in mouse DRG neurons, ASIC2 are predominantly

expressed (Hughes *et al.*, 2007). This could be an explanation why we did only see a small difference between ASIC3 knockout and wild type mice at 21 days after SNI.

#### 4.4.2 Thermal allodynia-like behaviour in the tail flick and the hot plate test

Thermal sensitivity was assessed with tail flick and hot plate apparatus. For the tail flick experiments, there were no significant differences between either of the ASIC ko mice and their wild type littermates. For the hot plate experiments, at 49, 52, and 55°C, there were significant differences at each temperature between ASIC1a and ASIC2 null mice and their wild-type littermates. ASIC1a null mice had increased thermal allodynia behaviors with the hot plate compared to wild type littermates. On the contrary, ASIC2 null mice had reduced thermal allodynia behaviors with the hot plate compared to wild type littermates. There were no significant differences at each temperature between ASIC3 null mice and wild-type littermates.

In a study, ASIC3 null mutant mice displayed more thermal allodynia-like behaviors, when stimuli of moderate to high intensity were used. This effect was observed in the hot-plate test (Chen *et al.*, 2002). It has also been shown that ASIC3 null mice had a reduced latency to withdrawal to tail stimulation at 52°C compared to wild type mice in the tail withdrawal test. ASIC1 and ASIC3 null mice show no difference of behaviour in Hargreaves' and tail withdrawal tests. It was also shown that in tail immersion and hot plate tests, a large antinociceptive effect was observed following both intrathecal and intracerebroventricular injections of PcTx1 (Mazucca *et al.*, 2007), which is in contradiction with our findings that ASIC1a null mice had increased thermal allodynia behaviors with the hot plate. A recent study has shown that the mean withdrawal latency to a slow radiant heat ramp was not different between ASIC1a, -2 and -3 triple knockout mice and wild type mice (Kang *et al.*, 2012). Most of the studies using ASIC null mice animals were done on ASIC3 null mice. Even if all the thermal tests done in these studies were not directly comparable, increased, decreased or unchanged thermal allodynia were described. In our hot plate study, there was no difference of response between ASIC3 null mice and wild type mice. This discrepancy in the results does not allow us to have a definitive conclusion on the role of ASICs in thermal sensation.

The opposite reaction of ASIC1a and ASIC2 knockout mice is very surprising and would need further investigations to elucidate the mechanisms. A study on the effect of the temperature on the function of ASICs showed that the temperature has small effects on the acid-induced currents in rat DRG neurons. (Blanchard & Kellenberger, 2011). As ASICs are activated by an extracellular acidification, even if this activation is modulated by temperature, it is difficult to imagine a mechanism in which ASICs would be the temperature sensor.

## 4.5 Conclusion

During my thesis, I have mainly worked on two projects. The aim of the first project was to determine the role of ASICs in neuropeptide secretion. We hypothesized that some neurons expressing ASIC current type 1 may mediate neuropeptide secretion in DRG neurons. This hypothesis was formulated from the discovery that most of the neurons expressing ASIC current type 1 were expressing neuropeptides. The aim of the study was to determine whether the activation by extracellular acidification of ASICs in DRG neurons induces the release of neuropeptides, and to determine the implication of other relevant ion channels in this process.

The second project was to determine the role of ASICs in neuropathic pain. We hypothesized that ASICs could have a role in neuropathic pain. This hypothesis was formulated based on the observation that in a model of neuropathic pain performed on rat, the relative expressions of the different ASIC subunits in DRG neurons were modified by the nerve injury.

The experiments done during my thesis concerning my first project showed the distribution of the different ASIC subunits and of TRPV1 in the rat DRG neurons. We showed that different ASIC subunits and TRPV1 are co-expressed with neuropeptides CGRP and SP. Different populations of DRG neurons were described according to their response to extracellular acidification and to various inhibitors. We have described a population of small diameter neurons which express ASICs. Some of the ASIC-expressing neurons form a sub-population of neurons expressing only ASIC1a homomeric channels. Another population insensitive to amiloride was found. This population likely expresses another acid-sensing channel, TRPV1. We showed that  $Ca_v$ s were involved in the ASIC-dependent increase of intracellular calcium concentration. We proposed a mechanism in which the activation of ASICs depolarizes the cell membrane and activates  $Ca_v$  channels to let enter  $Ca^{2+}$  in the neuron. Experiments on PcTx1-sensitive neurons expressing ASIC1a homomeric channels showed that  $Ca_v$  were not involved in this population of neurons and that  $Ca^{2+}$  likely enters the neurons via ASIC1a homomeric channels. We have shown, despite our first hypothesis that ASICs are able to trigger neuropeptides secretion that it was not the case in our conditions. ASICs don't seem to play a role in CGRP secretion. We found that TRPV1 was able to trigger the secretion of neuropeptides. ASICs and especially ASIC1a are preferentially expressed in peptidergic small diameter neurons and play a role in the increase of intracellular calcium concentration.

The second project was based on behavioral experiments performed with ASIC1a, -2 and -3 knockout mice. Mechanical allodynia behaviour was induced by SNI in mice. There were no differences between the wild-type and the ASIC1, or ASIC2, null mice at baseline 2 and at 21 days after SNI. There was a significant difference between the wild-type and the ASIC3 null mice at 21 day SNI. ASIC3 null mice were less sensitive than wild type littermates. Hot plate experiments showed that

ASIC1a null mice had increased thermal allodynia behaviours compared to wild type littermates and that on the contrary, ASIC2 null mice had reduced thermal allodynia behaviours compared to wild type littermates.

## 4.6 Perspectives

Concerning the neuropeptide secretion project, all the experiments were done *in vitro*. It would be interesting to perform *in vivo* experiments to further investigate the role of extracellular acidification and neuronal ASICs in neuropeptides secretion. We have already tried to performed experiments in which we measure the plasma extravasation in the skin as an indirect measure of the neuropeptides secretion. Briefly, anesthetized rat was intravenously injected with Evans blue dye which binds to the albumin of the blood. Acidic solutions were subcutaneously injected. A biopsy was taken at the site of injection and the blue dye that leaked into the skin was dissolved and measured. As this kind of experiment was difficult to make, an alternative would be to measure the increase of the blood flow with an Ultrasonic Doppler blood flow measuring apparatus.

Knock-out animal would be very useful to be sure that ASICs play no role in CGRP secretion. But as mentioned before, mice are not the best model concerning ASIC channels as their distribution is completely different of the distribution in rat. We could use the dominant negative form of the ASIC3 subunit generated by Mogil et al. (Mogil *et al.*, 2005) and pack it into a virus. The virus would be intrathecally injected in DRG. Neurons of these DRG would be dissociated and used to make a secretion assay.

For the behaviour experiments, it would be more useful to use rats instead of mice for the reason already described above. We could use the same virus as described above to test if a complete ASIC knockout rat would have different mechanical responses after the SNI model. If a difference was found, we could make knockdown rat for individual ASIC subunits to characterize which ASIC subunits would be implicated in mechanical allodynia after the SNI model.

## 5. Annexes

### 5.1 Supplementary images of in-situ hybridization on DRG neurons

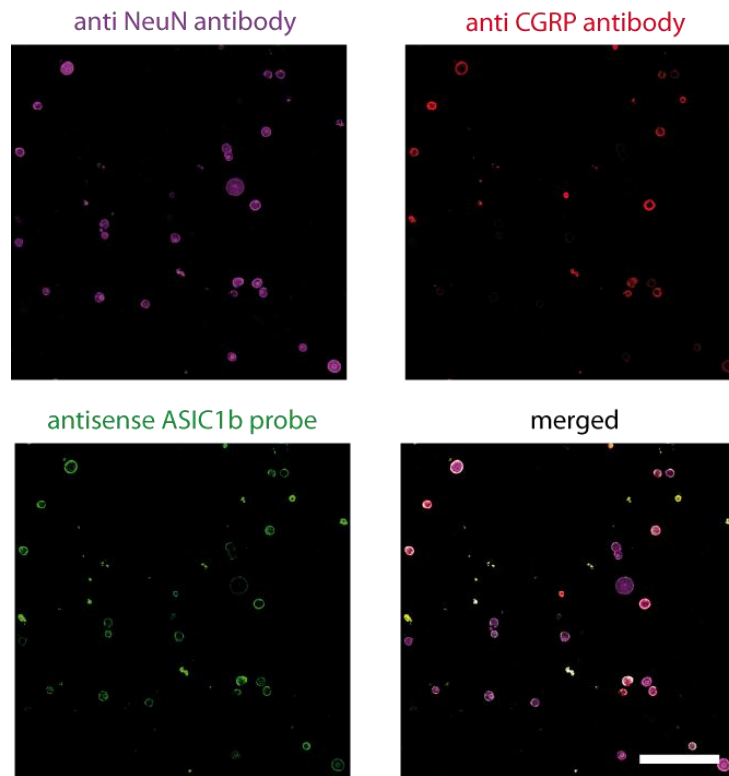


**Figure S1: Example of staining of ASIC1b with in-situ hybridization on DRG neurons**

ASIC1b antisense probe, shown in green, and anti CGRP antibody, shown in red are used. Scale bar: 100  $\mu\text{m}$ . In the merged image, cells which are positive for NeuN, CGRP and ASIC1b appear yellow.

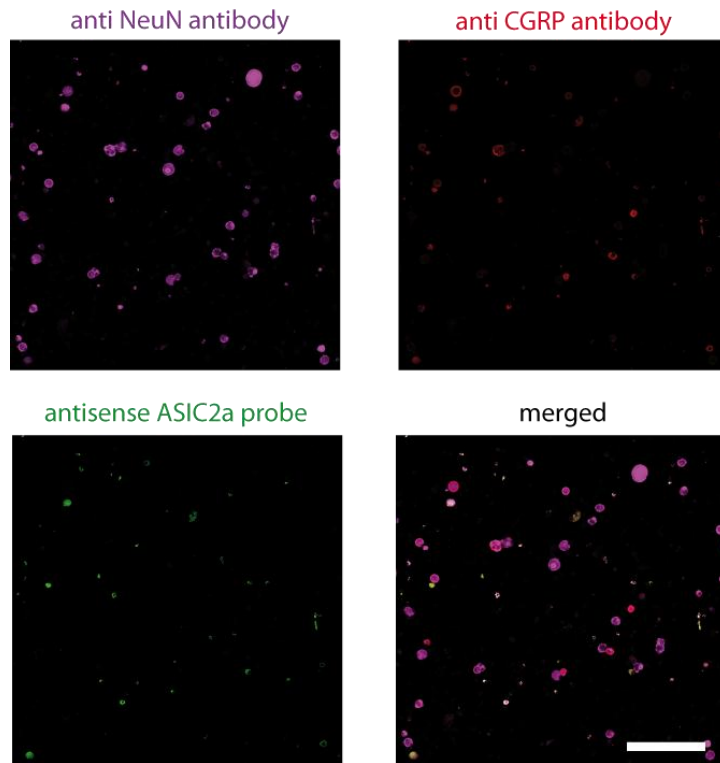


**Figure S2: Example of staining of ASIC2a with in-situ hybridization on DRG neurons** ASIC2a antisense probe, shown in green, and anti CGRP antibody, shown in red are used. Scale bar: 100  $\mu\text{m}$ . In the merged image, cells which are positive for NeuN, CGRP and ASIC2a appear yellow.

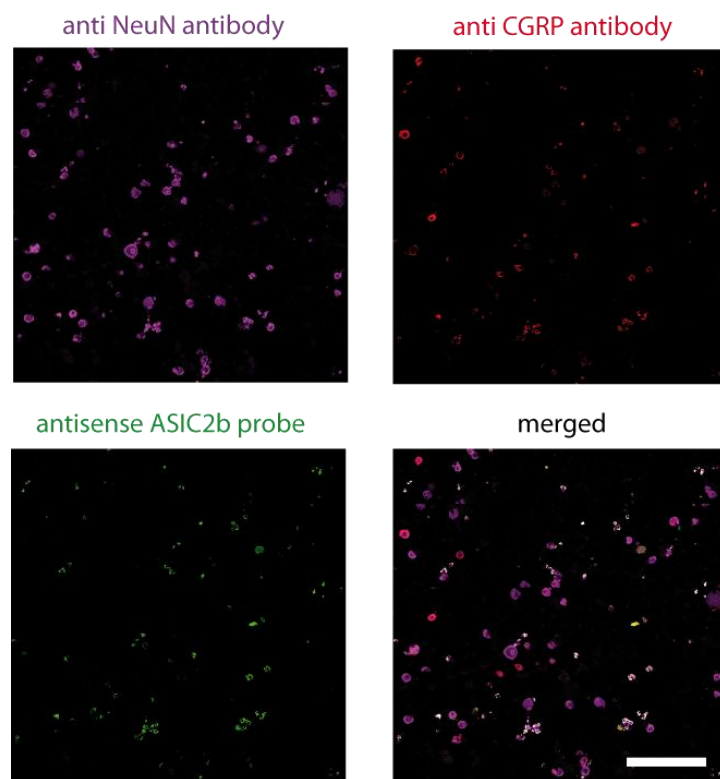


**Figure S3: Example of staining of ASIC2b with in-situ hybridization on DRG neurons** ASIC2b antisense probe, shown in green, and anti CGRP antibody, shown in red are used. Scale bar: 100  $\mu\text{m}$ . In the merged image, cells which are positive for NeuN, CGRP and ASIC2b appear yellow.

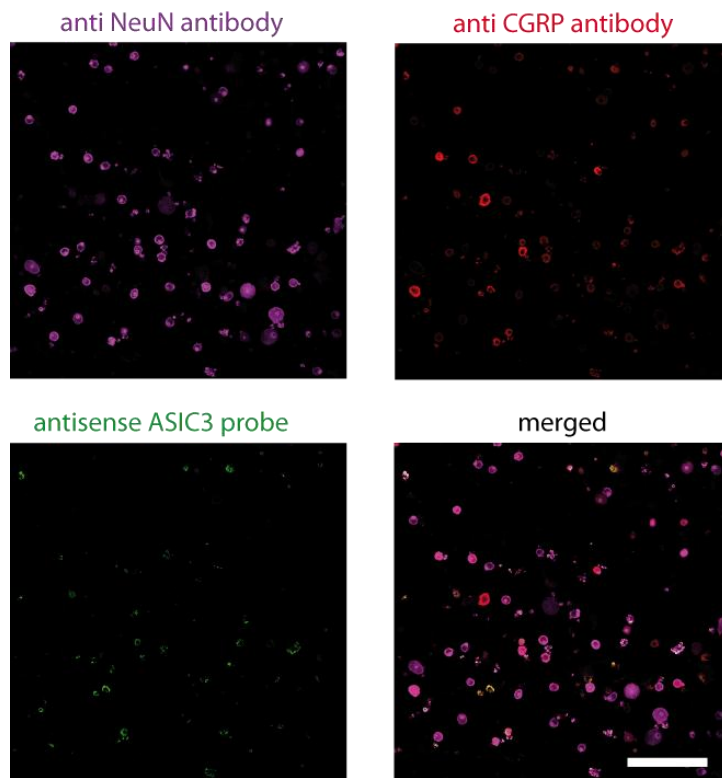


**Figure S4: Example of staining of ASIC3 with in-situ hybridization on DRG neurons**  
ASIC3 antisense probe, shown in green, and anti CGRP antibody, shown in red are used. Scale bar: 100  $\mu\text{m}$ . In the merged image, cells which are positive for NeuN, CGRP and ASIC3 appear yellow.



## 6. References

- Abelli, L., Maggi, C.A., Rovero, P., Del Bianco, E., Regoli, D., Drapeau, G. & Giachetti, A. (1991) Effect of synthetic tachykinin analogues on airway microvascular leakage in rats and guinea-pigs: evidence for the involvement of NK-1 receptors. *J Auton Pharmacol*, **11**, 267-275.
- Akopian, A.N., Sivilotti, L. & Wood, J.N. (1996) A tetrodotoxin-resistant voltage-gated sodium channel expressed by sensory neurons. *Nature*, **379**, 257-262.
- Alvarez de la Rosa, D., Krueger, S.R., Kolar, A., Shao, D., Fitzsimonds, R.M. & Canessa, C.M. (2003) Distribution, subcellular localization and ontogeny of ASIC1 in the mammalian central nervous system. *The Journal of physiology*, **546**, 77-87.
- Andrey, F., Tsintsadze, T., Volkova, T., Lozovaya, N. & Krishtal, O. (2005) Acid sensing ionic channels: modulation by redox reagents. *Biochim Biophys Acta*, **1745**, 1-6.
- Asakura, K., Kanemasa, T., Minagawa, K., Kagawa, K., Yagami, T., Nakajima, M. & Ninomiya, M. (2000) alpha-eudesmol, a P/Q-type Ca(2+) channel blocker, inhibits neurogenic vasodilation and extravasation following electrical stimulation of trigeminal ganglion. *Brain research*, **873**, 94-101.
- Askwith, C.C., Cheng, C., Ikuma, M., Benson, C., Price, M.P. & Welsh, M.J. (2000) Neuropeptide FF and FMRFamide potentiate acid-evoked currents from sensory neurons and proton-gated DEG/ENaC channels. *Neuron*, **26**, 133-141.
- Askwith, C.C., Wemmie, J.A., Price, M.P., Rokhlina, T. & Welsh, M.J. (2004) Acid-sensing ion channel 2 (ASIC2) modulates ASIC1 H+-activated currents in hippocampal neurons. *J Biol Chem*, **279**, 18296-18305.
- Auer, J., Reeh, P.W. & Fischer, M.J. (2010) Acid-induced CGRP release from the stomach does not depend on TRPV1 or ASIC3. *Neurogastroenterol Motil*, **22**, 680-687.
- Babini, E., Paukert, M., Geisler, H.S. & Grunder, S. (2002) Alternative splicing and interaction with di- and polyvalent cations control the dynamic range of acid-sensing ion channel 1 (ASIC1). *J Biol Chem*, **277**, 41597-41603.
- Baron, A., Schaefer, L., Lingueglia, E., Champigny, G. & Lazdunski, M. (2001) Zn<sup>2+</sup> and H<sup>+</sup> are coactivators of acid-sensing ion channels. *The Journal of biological chemistry*, **276**, 35361-35367.
- Baron, A., Voilley, N., Lazdunski, M. & Lingueglia, E. (2008) Acid sensing ion channels in dorsal spinal cord neurons. *J Neurosci*, **28**, 1498-1508.

- Basbaum, A.I., Bautista, D.M., Scherrer, G. & Julius, D. (2009) Cellular and molecular mechanisms of pain. *Cell*, **139**, 267-284.
- Bassler, E.L., Ngo-Anh, T.J., Geisler, H.S., Ruppersberg, J.P. & Grunder, S. (2001) Molecular and functional characterization of acid-sensing ion channel (ASIC) 1b. *J Biol Chem*, **276**, 33782-33787.
- Bautista, D.M., Siemens, J., Glazer, J.M., Tsuruda, P.R., Basbaum, A.I., Stucky, C.L., Jordt, S.E. & Julius, D. (2007) The menthol receptor TRPM8 is the principal detector of environmental cold. *Nature*, **448**, 204-208.
- Benarroch, E.E. (2011) CGRP: sensory neuropeptide with multiple neurologic implications. *Neurology*, **77**, 281-287.
- Benemei, S., Nicoletti, P., Capone, J.G. & Geppetti, P. (2009) CGRP receptors in the control of pain and inflammation. *Current opinion in pharmacology*, **9**, 9-14.
- Biagini, G., Babinski, K., Avoli, M., Marcinkiewicz, M. & Seguela, P. (2001) Regional and subunit-specific downregulation of acid-sensing ion channels in the pilocarpine model of epilepsy. *Neurobiol Dis*, **8**, 45-58.
- Black, J.A., Dib-Hajj, S., McNabola, K., Jeste, S., Rizzo, M.A., Kocsis, J.D. & Waxman, S.G. (1996) Spinal sensory neurons express multiple sodium channel alpha-subunit mRNAs. *Brain research. Molecular brain research*, **43**, 117-131.
- Blanchard, M.G. & Kellenberger, S. (2011) Effect of a temperature increase in the non-noxious range on proton-evoked ASIC and TRPV1 activity. *Pflugers Archiv : European journal of physiology*, **461**, 123-139.
- Blanchard, M.G., Rash, L.D. & Kellenberger, S. (2011) Inhibition of voltage-gated Na(+) currents in sensory neurons by the sea anemone toxin APETx2. *Br J Pharmacol*.
- Blaustein, M.P. & Lederer, W.J. (1999) Sodium/calcium exchange: its physiological implications. *Physiological reviews*, **79**, 763-854.
- Bobrow, M.N. & Moen, P.T. (2001) Tyramide Signal Amplification (TSA) Systems for the Enhancement of ISH Signals in Cytogenetics *Current Protocols in Cytometry*. John Wiley & Sons, Inc.
- Bohlen, C.J., Chesler, A.T., Sharif-Naeini, R., Medzihradzsky, K.F., Zhou, S., King, D., Sanchez, E.E., Burlingame, A.L., Basbaum, A.I. & Julius, D. (2011) A heteromeric Texas coral snake toxin targets acid-sensing ion channels to produce pain. *Nature*, **479**, 410-414.

- Bourinet, E., Alloui, A., Monteil, A., Barrere, C., Couette, B., Poirot, O., Pages, A., McRory, J., Snutch, T.P., Eschalier, A. & Nargeot, J. (2005) Silencing of the Cav3.2 T-type calcium channel gene in sensory neurons demonstrates its major role in nociception. *The EMBO journal*, **24**, 315-324.
- Bourquin, A.F., Suveges, M., Pertin, M., Gilliard, N., Sardy, S., Davison, A.C., Spahn, D.R. & Decosterd, I. (2006) Assessment and analysis of mechanical allodynia-like behavior induced by spared nerve injury (SNI) in the mouse. *Pain*, **122**, 14 e11-14.
- Brain, S.D. & Grant, A.D. (2004) Vascular actions of calcitonin gene-related peptide and adrenomedullin. *Physiological reviews*, **84**, 903-934.
- Burnes, L.A., Kolker, S.J., Danielson, J.F., Walder, R.Y. & Sluka, K.A. (2008) Enhanced muscle fatigue occurs in male but not female ASIC3<sup>-/-</sup> mice. *Am J Physiol Regul Integr Comp Physiol*, **294**, R1347-1355.
- Canessa, C.M., Horisberger, J.D. & Rossier, B.C. (1993) Epithelial sodium channel related to proteins involved in neurodegeneration. *Nature*, **361**, 467-470.
- Catarsi, S., Babinski, K. & Seguela, P. (2001) Selective modulation of heteromeric ASIC proton-gated channels by neuropeptide FF. *Neuropharmacology*, **41**, 592-600.
- Caterina, M.J., Leffler, A., Malmberg, A.B., Martin, W.J., Trafton, J., Petersen-Zeitz, K.R., Koltzenburg, M., Basbaum, A.I. & Julius, D. (2000) Impaired nociception and pain sensation in mice lacking the capsaicin receptor. *Science*, **288**, 306-313.
- Caterina, M.J., Rosen, T.A., Tominaga, M., Brake, A.J. & Julius, D. (1999) A capsaicin-receptor homologue with a high threshold for noxious heat. *Nature*, **398**, 436-441.
- Caterina, M.J., Schumacher, M.A., Tominaga, M., Rosen, T.A., Levine, J.D. & Julius, D. (1997) The capsaicin receptor: a heat-activated ion channel in the pain pathway. *Nature*, **389**, 816-824.
- Catterall, W.A. (2000) From ionic currents to molecular mechanisms: the structure and function of voltage-gated sodium channels. *Neuron*, **26**, 13-25.
- Catterall, W.A. & Few, A.P. (2008) Calcium channel regulation and presynaptic plasticity. *Neuron*, **59**, 882-901.
- Catterall, W.A., Goldin, A.L. & Waxman, S.G. (2005a) International Union of Pharmacology. XLVII. Nomenclature and structure-function relationships of voltage-gated sodium channels. *Pharmacol Rev*, **57**, 397-409.

- Catterall, W.A., Perez-Reyes, E., Snutch, T.P. & Striessnig, J. (2005b) International Union of Pharmacology. XLVIII. Nomenclature and structure-function relationships of voltage-gated calcium channels. *Pharmacol Rev*, **57**, 411-425.
- Chalfie, M., Driscoll, M. & Huang, M. (1993) Degenerin similarities. *Nature*, **361**, 504.
- Chanda, M.L. & Mogil, J.S. (2006) Sex differences in the effects of amiloride on formalin test nociception in mice. *Am J Physiol Regul Integr Comp Physiol*, **291**, R335-342.
- Chao, M.V. (2003) Neurotrophins and their receptors: a convergence point for many signalling pathways. *Nature reviews. Neuroscience*, **4**, 299-309.
- Chen, C.C., Zimmer, A., Sun, W.H., Hall, J. & Brownstein, M.J. (2002) A role for ASIC3 in the modulation of high-intensity pain stimuli. *Proc Natl Acad Sci U S A*, **99**, 8992-8997.
- Chen, X., Kalbacher, H. & Grunder, S. (2005) The tarantula toxin psalmotoxin 1 inhibits acid-sensing ion channel (ASIC) 1a by increasing its apparent H<sup>+</sup> affinity. *J Gen Physiol*, **126**, 71-79.
- Cho, J.H. & Askwith, C.C. (2007) Potentiation of acid-sensing ion channels by sulfhydryl compounds. *Am J Physiol Cell Physiol*, **292**, C2161-2174.
- Chu, X.P., Close, N., Saugstad, J.A. & Xiong, Z.G. (2006) ASIC1a-specific modulation of acid-sensing ion channels in mouse cortical neurons by redox reagents. *J Neurosci*, **26**, 5329-5339.
- Chu, X.P., Miesch, J., Johnson, M., Root, L., Zhu, X.M., Chen, D., Simon, R.P. & Xiong, Z.G. (2002) Proton-gated channels in PC12 cells. *J Neurophysiol*, **87**, 2555-2561.
- Chu, X.P., Wemmie, J.A., Wang, W.Z., Zhu, X.M., Saugstad, J.A., Price, M.P., Simon, R.P. & Xiong, Z.G. (2004) Subunit-dependent high-affinity zinc inhibition of acid-sensing ion channels. *J Neurosci*, **24**, 8678-8689.
- Chuang, H.H., Prescott, E.D., Kong, H., Shields, S., Jordt, S.E., Basbaum, A.I., Chao, M.V. & Julius, D. (2001) Bradykinin and nerve growth factor release the capsaicin receptor from PtdIns(4,5)P<sub>2</sub>-mediated inhibition. *Nature*, **411**, 957-962.
- Colburn, R.W., Lubin, M.L., Stone, D.J., Jr., Wang, Y., Lawrence, D., D'Andrea, M.R., Brandt, M.R., Liu, Y., Flores, C.M. & Qin, N. (2007) Attenuated cold sensitivity in TRPM8 null mice. *Neuron*, **54**, 379-386.
- Corey, D.P., Garcia-Anoveros, J., Holt, J.R., Kwan, K.Y., Lin, S.Y., Vollrath, M.A., Amalfitano, A., Cheung, E.L., Derfler, B.H., Duggan, A., Geleoc, G.S., Gray, P.A., Hoffman, M.P., Rehm,

- H.L., Tamasauskas, D. & Zhang, D.S. (2004) TRPA1 is a candidate for the mechanosensitive transduction channel of vertebrate hair cells. *Nature*, **432**, 723-730.
- Coryell, M.W., Wunsch, A.M., Haenfler, J.M., Allen, J.E., McBride, J.L., Davidson, B.L. & Wemmie, J.A. (2008) Restoring Acid-sensing ion channel-1a in the amygdala of knock-out mice rescues fear memory but not unconditioned fear responses. *The Journal of neuroscience : the official journal of the Society for Neuroscience*, **28**, 13738-13741.
- Coryell, M.W., Ziemann, A.E., Westmoreland, P.J., Haenfler, J.M., Kurjakovic, Z., Zha, X.M., Price, M., Schnizler, M.K. & Wemmie, J.A. (2007) Targeting ASIC1a reduces innate fear and alters neuronal activity in the fear circuit. *Biol Psychiatry*, **62**, 1140-1148.
- Cottrell, G.A. (1989) The biology of the FMRFamide-series of peptides in molluscs with special reference to Helix. *Comp Biochem Physiol A Comp Physiol*, **93**, 41-45.
- Cox, J.J., Reimann, F., Nicholas, A.K., Thornton, G., Roberts, E., Springell, K., Karbani, G., Jafri, H., Mannan, J., Raashid, Y., Al-Gazali, L., Hamamy, H., Valente, E.M., Gorman, S., Williams, R., McHale, D.P., Wood, J.N., Gribble, F.M. & Woods, C.G. (2006) An SCN9A channelopathy causes congenital inability to experience pain. *Nature*, **444**, 894-898.
- Cuello, A.C., Jessell, T.M., Kanazawa, I. & Iversen, L.L. (1977) Substance P: localization in synaptic vesicles in rat central nervous system. *Journal of neurochemistry*, **29**, 747-751.
- Cummins, T.R., Dib-Hajj, S.D. & Waxman, S.G. (2004) Electrophysiological properties of mutant Nav1.7 sodium channels in a painful inherited neuropathy. *The Journal of neuroscience : the official journal of the Society for Neuroscience*, **24**, 8232-8236.
- Davis, J.B., Gray, J., Gunthorpe, M.J., Hatcher, J.P., Davey, P.T., Overend, P., Harries, M.H., Latcham, J., Clapham, C., Atkinson, K., Hughes, S.A., Rance, K., Grau, E., Harper, A.J., Pugh, P.L., Rogers, D.C., Bingham, S., Randall, A. & Sheardown, S.A. (2000) Vanilloid receptor-1 is essential for inflammatory thermal hyperalgesia. *Nature*, **405**, 183-187.
- de Weille, J. & Bassilana, F. (2001) Dependence of the acid-sensitive ion channel, ASIC1a, on extracellular Ca(2+) ions. *Brain Res*, **900**, 277-281.
- Decosterd, I., Allchorne, A. & Woolf, C.J. (2004) Differential analgesic sensitivity of two distinct neuropathic pain models. *Anesthesia and analgesia*, **99**, 457-463, table of contents.
- Deval, E., Noel, J., Gasull, X., Delaunay, A., Alloui, A., Friend, V., Eschalier, A., Lazdunski, M. & Lingueglia, E. (2011) Acid-sensing ion channels in postoperative pain. *The Journal of neuroscience : the official journal of the Society for Neuroscience*, **31**, 6059-6066.

- Deval, E., Noel, J., Lay, N., Alloui, A., Diochot, S., Friend, V., Jodar, M., Lazdunski, M. & Lingueglia, E. (2008) ASIC3, a sensor of acidic and primary inflammatory pain. *The EMBO journal*, **27**, 3047-3055.
- Dewey, W.L., Harris, L.S., Howes, J.F. & Nuite, J.A. (1970) The effect of various neurohumoral modulators on the activity of morphine and the narcotic antagonists in the tail-flick and phenylquinone tests. *The Journal of pharmacology and experimental therapeutics*, **175**, 435-442.
- Dhaka, A., Murray, A.N., Mathur, J., Earley, T.J., Petrus, M.J. & Patapoutian, A. (2007) TRPM8 is required for cold sensation in mice. *Neuron*, **54**, 371-378.
- Dib-Hajj, S.D., Cummins, T.R., Black, J.A. & Waxman, S.G. (2010) Sodium channels in normal and pathological pain. *Annu Rev Neurosci*, **33**, 325-347.
- Dib-Hajj, S.D., Rush, A.M., Cummins, T.R., Hisama, F.M., Novella, S., Tyrrell, L., Marshall, L. & Waxman, S.G. (2005) Gain-of-function mutation in Nav1.7 in familial erythromelalgia induces bursting of sensory neurons. *Brain : a journal of neurology*, **128**, 1847-1854.
- Dib-Hajj, S.D., Tyrrell, L., Black, J.A. & Waxman, S.G. (1998) Na<sub>v</sub>1.7, a novel voltage-gated Na channel, is expressed preferentially in peripheral sensory neurons and down-regulated after axotomy. *Proceedings of the National Academy of Sciences of the United States of America*, **95**, 8963-8968.
- Diochot, S., Baron, A., Rash, L.D., Deval, E., Escoubas, P., Scarzello, S., Salinas, M. & Lazdunski, M. (2004) A new sea anemone peptide, APETx2, inhibits ASIC3, a major acid-sensitive channel in sensory neurons. *The EMBO journal*, **23**, 1516-1525.
- Dirajlal, S., Pauers, L.E. & Stucky, C.L. (2003) Differential response properties of IB(4)-positive and -negative unmyelinated sensory neurons to protons and capsaicin. *Journal of neurophysiology*, **89**, 513-524.
- Dorofeeva, N.A., Barygin, O.I., Staruschenko, A., Bolshakov, K.V. & Magazanik, L.G. (2008) Mechanisms of non-steroid anti-inflammatory drugs action on ASICs expressed in hippocampal interneurons. *J Neurochem*, **106**, 429-441.
- Dou, H., Xu, J., Wang, Z., Smith, A.N., Soleimani, M., Karet, F.E., Greinwald, J.H., Jr. & Choo, D. (2004) Co-expression of pendrin, vacuolar H<sup>+</sup>-ATPase alpha4-subunit and carbonic anhydrase II in epithelial cells of the murine endolymphatic sac. *J Histochem Cytochem*, **52**, 1377-1384.
- Duan, B., Wu, L.J., Yu, Y.Q., Ding, Y., Jing, L., Xu, L., Chen, J. & Xu, T.L. (2007) Upregulation of acid-sensing ion channel ASIC1a in spinal dorsal horn neurons contributes to inflammatory pain hypersensitivity. *J Neurosci*, **27**, 11139-11148.

- Dube, G.R., Lehto, S.G., Breese, N.M., Baker, S.J., Wang, X., Matulenko, M.A., Honore, P., Stewart, A.O., Moreland, R.B. & Brioni, J.D. (2005) Electrophysiological and in vivo characterization of A-317567, a novel blocker of acid sensing ion channels. *Pain*, **117**, 88-96.
- Ebner, K. & Singewald, N. (2006) The role of substance P in stress and anxiety responses. *Amino Acids*, **31**, 251-272.
- Erdtmann-Vourliotis, M., Mayer, P., Riechert, U., Handel, M., Kriebitzsch, J. & Holtt, V. (1999) Rational design of oligonucleotide probes to avoid optimization steps in in situ hybridization. *Brain Res Brain Res Protoc*, **4**, 82-91.
- Ertel, E.A., Campbell, K.P., Harpold, M.M., Hofmann, F., Mori, Y., Perez-Reyes, E., Schwartz, A., Snutch, T.P., Tanabe, T., Birnbaumer, L., Tsien, R.W. & Catterall, W.A. (2000) Nomenclature of voltage-gated calcium channels. *Neuron*, **25**, 533-535.
- Escoubas, P., De Weille, J.R., Lecoq, A., Diochot, S., Waldmann, R., Champigny, G., Moinier, D., Menez, A. & Lazdunski, M. (2000) Isolation of a tarantula toxin specific for a class of proton-gated Na<sup>+</sup> channels. *J Biol Chem*, **275**, 25116-25121.
- Ettaiche, M., Guy, N., Hofman, P., Lazdunski, M. & Waldmann, R. (2004) Acid-sensing ion channel 2 is important for retinal function and protects against light-induced retinal degeneration. *J Neurosci*, **24**, 1005-1012.
- Evans, A.R., Nicol, G.D. & Vasko, M.R. (1996) Differential regulation of evoked peptide release by voltage-sensitive calcium channels in rat sensory neurons. *Brain research*, **712**, 265-273.
- Firsov, D., Gautschi, I., Merillat, A.M., Rossier, B.C. & Schild, L. (1998) The heterotetrameric architecture of the epithelial sodium channel (ENaC). *The EMBO journal*, **17**, 344-352.
- Fischer, T.Z. & Waxman, S.G. (2010) Familial pain syndromes from mutations of the NaV1.7 sodium channel. *Annals of the New York Academy of Sciences*, **1184**, 196-207.
- Fukuda, T., Ichikawa, H., Terayama, R., Yamaai, T., Kuboki, T. & Sugimoto, T. (2006) ASIC3-immunoreactive neurons in the rat vagal and glossopharyngeal sensory ganglia. *Brain research*, **1081**, 150-155.
- Gannon, K.P., Vanlandingham, L.G., Jernigan, N.L., Grifoni, S.C., Hamilton, G. & Drummond, H.A. (2008a) Impaired pressure-induced constriction in mouse middle cerebral arteries of ASIC2 knockout mice. *Am J Physiol Heart Circ Physiol*, **294**, H1793-1803.
- Gannon, K.P., Vanlandingham, L.G., Jernigan, N.L., Grifoni, S.C., Hamilton, G. & Drummond, H.A. (2008b) Impaired pressure-induced constriction in mouse middle cerebral arteries of ASIC2

- knockout mice. *American journal of physiology. Heart and circulatory physiology*, **294**, H1793-1803.
- Gao, J., Wu, L.J., Xu, L. & Xu, T.L. (2004) Properties of the proton-evoked currents and their modulation by Ca<sup>2+</sup> and Zn<sup>2+</sup> in the acutely dissociated hippocampus CA1 neurons. *Brain research*, **1017**, 197-207.
- Gonzales, E.B., Kawate, T. & Gouaux, E. (2009) Pore architecture and ion sites in acid-sensing ion channels and P2X receptors. *Nature*, **460**, 599-604.
- Grady, E.F., Garland, A.M., Gamp, P.D., Lovett, M., Payan, D.G. & Bunnett, N.W. (1995) Delineation of the endocytic pathway of substance P and its seven-transmembrane domain NK1 receptor. *Molecular biology of the cell*, **6**, 509-524.
- Green, K.A., Falconer, S.W. & Cottrell, G.A. (1994) The neuropeptide Phe-Met-Arg-Phe-NH<sub>2</sub> (FMRFamide) directly gates two ion channels in an identified Helix neurone. *Pflugers Archiv : European journal of physiology*, **428**, 232-240.
- Grunder, S., Geissler, H.S., Bassler, E.L. & Ruppersberg, J.P. (2000) A new member of acid-sensing ion channels from pituitary gland. *Neuroreport*, **11**, 1607-1611.
- Gu, X.L. & Yu, L.C. (2007) The colocalization of CGRP receptor and AMPA receptor in the spinal dorsal horn neuron of rat: a morphological and electrophysiological study. *Neuroscience letters*, **414**, 237-241.
- Henke, H., Sigrist, S., Lang, W., Schneider, J. & Fischer, J.A. (1987) Comparison of binding sites for the calcitonin gene-related peptides I and II in man. *Brain research*, **410**, 404-408.
- Hesselager, M., Timmermann, D.B. & Ahring, P.K. (2004) pH Dependency and desensitization kinetics of heterologously expressed combinations of acid-sensing ion channel subunits. *J Biol Chem*, **279**, 11006-11015.
- Hildebrand, M.S., de Silva, M.G., Klockars, T., Rose, E., Price, M., Smith, R.J., McGuirt, W.T., Christopoulos, H., Petit, C. & Dahl, H.H. (2004) Characterisation of DRASIC in the mouse inner ear. *Hear Res*, **190**, 149-160.
- Hughes, P.A., Brierley, S.M., Young, R.L. & Blackshaw, L.A. (2007) Localization and comparative analysis of acid-sensing ion channel (ASIC1, 2, and 3) mRNA expression in mouse colonic sensory neurons within thoracolumbar dorsal root ganglia. *J Comp Neurol*, **500**, 863-875.
- Hughey, R.P., Carattino, M.D. & Kleyman, T.R. (2007) Role of proteolysis in the activation of epithelial sodium channels. *Curr Opin Nephrol Hypertens*, **16**, 444-450.



- Hughey, R.P., Mueller, G.M., Bruns, J.B., Kinlough, C.L., Poland, P.A., Harkleroad, K.L., Carattino, M.D. & Kleyman, T.R. (2003) Maturation of the epithelial Na<sup>+</sup> channel involves proteolytic processing of the alpha- and gamma-subunits. *The Journal of biological chemistry*, **278**, 37073-37082.
- Huque, T., Cowart, B.J., Dankulich-Nagrudny, L., Pribitkin, E.A., Bayley, D.L., Spielman, A.I., Feldman, R.S., Mackler, S.A. & Brand, J.G. (2009) Sour ageusia in two individuals implicates ion channels of the ASIC and PKD families in human sour taste perception at the anterior tongue. *PloS one*, **4**, e7347.
- Ikeuchi, M., Kolker, S.J., Burnes, L.A., Walder, R.Y. & Sluka, K.A. (2008) Role of ASIC3 in the primary and secondary hyperalgesia produced by joint inflammation in mice. *Pain*, **137**, 662-669.
- Immke, D.C. & McCleskey, E.W. (2003) Protons open acid-sensing ion channels by catalyzing relief of Ca<sup>2+</sup> blockade. *Neuron*, **37**, 75-84.
- Jasti, J., Furukawa, H., Gonzales, E.B. & Gouaux, E. (2007) Structure of acid-sensing ion channel 1 at 1.9 Å resolution and low pH. *Nature*, **449**, 316-323.
- Jiang, N., Rau, K.K., Johnson, R.D. & Cooper, B.Y. (2006) Proton sensitivity Ca<sup>2+</sup> permeability and molecular basis of acid-sensing ion channels expressed in glabrous and hairy skin afferents. *J Neurophysiol*, **95**, 2466-2478.
- Jones, N.G., Slater, R., Cadiou, H., McNaughton, P. & McMahon, S.B. (2004) Acid-induced pain and its modulation in humans. *J Neurosci*, **24**, 10974-10979.
- Jordt, S.E., Bautista, D.M., Chuang, H.H., McKemy, D.D., Zygmunt, P.M., Hogestatt, E.D., Meng, I.D. & Julius, D. (2004) Mustard oils and cannabinoids excite sensory nerve fibres through the TRP channel ANKTM1. *Nature*, **427**, 260-265.
- Jovov, B., Tousson, A., McMahon, L.L. & Benos, D.J. (2003) Immunolocalization of the acid-sensing ion channel 2a in the rat cerebellum. *Histochem Cell Biol*, **119**, 437-446.
- Julius, D. & Basbaum, A.I. (2001) Molecular mechanisms of nociception. *Nature*, **413**, 203-210.
- Kang, S., Jang, J.H., Price, M.P., Gautam, M., Benson, C.J., Gong, H., Welsh, M.J. & Brennan, T.J. (2012) Simultaneous Disruption of Mouse ASIC1a, ASIC2 and ASIC3 Genes Enhances Cutaneous Mechanosensitivity. *PloS one*, **7**, e35225.

- Karashima, Y., Damann, N., Prenen, J., Talavera, K., Segal, A., Voets, T. & Nilius, B. (2007) Bimodal action of menthol on the transient receptor potential channel TRPA1. *The Journal of neuroscience : the official journal of the Society for Neuroscience*, **27**, 9874-9884.
- Karashima, Y., Talavera, K., Everaerts, W., Janssens, A., Kwan, K.Y., Vennekens, R., Nilius, B. & Voets, T. (2009) TRPA1 acts as a cold sensor in vitro and in vivo. *Proceedings of the National Academy of Sciences of the United States of America*, **106**, 1273-1278.
- Kaur, R., O'Shaughnessy, C.T., Jarvie, E.M., Winchester, W.J. & McLean, P.G. (2009) Characterization of a calcitonin gene-related peptide release assay in rat isolated distal colon. *Arch Pharm Res*, **32**, 1775-1781.
- Kawamata, T., Ninomiya, T., Toriyabe, M., Yamamoto, J., Niiyama, Y., Omote, K. & Namiki, A. (2006) Immunohistochemical analysis of acid-sensing ion channel 2 expression in rat dorsal root ganglion and effects of axotomy. *Neuroscience*, **143**, 175-187.
- Kellenberger, S. & Schild, L. (2002) Epithelial sodium channel/degenerin family of ion channels: a variety of functions for a shared structure. *Physiol Rev*, **82**, 735-767.
- Kichko, T.I. & Reeh, P.W. (2009) TRPV1 controls acid- and heat-induced calcitonin gene-related peptide release and sensitization by bradykinin in the isolated mouse trachea. *The European journal of neuroscience*, **29**, 1896-1904.
- Kleyman, T.R., Carattino, M.D. & Hughey, R.P. (2009) ENaC at the cutting edge: regulation of epithelial sodium channels by proteases. *The Journal of biological chemistry*, **284**, 20447-20451.
- Kokaia, Z. (2001) In Situ Hybridization Histochemistry *Current Protocols in Toxicology*. John Wiley & Sons, Inc.
- Kosari, F., Sheng, S., Li, J., Mak, D.O., Foskett, J.K. & Kleyman, T.R. (1998) Subunit stoichiometry of the epithelial sodium channel. *The Journal of biological chemistry*, **273**, 13469-13474.
- Kremeyer, B., Lopera, F., Cox, J.J., Momin, A., Rugiero, F., Marsh, S., Woods, C.G., Jones, N.G., Paterson, K.J., Fricker, F.R., Villegas, A., Acosta, N., Pineda-Trujillo, N.G., Ramirez, J.D., Zea, J., Burley, M.W., Bedoya, G., Bennett, D.L., Wood, J.N. & Ruiz-Linares, A. (2010) A gain-of-function mutation in TRPA1 causes familial episodic pain syndrome. *Neuron*, **66**, 671-680.
- Lee, H. & Caterina, M.J. (2005) TRPV channels as thermosensory receptors in epithelial cells. *Pflugers Archiv : European journal of physiology*, **451**, 160-167.

- Leffler, A., Fischer, M.J., Rehner, D., Kienel, S., Kistner, K., Sauer, S.K., Gavva, N.R., Reeh, P.W. & Nau, C. (2008) The vanilloid receptor TRPV1 is activated and sensitized by local anesthetics in rodent sensory neurons. *The Journal of clinical investigation*, **118**, 763-776.
- Lembeck, F. & Holzer, P. (1979) Substance P as neurogenic mediator of antidromic vasodilation and neurogenic plasma extravasation. *Naunyn Schmiedebergs Arch Pharmacol*, **310**, 175-183.
- Light, A.R., Huguen, R.W., Zhang, J., Rainier, J., Liu, Z. & Lee, J. (2008) Dorsal root ganglion neurons innervating skeletal muscle respond to physiological combinations of protons, ATP, and lactate mediated by ASIC, P2X, and TRPV1. *Journal of neurophysiology*, **100**, 1184-1201.
- Lingueglia, E., Champigny, G., Lazdunski, M. & Barbry, P. (1995) Cloning of the amiloride-sensitive FMRFamide peptide-gated sodium channel. *Nature*, **378**, 730-733.
- Lingueglia, E., de Weille, J.R., Bassilana, F., Heurteaux, C., Sakai, H., Waldmann, R. & Lazdunski, M. (1997) A modulatory subunit of acid sensing ion channels in brain and dorsal root ganglion cells. *J Biol Chem*, **272**, 29778-29783.
- Lingueglia, E., Deval, E. & Lazdunski, M. (2006) FMRFamide-gated sodium channel and ASIC channels: a new class of ionotropic receptors for FMRFamide and related peptides. *Peptides*, **27**, 1138-1152.
- Liu, M. & Wood, J.N. (2011) The roles of sodium channels in nociception: implications for mechanisms of neuropathic pain. *Pain Med*, **12 Suppl 3**, S93-99.
- Lu, Y., Ma, X., Sabharwal, R., Snitsarev, V., Morgan, D., Rahmouni, K., Drummond, H.A., Whiteis, C.A., Costa, V., Price, M., Benson, C., Welsh, M.J., Chapleau, M.W. & Abboud, F.M. (2009) The ion channel ASIC2 is required for baroreceptor and autonomic control of the circulation. *Neuron*, **64**, 885-897.
- Mamet, J., Baron, A., Lazdunski, M. & Voilley, N. (2002) Proinflammatory mediators, stimulators of sensory neuron excitability via the expression of acid-sensing ion channels. *J Neurosci*, **22**, 10662-10670.
- Masereel, B., Pochet, L. & Laeckmann, D. (2003) An overview of inhibitors of Na(+)/H(+) exchanger. *Eur J Med Chem*, **38**, 547-554.
- Mazzuca, M., Heurteaux, C., Alloui, A., Diochot, S., Baron, A., Voilley, N., Blondeau, N., Escoubas, P., Gelot, A., Cupo, A., Zimmer, A., Zimmer, A.M., Eschalier, A. & Lazdunski, M. (2007) A tarantula peptide against pain via ASIC1a channels and opioid mechanisms. *Nat Neurosci*, **10**, 943-945.

- McKemy, D.D., Neuhauser, W.M. & Julius, D. (2002) Identification of a cold receptor reveals a general role for TRP channels in thermosensation. *Nature*, **416**, 52-58.
- McLatchie, L.M., Fraser, N.J., Main, M.J., Wise, A., Brown, J., Thompson, N., Solari, R., Lee, M.G. & Foord, S.M. (1998) RAMPs regulate the transport and ligand specificity of the calcitonin-receptor-like receptor. *Nature*, **393**, 333-339.
- McNamara, C.R., Mandel-Brehm, J., Bautista, D.M., Siemens, J., Deranian, K.L., Zhao, M., Hayward, N.J., Chong, J.A., Julius, D., Moran, M.M. & Fanger, C.M. (2007) TRPA1 mediates formalin-induced pain. *Proceedings of the National Academy of Sciences of the United States of America*, **104**, 13525-13530.
- Meng, J., Wang, J., Lawrence, G. & Dolly, J.O. (2007) Synaptobrevin I mediates exocytosis of CGRP from sensory neurons and inhibition by botulinum toxins reflects their anti-nociceptive potential. *J Cell Sci*, **120**, 2864-2874.
- Mocanu, M.M., Gadgil, S., Yellon, D.M. & Baxter, G.F. (1999) Mibefradil, a T-type and L-type calcium channel blocker, limits infarct size through a glibenclamide-sensitive mechanism. *Cardiovasc Drugs Ther*, **13**, 115-122.
- Mogil, J.S., Breese, N.M., Witty, M.F., Ritchie, J., Rainville, M.L., Ase, A., Abbadi, N., Stucky, C.L. & Seguela, P. (2005) Transgenic expression of a dominant-negative ASIC3 subunit leads to increased sensitivity to mechanical and inflammatory stimuli. *J Neurosci*, **25**, 9893-9901.
- Mohapatra, D.P., Wang, S.Y., Wang, G.K. & Nau, C. (2003) A tyrosine residue in TM6 of the Vanilloid Receptor TRPV1 involved in desensitization and calcium permeability of capsaicin-activated currents. *Molecular and cellular neurosciences*, **23**, 314-324.
- Montell, C. & Rubin, G.M. (1989) Molecular characterization of the *Drosophila* trp locus: a putative integral membrane protein required for phototransduction. *Neuron*, **2**, 1313-1323.
- Negoescu, A., Labat-Moleur, F., Lorimier, P., Lamarcq, L., Guillermet, C., Chambaz, E. & Brambilla, E. (1994) F(ab) secondary antibodies: a general method for double immunolabeling with primary antisera from the same species. Efficiency control by chemiluminescence. *J Histochem Cytochem*, **42**, 433-437.
- Nielsen, K.J., Schroeder, T. & Lewis, R. (2000) Structure-activity relationships of omega-conotoxins at N-type voltage-sensitive calcium channels. *J Mol Recognit*, **13**, 55-70.
- Pan, X.Q., Gonzalez, J.A., Chang, S., Chacko, S., Wein, A.J. & Malykhina, A.P. (2010) Experimental colitis triggers the release of substance P and calcitonin gene-related peptide in the urinary bladder via TRPV1 signaling pathways. *Exp Neurol*, **225**, 262-273.

- Park, J. & Luo, Z.D. (2010) Calcium channel functions in pain processing. *Channels (Austin)*, **4**, 510-517.
- Paukert, M., Babini, E., Pusch, M. & Grunder, S. (2004) Identification of the Ca<sup>2+</sup> blocking site of acid-sensing ion channel (ASIC) 1: implications for channel gating. *J Gen Physiol*, **124**, 383-394.
- Payandeh, J., Scheuer, T., Zheng, N. & Catterall, W.A. (2011) The crystal structure of a voltage-gated sodium channel. *Nature*, **475**, 353-358.
- Peier, A.M., Moqrich, A., Hergarden, A.C., Reeve, A.J., Andersson, D.A., Story, G.M., Earley, T.J., Dragoni, I., McIntyre, P., Bevan, S. & Patapoutian, A. (2002) A TRP channel that senses cold stimuli and menthol. *Cell*, **108**, 705-715.
- Peng, B.G., Ahmad, S., Chen, S., Chen, P., Price, M.P. & Lin, X. (2004) Acid-sensing ion channel 2 contributes a major component to acid-evoked excitatory responses in spiral ganglion neurons and plays a role in noise susceptibility of mice. *J Neurosci*, **24**, 10167-10175.
- Perl, E.R. (2007) Ideas about pain, a historical view. *Nature reviews. Neuroscience*, **8**, 71-80.
- Persson, S., Le Greves, P., Thornwall, M., Eriksson, U., Silberring, J. & Nyberg, F. (1995) Neuropeptide converting and processing enzymes in the spinal cord and cerebrospinal fluid. *Prog Brain Res*, **104**, 111-130.
- Petruska, J.C., Napaporn, J., Johnson, R.D. & Cooper, B.Y. (2002) Chemical responsiveness and histochemical phenotype of electrophysiologically classified cells of the adult rat dorsal root ganglion. *Neuroscience*, **115**, 15-30.
- Petruska, J.C., Napaporn, J., Johnson, R.D., Gu, J.G. & Cooper, B.Y. (2000) Subclassified acutely dissociated cells of rat DRG: histochemistry and patterns of capsaicin-, proton-, and ATP-activated currents. *Journal of neurophysiology*, **84**, 2365-2379.
- Poirot, O., Berta, T., Decosterd, I. & Kellenberger, S. (2006) Distinct ASIC currents are expressed in rat putative nociceptors and are modulated by nerve injury. *J Physiol*, **576**, 215-234.
- Poirot, O., Vukicevic, M., Boesch, A. & Kellenberger, S. (2004) Selective regulation of acid-sensing ion channel 1 by serine proteases. *J Biol Chem*, **279**, 38448-38457.
- Pomonis, J.D., Harrison, J.E., Mark, L., Bristol, D.R., Valenzano, K.J. & Walker, K. (2003) N-(4-Tertiarybutylphenyl)-4-(3-cholorpyridin-2-yl)tetrahydropyrazine-1(2H)-carbox-amide (BCTC), a novel, orally effective vanilloid receptor 1 antagonist with analgesic properties: II. in vivo characterization in rat models of inflammatory and neuropathic pain. *The Journal of pharmacology and experimental therapeutics*, **306**, 387-393.

- Poyner, D.R. (1992) Calcitonin gene-related peptide: multiple actions, multiple receptors. *Pharmacol Ther*, **56**, 23-51.
- Price, M.P., Lewin, G.R., McIlwrath, S.L., Cheng, C., Xie, J., Heppenstall, P.A., Stucky, C.L., Mannsfeldt, A.G., Brennan, T.J., Drummond, H.A., Qiao, J., Benson, C.J., Tarr, D.E., Hrstka, R.F., Yang, B., Williamson, R.A. & Welsh, M.J. (2000) The mammalian sodium channel BNC1 is required for normal touch sensation. *Nature*, **407**, 1007-1011.
- Price, M.P., McIlwrath, S.L., Xie, J., Cheng, C., Qiao, J., Tarr, D.E., Sluka, K.A., Brennan, T.J., Lewin, G.R. & Welsh, M.J. (2001) The DRASIC cation channel contributes to the detection of cutaneous touch and acid stimuli in mice. *Neuron*, **32**, 1071-1083.
- Purves, D. (2008) *Neuroscience*. Sinauer, Sunderland Mass.
- Richardson, J.D. & Vasko, M.R. (2002) Cellular mechanisms of neurogenic inflammation. *The Journal of pharmacology and experimental therapeutics*, **302**, 839-845.
- Richter, T.A., Dvoryanchikov, G.A., Roper, S.D. & Chaudhari, N. (2004) Acid-sensing ion channel-2 is not necessary for sour taste in mice. *J Neurosci*, **24**, 4088-4091.
- Roza, C., Puel, J.L., Kress, M., Baron, A., Diochot, S., Lazdunski, M. & Waldmann, R. (2004) Knockout of the ASIC2 channel in mice does not impair cutaneous mechanosensation, visceral mechanonociception and hearing. *The Journal of physiology*, **558**, 659-669.
- Rugiero, F., Mistry, M., Sage, D., Black, J.A., Waxman, S.G., Crest, M., Clerc, N., Delmas, P. & Gola, M. (2003) Selective expression of a persistent tetrodotoxin-resistant Na<sup>+</sup> current and NaV1.9 subunit in myenteric sensory neurons. *The Journal of neuroscience : the official journal of the Society for Neuroscience*, **23**, 2715-2725.
- Sage, D., Salin, P., Alcaraz, G., Castets, F., Giraud, P., Crest, M., Mazet, B. & Clerc, N. (2007) Na(v)1.7 and Na(v)1.3 are the only tetrodotoxin-sensitive sodium channels expressed by the adult guinea pig enteric nervous system. *The Journal of comparative neurology*, **504**, 363-378.
- Samways, D.S., Harkins, A.B. & Egan, T.M. (2009) Native and recombinant ASIC1a receptors conduct negligible Ca<sup>2+</sup> entry. *Cell calcium*, **45**, 319-325.
- Samways, D.S., Khakh, B.S. & Egan, T.M. (2008) Tunable calcium current through TRPV1 receptor channels. *The Journal of biological chemistry*, **283**, 31274-31278.
- Schild, L., Schneeberger, E., Gautschi, I. & Firsov, D. (1997) Identification of amino acid residues in the alpha, beta, and gamma subunits of the epithelial sodium channel (ENaC) involved in amiloride block and ion permeation. *The Journal of general physiology*, **109**, 15-26.

- Schmidtko, A., Lotsch, J., Freynhagen, R. & Geisslinger, G. (2010) Ziconotide for treatment of severe chronic pain. *Lancet*, **375**, 1569-1577.
- Seybold, V.S. (2009) The role of peptides in central sensitization. *Handbook of experimental pharmacology*, 451-491.
- Sherwood, T.W. & Askwith, C.C. (2008) Endogenous arginine-phenylalanine-amide-related peptides alter steady-state desensitization of ASIC1a. *J Biol Chem*, **283**, 1818-1830.
- Sherwood, T.W. & Askwith, C.C. (2009) Dynorphin opioid peptides enhance acid-sensing ion channel 1a activity and acidosis-induced neuronal death. *The Journal of neuroscience : the official journal of the Society for Neuroscience*, **29**, 14371-14380.
- Shimada, S., Ueda, T., Ishida, Y., Yamamoto, T. & Ugawa, S. (2006) Acid-sensing ion channels in taste buds. *Arch Histol Cytol*, **69**, 227-231.
- Sluka, K.A., Price, M.P., Breese, N.M., Stucky, C.L., Wemmie, J.A. & Welsh, M.J. (2003) Chronic hyperalgesia induced by repeated acid injections in muscle is abolished by the loss of ASIC3, but not ASIC1. *Pain*, **106**, 229-239.
- Sluka, K.A., Radhakrishnan, R., Benson, C.J., Eshcol, J.O., Price, M.P., Babinski, K., Audette, K.M., Yeomans, D.C. & Wilson, S.P. (2007) ASIC3 in muscle mediates mechanical, but not heat, hyperalgesia associated with muscle inflammation. *Pain*, **129**, 102-112.
- Smith, M.T., Cabot, P.J., Ross, F.B., Robertson, A.D. & Lewis, R.J. (2002) The novel N-type calcium channel blocker, AM336, produces potent dose-dependent antinociception after intrathecal dosing in rats and inhibits substance P release in rat spinal cord slices. *Pain*, **96**, 119-127.
- Snider, W.D. & McMahon, S.B. (1998) Tackling pain at the source: new ideas about nociceptors. *Neuron*, **20**, 629-632.
- Snijdelaar, D.G., Dirksen, R., Slappendel, R. & Crul, B.J. (2000) Substance P. *European journal of pain*, **4**, 121-135.
- Staniland, A.A. & McMahon, S.B. (2008) Mice lacking acid-sensing ion channels (ASIC) 1 or 2, but not ASIC3, show increased pain behaviour in the formalin test. *Eur J Pain*.
- Strecker, T., Messlinger, K., Weyand, M. & Reeh, P.W. (2005) Role of different proton-sensitive channels in releasing calcitonin gene-related peptide from isolated hearts of mutant mice. *Cardiovasc Res*, **65**, 405-410.

- Talavera, K., Gees, M., Karashima, Y., Meseguer, V.M., Vanoirbeek, J.A., Damann, N., Everaerts, W., Benoit, M., Janssens, A., Vennekens, R., Viana, F., Nemery, B., Nilius, B. & Voets, T. (2009) Nicotine activates the chemosensory cation channel TRPA1. *Nature neuroscience*, **12**, 1293-1299.
- Tang, H.B., Shiba, E., Li, Y.S., Morioka, N., Zheng, T.X., Ogata, N. & Nakata, Y. (2008) Involvement of voltage-gated sodium channel Na(v)1.8 in the regulation of the release and synthesis of substance P in adult mouse dorsal root ganglion neurons. *J Pharmacol Sci*, **108**, 190-197.
- Todorovic, S.M. & Jevtovic-Todorovic, V. (2006) The role of T-type calcium channels in peripheral and central pain processing. *CNS Neurol Disord Drug Targets*, **5**, 639-653.
- Toledo-Aral, J.J., Moss, B.L., He, Z.J., Koszowski, A.G., Whisenand, T., Levinson, S.R., Wolf, J.J., Silos-Santiago, I., Halegoua, S. & Mandel, G. (1997) Identification of PN1, a predominant voltage-dependent sodium channel expressed principally in peripheral neurons. *Proceedings of the National Academy of Sciences of the United States of America*, **94**, 1527-1532.
- Tominaga, M., Caterina, M.J., Malmberg, A.B., Rosen, T.A., Gilbert, H., Skinner, K., Raumann, B.E., Basbaum, A.I. & Julius, D. (1998) The cloned capsaicin receptor integrates multiple pain-producing stimuli. *Neuron*, **21**, 531-543.
- Triggle, D.J. (2003) 1,4-Dihydropyridines as calcium channel ligands and privileged structures. *Cell Mol Neurobiol*, **23**, 293-303.
- Tschopp, F.A., Henke, H., Petermann, J.B., Tobler, P.H., Janzer, R., Hokfelt, T., Lundberg, J.M., Cuello, C. & Fischer, J.A. (1985) Calcitonin gene-related peptide and its binding sites in the human central nervous system and pituitary. *Proceedings of the National Academy of Sciences of the United States of America*, **82**, 248-252.
- Tsukagoshi, M., Goris, R.C. & Funakoshi, K. (2006) Differential distribution of vanilloid receptors in the primary sensory neurons projecting to the dorsal skin and muscles. *Histochemistry and cell biology*, **126**, 343-352.
- Ugawa, S., Ueda, T., Ishida, Y., Nishigaki, M., Shibata, Y. & Shimada, S. (2002) Amiloride-blockable acid-sensing ion channels are leading acid sensors expressed in human nociceptors. *J Clin Invest*, **110**, 1185-1190.
- Ugawa, S., Ueda, T., Yamamura, H. & Shimada, S. (2005) In situ hybridization evidence for the coexistence of ASIC and TRPV1 within rat single sensory neurons. *Brain Res Mol Brain Res*, **136**, 125-133.
- V. Euler, U. & Gaddum, J.H. (1931) An unidentified depressor substance in certain tissue extracts. *The Journal of physiology*, **72**, 74-87.



- Vallet, V., Chraïbi, A., Gaeggeler, H.P., Horisberger, J.D. & Rossier, B.C. (1997) An epithelial serine protease activates the amiloride-sensitive sodium channel. *Nature*, **389**, 607-610.
- Verdru, P., De Greef, C., Mertens, L., Carmeliet, E. & Callewaert, G. (1997) Na<sup>(+)</sup>-Ca<sup>2+</sup> exchange in rat dorsal root ganglion neurons. *Journal of neurophysiology*, **77**, 484-490.
- Villalon, C.M. & Olesen, J. (2009) The role of CGRP in the pathophysiology of migraine and efficacy of CGRP receptor antagonists as acute antimigraine drugs. *Pharmacol Ther*, **124**, 309-323.
- Voets, T., Droogmans, G., Wissenbach, U., Janssens, A., Flockerzi, V. & Nilius, B. (2004) The principle of temperature-dependent gating in cold- and heat-sensitive TRP channels. *Nature*, **430**, 748-754.
- Voilley, N., de Weille, J., Mamet, J. & Lazdunski, M. (2001) Nonsteroid anti-inflammatory drugs inhibit both the activity and the inflammation-induced expression of acid-sensing ion channels in nociceptors. *J Neurosci*, **21**, 8026-8033.
- Vukicevic, M. & Kellenberger, S. (2004) Modulatory effects of acid-sensing ion channels on action potential generation in hippocampal neurons. *Am J Physiol Cell Physiol*, **287**, C682-690.
- Vukicevic, M., Weder, G., Boillat, A., Boesch, A. & Kellenberger, S. (2006) Trypsin cleaves acid-sensing ion channel 1a in a domain that is critical for channel gating. *J Biol Chem*, **281**, 714-722.
- Walder, R.Y., Gautam, M., Wilson, S.P., Benson, C.J. & Sluka, K.A. (2011) Selective targeting of ASIC3 using artificial miRNAs inhibits primary and secondary hyperalgesia after muscle inflammation. *Pain*, **152**, 2348-2356.
- Walder, R.Y., Rasmussen, L.A., Rainier, J.D., Light, A.R., Wemmie, J.A. & Sluka, K.A. (2010) ASIC1 and ASIC3 play different roles in the development of Hyperalgesia after inflammatory muscle injury. *J Pain*, **11**, 210-218.
- Waldmann, R., Champigny, G., Bassilana, F., Heurteaux, C. & Lazdunski, M. (1997) A proton-gated cation channel involved in acid-sensing. *Nature*, **386**, 173-177.
- Waldmann, R. & Lazdunski, M. (1998) H<sup>(+)</sup>-gated cation channels: neuronal acid sensors in the NaC/DEG family of ion channels. *Current opinion in neurobiology*, **8**, 418-424.
- Walker, C.S., Conner, A.C., Poyner, D.R. & Hay, D.L. (2010) Regulation of signal transduction by calcitonin gene-related peptide receptors. *Trends Pharmacol Sci*, **31**, 476-483.

- Wang, H. & Woolf, C.J. (2005) Pain TRPs. *Neuron*, **46**, 9-12.
- Waxman, S.G., Kocsis, J.D. & Black, J.A. (1994) Type III sodium channel mRNA is expressed in embryonic but not adult spinal sensory neurons, and is reexpressed following axotomy. *Journal of neurophysiology*, **72**, 466-470.
- Wemmie, J.A., Askwith, C.C., Lamani, E., Cassell, M.D., Freeman, J.H., Jr. & Welsh, M.J. (2003) Acid-sensing ion channel 1 is localized in brain regions with high synaptic density and contributes to fear conditioning. *J Neurosci*, **23**, 5496-5502.
- Wemmie, J.A., Chen, J., Askwith, C.C., Hruska-Hageman, A.M., Price, M.P., Nolan, B.C., Yoder, P.G., Lamani, E., Hoshi, T., Freeman, J.H., Jr. & Welsh, M.J. (2002) The acid-activated ion channel ASIC contributes to synaptic plasticity, learning, and memory. *Neuron*, **34**, 463-477.
- Wemmie, J.A., Price, M.P. & Welsh, M.J. (2006) Acid-sensing ion channels: advances, questions and therapeutic opportunities. *Trends Neurosci*, **29**, 578-586.
- Westenbroek, R.E., Hoskins, L. & Catterall, W.A. (1998) Localization of Ca<sup>2+</sup> channel subtypes on rat spinal motor neurons, interneurons, and nerve terminals. *The Journal of neuroscience : the official journal of the Society for Neuroscience*, **18**, 6319-6330.
- Wetsel, W.C. (2011) Sensing hot and cold with TRP channels. *Int J Hyperthermia*, **27**, 388-398.
- Woolf, C.J. (2004) Pain: moving from symptom control toward mechanism-specific pharmacologic management. *Ann Intern Med*, **140**, 441-451.
- Wu, L.J., Duan, B., Mei, Y.D., Gao, J., Chen, J.G., Zhuo, M., Xu, L., Wu, M. & Xu, T.L. (2004) Characterization of acid-sensing ion channels in dorsal horn neurons of rat spinal cord. *J Biol Chem*, **279**, 43716-43724.
- Wu, W.L., Wang, C.H., Huang, E.Y. & Chen, C.C. (2009) Asic3(-/-) female mice with hearing deficit affects social development of pups. *PloS one*, **4**, e6508.
- Xie, J., Price, M.P., Berger, A.L. & Welsh, M.J. (2002) DRASIC contributes to pH-gated currents in large dorsal root ganglion sensory neurons by forming heteromultimeric channels. *J Neurophysiol*, **87**, 2835-2843.
- Xie, J., Price, M.P., Wemmie, J.A., Askwith, C.C. & Welsh, M.J. (2003) ASIC3 and ASIC1 mediate FMRamide-related peptide enhancement of H<sup>+</sup>-gated currents in cultured dorsal root ganglion neurons. *J Neurophysiol*, **89**, 2459-2465.

- Xiong, Z.G., Zhu, X.M., Chu, X.P., Minami, M., Hey, J., Wei, W.L., MacDonald, J.F., Wemmie, J.A., Price, M.P., Welsh, M.J. & Simon, R.P. (2004) Neuroprotection in ischemia: blocking calcium-permeable acid-sensing ion channels. *Cell*, **118**, 687-698.
- Xu, X.J., Dalsgaard, C.J., Maggi, C.A. & Wiesenfeld-Hallin, Z. (1992) NK-1, but not NK-2, tachykinin receptors mediate plasma extravasation induced by antidromic C-fiber stimulation in rat hindpaw: demonstrated with the NK-1 antagonist CP-96,345 and the NK-2 antagonist Men 10207. *Neuroscience letters*, **139**, 249-252.
- Yang, Y., Wang, Y., Li, S., Xu, Z., Li, H., Ma, L., Fan, J., Bu, D., Liu, B., Fan, Z., Wu, G., Jin, J., Ding, B., Zhu, X. & Shen, Y. (2004) Mutations in SCN9A, encoding a sodium channel alpha subunit, in patients with primary erythralgia. *J Med Genet*, **41**, 171-174.
- Yen, Y.T., Tu, P.H., Chen, C.J., Lin, Y.W., Hsieh, S.T. & Chen, C.C. (2009) Role of acid-sensing ion channel 3 in sub-acute-phase inflammation. *Molecular pain*, **5**, 1.
- Yermolaieva, O., Leonard, A.S., Schnizler, M.K., Abboud, F.M. & Welsh, M.J. (2004) Extracellular acidosis increases neuronal cell calcium by activating acid-sensing ion channel 1a. *Proc Natl Acad Sci U S A*, **101**, 6752-6757.
- Yu, F.H., Yarov-Yarovoy, V., Gutman, G.A. & Catterall, W.A. (2005) Overview of molecular relationships in the voltage-gated ion channel superfamily. *Pharmacol Rev*, **57**, 387-395.
- Yu, L.C., Hou, J.F., Fu, F.H. & Zhang, Y.X. (2009) Roles of calcitonin gene-related peptide and its receptors in pain-related behavioral responses in the central nervous system. *Neurosci Biobehav Rev*, **33**, 1185-1191.
- Yu, Y., Chen, Z., Li, W.G., Cao, H., Feng, E.G., Yu, F., Liu, H., Jiang, H. & Xu, T.L. (2010) A nonproton ligand sensor in the acid-sensing ion channel. *Neuron*, **68**, 61-72.
- Ziemann, A.E., Allen, J.E., Dahdaleh, N.S., Drebot, II, Coryell, M.W., Wunsch, A.M., Lynch, C.M., Faraci, F.M., Howard, M.A., 3rd, Welsh, M.J. & Wemmie, J.A. (2009) The amygdala is a chemosensor that detects carbon dioxide and acidosis to elicit fear behavior. *Cell*, **139**, 1012-1021.
- Zimmermann, M. (1983) Ethical guidelines for investigations of experimental pain in conscious animals. *Pain*, **16**, 109-110.